



HAL
open science

Measurements of the top quark branching ratios into channels with leptons and quarks with the ATLAS detector

G. Aad, M.K. Ayoub, A. Bassalat, C. Becot, S. Binet, C. Bourdarios, J.B. de Vivie De Regie, D. Delgove, L. Duflot, M. Escalier, et al.

► **To cite this version:**

G. Aad, M.K. Ayoub, A. Bassalat, C. Becot, S. Binet, et al.. Measurements of the top quark branching ratios into channels with leptons and quarks with the ATLAS detector. *Physical Review D*, 2015, 92, pp.072005. 10.1103/PhysRevD.92.072005 . in2p3-01164723

HAL Id: in2p3-01164723

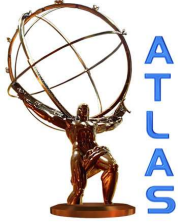
<https://hal.in2p3.fr/in2p3-01164723>

Submitted on 13 Sep 2023

HAL is a multi-disciplinary open access archive for the deposit and dissemination of scientific research documents, whether they are published or not. The documents may come from teaching and research institutions in France or abroad, or from public or private research centers.

L'archive ouverte pluridisciplinaire **HAL**, est destinée au dépôt et à la diffusion de documents scientifiques de niveau recherche, publiés ou non, émanant des établissements d'enseignement et de recherche français ou étrangers, des laboratoires publics ou privés.

EUROPEAN ORGANISATION FOR NUCLEAR RESEARCH (CERN)



Submitted to: PRD



CERN-PH-EP-2015-108
June 18, 2016

arXiv:1506.05074v4 [hep-ex] 15 Jun 2016

Measurements of the top quark branching ratios into channels with leptons and quarks with the ATLAS detector

The ATLAS Collaboration

Abstract

Measurements of the branching ratios of top quark decays into leptons and jets using events with $t\bar{t}$ (top antitop) pairs are reported. Events were recorded with the ATLAS detector at the LHC in pp collisions at a center-of-mass energy of 7 TeV. The collected data sample corresponds to an integrated luminosity of 4.6 fb^{-1} . The measured top quark branching ratios agree with the Standard Model predictions within the measurement uncertainties of a few percent.

© 2016 CERN for the benefit of the ATLAS Collaboration.

Reproduction of this article or parts of it is allowed as specified in the CC-BY-3.0 license.

Contents

1	Introduction	3
2	Analysis Overview	3
3	ATLAS Detector	4
4	Data and Monte Carlo Samples	5
5	Event Selection	5
6	Single-lepton + jets channel	7
6.1	Background templates	8
6.2	Fits to mass distributions	10
7	Dilepton + jets channel	15
8	Lepton+τ_{had}+jets channel	18
8.1	Tau background templates	18
8.2	Signal extraction by fitting to BDT_j shape	20
8.3	Fit results	21
9	Measuring Cross Section and Branching Ratios	23
10	Systematic Uncertainties	26
11	Results	30
12	Conclusion	30

1 Introduction

In the Standard Model (SM), 100% of the top quark decays contain a W boson and a down-type quark. Measurements of the ratio of top branching fractions $B(t \rightarrow W+b\text{-quark})/B(t \rightarrow W+\text{down-type quark})$ [1] and of single top production [2–4] have shown that more than 95% of the decays are to a W boson and a b -quark. In the SM the branching ratio to the different leptons is the same since the decay proceeds via a W boson, but in models of new physics, e.g. supersymmetry (SUSY), final states with τ leptons can be enhanced or suppressed [5]; thus measuring the inclusive cross section using final states with τ leptons can be a good probe for new physics. The measured values of the top quark branching ratios will deviate with respect to the SM predictions if the data sample selected to extract $t\bar{t}$ events contains final states without two W bosons. Examples of processes that would cause deviations include events with a top quark decaying to charged Higgs boson or with SUSY particles decaying to the supersymmetric partner of the τ lepton ($\tilde{\tau}$). Limits on the top quark branching ratio to a charged Higgs boson and a b -quark have been published by the CDF [6], D0 [7, 8], ATLAS [9, 10] and CMS [11] collaborations. Another example of a final state that can change the observed branching ratios is the pair production of supersymmetric partners of the top quark (\tilde{t}) decaying into $b\nu_\tau\tilde{\tau}$ followed by the $\tilde{\tau}$ decay into a τ lepton and the gravitino, predicted by gauge-mediated SUSY breaking models [12].

This article presents the first direct measurement of the top quark semileptonic and all-hadronic branching ratios. The branching ratios can be more sensitive probes of deviations from SM expectations than measuring cross sections in different channels, because of cancellation of systematic uncertainties. The large number of $t\bar{t}$ pairs produced at the LHC provides an opportunity to measure top quark branching ratios with high precision. These top quark branching ratios are expected to be determined by the W boson branching ratios, which have been measured at LEP [15] to be in good agreement with the SM expectations [16]. Observing any deviation would be an indication of non-SM processes contributing to final states dominated by $t\bar{t}$ production. This article also presents a measurement of the inclusive $t\bar{t}$ cross section using events with an isolated charged lepton (μ or e) and a τ lepton decaying hadronically (τ_{had}). Previous measurements of the cross section at $\sqrt{s} = 7$ TeV in this channel have been published by the ATLAS and CMS collaborations [13, 14].

The analysis uses the full data sample, 4.6 fb^{-1} , collected by the ATLAS experiment at the LHC from pp collisions at $\sqrt{s} = 7$ TeV between March and November 2011. Kinematic selection criteria are applied that require one or both of the top and antitop quarks to decay into a final state with one isolated lepton and a jet. At least one jet in the event must be tagged as originating from a b -quark (b -tag). Seven mutually exclusive final states are used in this analysis: $e+\text{jets}$, $\mu+\text{jets}$, $ee+\text{jets}$, $\mu\mu+\text{jets}$, $e\mu+\text{jets}$, $e\tau_{\text{had}}+\text{jets}$ and $\mu\tau_{\text{had}}+\text{jets}$. Branching ratios for semileptonic and purely hadronic top quark decays are obtained by combining these seven final states assuming that only SM processes contribute to the background and the top branching ratios to leptons and jets add up to one.

2 Analysis Overview

Data samples enriched with $t\bar{t}$ events are selected by means of criteria that are designed to accept two W bosons and at least one b -quark. In every event, either an electron or a muon is required, with the aim to select $W \rightarrow \ell\nu$, where ℓ stands for either e or μ . The ℓ may be produced directly in $W \rightarrow \ell\nu$ boson decays or indirectly in $W \rightarrow \tau\nu$ decays. Separate event channels are classified depending on the decay of a second W boson: $W \rightarrow \text{jets}$ for $\ell+\text{jets}$, $W \rightarrow \ell\nu$ for $\ell\ell'+\text{jets}$, or $W \rightarrow \tau_{\text{had}}\nu$ for $\ell\tau_{\text{had}}+\text{jets}$. Since

the analysis does not distinguish electrons or muons that originate from a τ lepton decay from those that come from direct $W \rightarrow e\nu$ and $W \rightarrow \mu\nu$ decays, both are included in the $W \rightarrow \ell\nu$ decays. The branching ratios are measured by taking ratios of the number of $t\bar{t}$ events extracted from the three channels; thus an important aspect of the event selection is to use similar criteria for the object selection in all final states, so as to allow the cancellation of systematic uncertainties in the ratios. Another important criterion is to ensure that no event contributes to more than one channel. The channel with the largest background and smallest number of signal events is that containing $\ell\tau_{\text{had}}+\text{jets}$; thus the event selection and analysis were optimized to reduce the uncertainty in that channel (see Sec. 5).

The number of $t\bar{t}$ events in a given channel is extracted by fitting background and signal templates to data distributions. The template shapes are fixed while their normalizations are allowed to vary. The signal templates are derived from $t\bar{t}$ Monte Carlo (MC) simulation, which assumes that the top quark decays to a W boson and a b -quark with a 100% branching ratio. This assumption affects the shape of the signal templates, and if it is not valid for the selected data, the measured branching ratios will deviate from the SM prediction. The amount of background varies significantly in each channel. It is almost negligible in the $e\mu+\text{jets}$ channel and larger than the signal in the $\ell\tau_{\text{had}}+\text{jets}$ channels. In the $\ell+\text{jets}$ channels, three invariant masses from two- and three-jet systems and a transverse mass distribution are fitted, as described in detail in Sec. 6, while in the $\ell\ell'+\text{jets}$ channels the dilepton effective mass distributions from two different missing transverse momentum ($E_{\text{T}}^{\text{miss}}$) regions are used (see Sec. 7). Because of the much larger background, which originates from jets misidentified as τ leptons, a very different approach is taken in the $\ell\tau_{\text{had}}+\text{jets}$ channel. Instead of fitting a kinematic distribution, the quantity fitted is a boosted decision tree (BDT) output [17], a multivariate discriminant that separates jets from τ leptons decaying to hadrons (see Sec. 8).

The details of how the inclusive production cross section and branching ratios are derived from the number of $t\bar{t}$ events obtained from each channel are discussed in Sec. 9. The systematic uncertainties of the measurements are estimated by varying each source of systematic uncertainty by $\pm 1\sigma$ in templates derived from MC simulation and fitting all the distributions with the new templates (see Sec. 10). The final results are given in Sec. 11.

3 ATLAS Detector

The ATLAS detector [18] at the LHC covers nearly the entire solid angle around the collision point.¹ It consists of an inner tracking detector surrounded by a thin superconducting solenoid, electromagnetic (EM) and hadronic calorimeters, and an external muon spectrometer incorporating three large superconducting toroid magnet assemblies. The inner tracking detector provides tracking information in a pseudorapidity range $|\eta| < 2.5$. The liquid-argon (LAr) EM sampling calorimeters cover a range of $|\eta| < 3.2$ with fine granularity. An iron/scintillator tile calorimeter provides hadronic energy measurements in the central rapidity range ($|\eta| < 1.7$). The endcap and forward regions are instrumented with LAr calorimeters for both the EM and hadronic energy measurements covering $|\eta| < 4.9$. The muon spectrometer provides precise tracking information in a range of $|\eta| < 2.7$.

¹ ATLAS uses a right-handed coordinate system with its origin at the nominal interaction point in the center of the detector and the z -axis along the beam pipe. The x -axis points to the center of the LHC ring, and the y -axis points upwards. The azimuthal angle ϕ is measured around the beam axis and the polar angle θ is the angle from the beam axis. The pseudorapidity is defined as $\eta = -\ln[\tan(\theta/2)]$. The distance ΔR in η - ϕ space is defined as $\Delta R = \sqrt{(\Delta\phi)^2 + (\Delta\eta)^2}$. The transverse momentum and energy are defined as $p_{\text{T}} = p \sin \theta$ and $E_{\text{T}} = E \sin \theta$, respectively

In 2011, ATLAS used a three-level trigger system to select events. The level-1 trigger is implemented in hardware using a subset of detector information to reduce the event rate to less than 75 kHz. This is followed by two software-based trigger levels, namely level-2 and the event filter, which together reduce the event rate to about 300 Hz recorded for analysis.

4 Data and Monte Carlo Samples

The present measurements use collision data with a center-of-mass energy of $\sqrt{s} = 7$ TeV taken in 2011 and selected with a single-electron or a single-muon trigger. Taking into account selection criteria for good data quality, the total integrated luminosity for the analyzed data sample is 4.6 fb^{-1} .

The $t\bar{t}$ signal is modeled using the POWHEG [19, 20] event generator, interfaced to PYTHIA6 (v6.421) [21] with the Perugia 2011C tune [22] for showering and hadronization, setting the top quark mass to 172.5 GeV and using the next-to-leading-order (NLO) parton distribution function (PDF) set CTEQ66 [23]. The $t\bar{t}$ production cross section used in the simulation is normalized to 177 pb as obtained from next-to-next-to-leading-order (NNLO) plus next-to-next-to-leading-logarithm (NNLL) calculations [24].

The calculation of the backgrounds uses MC simulations of W/Z production with multiple jets (matrix elements for the jets production include light quarks, c , \bar{c} , $c\bar{c}$, $b\bar{b}$), single-top-quark, and diboson (WW , WZ , ZZ) events. Single-top-quark events were generated using MC@NLO (v4.01) [25] interfaced with HERWIG (v6.520) [26] and JIMMY (v4.31) [27] to model parton showering, hadronization, and the underlying-event using PDF set CT10 [28]. W +jets events with up to five partons and Z +jets events with $m(\ell^+\ell^-) > 40$ GeV and up to five partons were generated by ALPGEN [29] (v2.13) interfaced to HERWIG plus JIMMY and the CTEQ6L1 [30] PDF set. The MLM matching scheme [31] of the ALPGEN generator is used to remove overlaps between matrix-element and parton-shower products. Diboson events were generated using HERWIG plus JIMMY and the MRSTMcal PDF set [32]. Scale factors are applied to each process to match next-to-leading-order predictions. The τ decays are handled by TAUOLA [33].

All samples of simulated events include the effect of multiple pp interactions in the same and neighboring bunch crossings (pile-up). On average, nine minimum-bias events are overlaid on all simulated events to match the pile-up conditions in data. The average number of pp collisions in a bunch crossing ($\langle\mu\rangle$) depends on the instantaneous luminosity, which increased over time; $\langle\mu\rangle$ varied from 5 at the beginning of the run period to approximately 18 at the end. The events are reweighted in order to make the distribution of the average number of interactions per bunch crossing match the one observed in data. All MC events are simulated with a detailed GEANT4-based detector simulation [34, 35] and are reconstructed with the same algorithms as used in data.

5 Event Selection

Events are selected using a single-muon trigger with a p_T threshold of 18 GeV or a single-electron trigger with a E_T threshold of 20 GeV, rising to 22 GeV during periods of high instantaneous luminosity. The p_T and E_T criteria used in the further analysis guarantee a high and constant trigger efficiency. The same triggers and reconstructed object definitions are applied to all channels.

Muon candidates are selected using tracks from the inner detector matched with tracks in the muon spectrometer [36]. They are required to have $p_T > 20$ GeV and $|\eta| < 2.5$ and to satisfy criteria designed to reduce the muon misidentification probability. The muon must have a longitudinal impact parameter (z_0) with respect to the primary vertex of less than 2 mm. In addition, to suppress muons from heavy-quark decays, muons must pass the isolation cuts: the calorimeter energy in a cone of size $\Delta R = 0.2$ around the muon track must be less than 4 GeV, and the scalar sum of the p_T of the tracks reconstructed in the inner tracker in a cone of $\Delta R = 0.3$ around the muon track must be less than 2.5 GeV. If a muon overlaps within a cone of $\Delta R = 0.4$ with an electron candidate or with a jet, as defined below, it is not considered to be isolated.

Electron candidates are required to satisfy cuts on calorimeter and tracking variables to separate isolated electrons from jets [37]. Electrons must fall into the region $|\eta_{\text{cluster}}| < 2.47$, where $|\eta_{\text{cluster}}|$ is the pseudorapidity of the calorimeter energy cluster associated with the electron, excluding the transition region between the barrel and endcap calorimeters at $1.37 < |\eta_{\text{cluster}}| < 1.52$, and have $E_T > 25$ GeV. The electrons must also pass an E_T isolation cut within a cone of $\Delta R = 0.2$ derived for 90% efficiency along with a p_T isolation cut within a cone of $\Delta R = 0.3$ derived for 90% efficiency for prompt electrons from $Z \rightarrow e^+e^-$ events. The electron must have z_0 with respect to the primary vertex of less than 2 mm. Finally, if the electron lies within a cone of $\Delta R = 0.4$ around the muon or between $0.2 < \Delta R \leq 0.4$ around a jet as defined below, the object is considered to be a muon or a jet, respectively.

Jets are reconstructed from clustered energy deposits in the calorimeters using the anti- k_r [38] algorithm with a radius parameter $R = 0.4$. Jets are required to have a transverse momentum $p_T > 25$ GeV and to be in the pseudorapidity range $|\eta| < 2.5$. The summed scalar p_T of tracks associated with the jet and associated with the primary vertex is required to be at least 75% of the summed p_T of all tracks associated with the jet [39]. Any jet close to a good electron, as defined above, is considered to be an electron if it lies within a cone of $\Delta R = 0.2$ around the electron.

Missing transverse momentum (E_T^{miss}) is the magnitude of the vector sum of the x and y components of the cluster energy in the calorimeters. Each cluster is calibrated according to which type of high- p_T object it is matched to, either electrons, jets, muons or photons.

Jets containing b -hadrons (b -jets) are identified (b -tagged) with a multivariate discriminant that exploits the long lifetimes, high masses and high decay multiplicities of b -hadrons. It makes use of track impact parameters and reconstructed secondary vertices. An operating point corresponding to an average efficiency of 70% and an average mistag rate for light-quark jets of 0.8% is used [40].

τ candidates are reconstructed using calorimeter jets as seeds. These seed jets are calibrated with the local calibration (LC) scheme [41, 42]. The τ candidate must have $E_T^\tau > 20$ GeV, $|\eta_\tau| < 2.3$, and only one track with $p_T > 4$ GeV associated with the τ candidate (77% of hadronic τ decays have only one track). The charge of the τ candidate is given by the charge of the associated track. Candidates with higher track multiplicity are not used as they do not improve the precision of the measurement because of much larger associated systematic uncertainties. The analysis makes use of a BDT for τ identification, a cut-based multivariate algorithm that optimizes signal and background separation [17].

The τ candidates that overlap within $\Delta R < 0.4$ of a b -tagged jet, a loose muon,² or an electron,³ are rejected and kept as jets or electrons. To remove the remaining electrons misidentified as τ candidates a medium BDT (BDT_e) electron veto is applied. BDT_e is a BDT trained to distinguish electrons and τ leptons using a $Z \rightarrow \tau\tau$ MC sample as signal and a $Z \rightarrow \ell\ell$ MC sample as background. The BDT_e uses four variables, the two most powerful being the ratio of high-threshold to low-threshold track hits in the transition radiator and the ratio of energy deposited in the EM calorimeter to the total energy deposited in the calorimeter. The medium working point corresponds to 85% efficiency for $Z \rightarrow \tau\tau$, Ref. [43]. The additional rejection factor for electrons after removing isolated electrons that overlap with τ candidates is 60. In addition, a muon veto that compares the track momentum in τ candidates with the energy deposited in the electromagnetic calorimeter is required to further reduce the muon background. It is tuned to 96% efficiency on signal (62% on background after overlap removal). A BDT to reject hadronic jets faking τ leptons, BDT_j , is trained with τ leptons from a $Z \rightarrow \tau\tau$ MC sample as signal and jets from data, selected from events with at least two jets, as background. The BDT_j uses eight variables, the most sensitive is the fraction of energy deposited in the region $\Delta R < 0.1$ with respect to all energy deposited in the region $\Delta R < 0.2$ around the τ candidate. Details of the BDT_e and BDT_j input variables and performance are given in Ref. [43].

The event selection requirements common to all channels are a primary vertex with at least five associated tracks with $p_T > 400$ MeV, at least one isolated high- p_T muon ($p_T > 20$ GeV) and/or isolated high- p_T electron ($p_T > 25$ GeV), at least two jets with $p_T > 25$ GeV, and at least one of them tagged as a b -jet. In addition, there are requirements specific to each channel. For the ℓ +jets channels the isolated-muon p_T threshold is raised from 20 GeV to 25 GeV to reduce the multijet background and exactly one isolated ℓ is required. The minimum number of jets with $p_T > 25$ GeV is raised to four. Events with τ candidates are removed. Removing events with τ candidates from the ℓ +jets channel results in an efficiency loss of 8.5%. For the $\ell\ell$ +jets channels, events are required to have exactly two isolated ℓ with opposite-sign charges and $E_T^{\text{miss}} > 30$ GeV. For the $\ell\tau_{\text{had}}$ +jets channels, exactly one isolated ℓ , $E_T^{\text{miss}} > 30$ GeV, and at least one τ candidate, are required. In addition the ℓ and the τ candidate must have opposite charge. The τ candidates that do not satisfy these requirements are kept as jets. The thresholds for lepton p_T , jet p_T and E_T^{miss} were optimized for the $\ell\tau_{\text{had}}$ +jets channel for maximum signal significance by means of a search in parameter space.

6 Single-lepton + jets channel

Three different classes of events contribute as a background to the $t\bar{t} \rightarrow \ell$ +jets channel:

1. events with one isolated ℓ originating from processes with one true lepton (W boson decay);
2. events with one jet misidentified as an isolated lepton and no other isolated lepton reconstructed;
3. events with one isolated lepton originating from processes with multiple true leptons but only one isolated lepton reconstructed.

² Loose muons are selected with all requirements described in Sec. 5 for good muons, except $p_T^\mu > 4$ GeV and no isolation requirements are applied.

³ These electrons are selected with all requirements described in Sec. 5 for good electrons, but electrons with $E_T > 20$ GeV are considered.

The number of $t\bar{t} \rightarrow \ell$ +jets events is extracted by fitting distributions of four invariant mass variables with templates for signal and backgrounds. The following mass variables provide good discrimination between signal and background:

1. m_{jj} : invariant mass of the two highest- p_T jets not designated as b -jets;
2. m_{b1jj} : invariant mass of the leading b -jet and the jets used to calculate m_{jj} ;
3. m_{b2jj} : invariant mass of the subleading b -jet and the jets used to calculate m_{jj} ;
4. m_T : transverse mass of ℓ and the E_T^{miss} , $m_T(\ell, E_T^{\text{miss}}) = \sqrt{(E_T^\ell + E_T^{\text{miss}})^2 - (p_x^\ell + E_x^{\text{miss}})^2 - (p_y^\ell + E_y^{\text{miss}})^2}$.

If an event has only one jet tagged as a b -jet, the highest- p_T jet that is not tagged is assumed to be a second b -jet. A few observations motivate the choice of mass distributions for the fit. The presence of a W boson decaying to a pair of quarks leads to a m_{jj} distribution that peaks at the W boson mass. The presence of a top quark decaying to $W(\rightarrow qq) + b$ will produce m_{b1jj} and m_{b2jj} distributions that peak at the top quark mass. The presence of a W boson decaying to $\ell + \nu$ manifests itself as a Jacobian peak in the m_T distribution when there are no additional high- p_T neutrinos in the event.

6.1 Background templates

The main backgrounds in the ℓ +jets channel are from $W(\rightarrow \ell\nu)$ +jets and other $t\bar{t}$ final states. There are also smaller contributions from single top, $Z(\rightarrow \ell\ell)$ +jets (with one lepton not identified) and multijet processes with one jet misidentified as a lepton. Background templates are derived from the MC simulations in all cases except multijet processes. The multijet background is very difficult to simulate due to the need for a very large sample and the fact that MC models do not reproduce that background well. Instead it is derived from a control data sample with nonisolated electrons and muons, keeping all other selection criteria the same. The distributions of a small expected contribution from $t\bar{t}$ is subtracted from the multijet control sample.

Figure 1 shows the m_{jj} , m_{b1jj} , m_{b2jj} and m_T distributions predicted by MC simulation and normalized to unity for W +jets, Z +jets, and $t\bar{t} \rightarrow \ell$ +jets events. It also shows these distributions for multijet events derived from the control data sample. The distributions from other $t\bar{t}$ channels are not shown as that background is normalized following the MC prediction of the ratio to the number of $t\bar{t} \rightarrow \ell$ +jets events. The figure demonstrates that the shape of all the invariant mass distributions from jets are quite distinct for $t\bar{t} \rightarrow \ell$ +jets while there is very little difference between the various backgrounds. The distributions for $t\bar{t} \rightarrow \ell$ +jets events show that they include top quarks decaying to $b+W$ with the W boson decaying to jets. On the other hand, the m_T distributions show that they include a W boson decaying leptonically in both the $t\bar{t} \rightarrow \ell$ +jets and W +jets channels but cannot discriminate between them. They do show a clear separation between final states with one W boson decaying leptonically and those with little intrinsic E_T^{miss} (Z +jets and multijets).

The background templates for Z +jets events from MC simulation are checked with Z +jets events from data by selecting events with two identified leptons and requiring the dilepton mass to be near the Z mass. Events are required to have two oppositely charged leptons ($p_T^e > 25$ GeV and $p_T^\mu > 20$ GeV), $70 \text{ GeV} < m_{\ell\ell} < 110$ GeV, $E_T^{\text{miss}} > 30$ GeV, and the same jet selections as for the ℓ +jets signal. The only significant background in the control data sample is from the $t\bar{t} \rightarrow \ell\ell'$ +jets channel. Figure 2 shows the m_{jj} , m_{b1jj} and m_{b2jj} distributions after merging ee and $\mu\mu$ events for ALPGEN Z +jets MC simulation

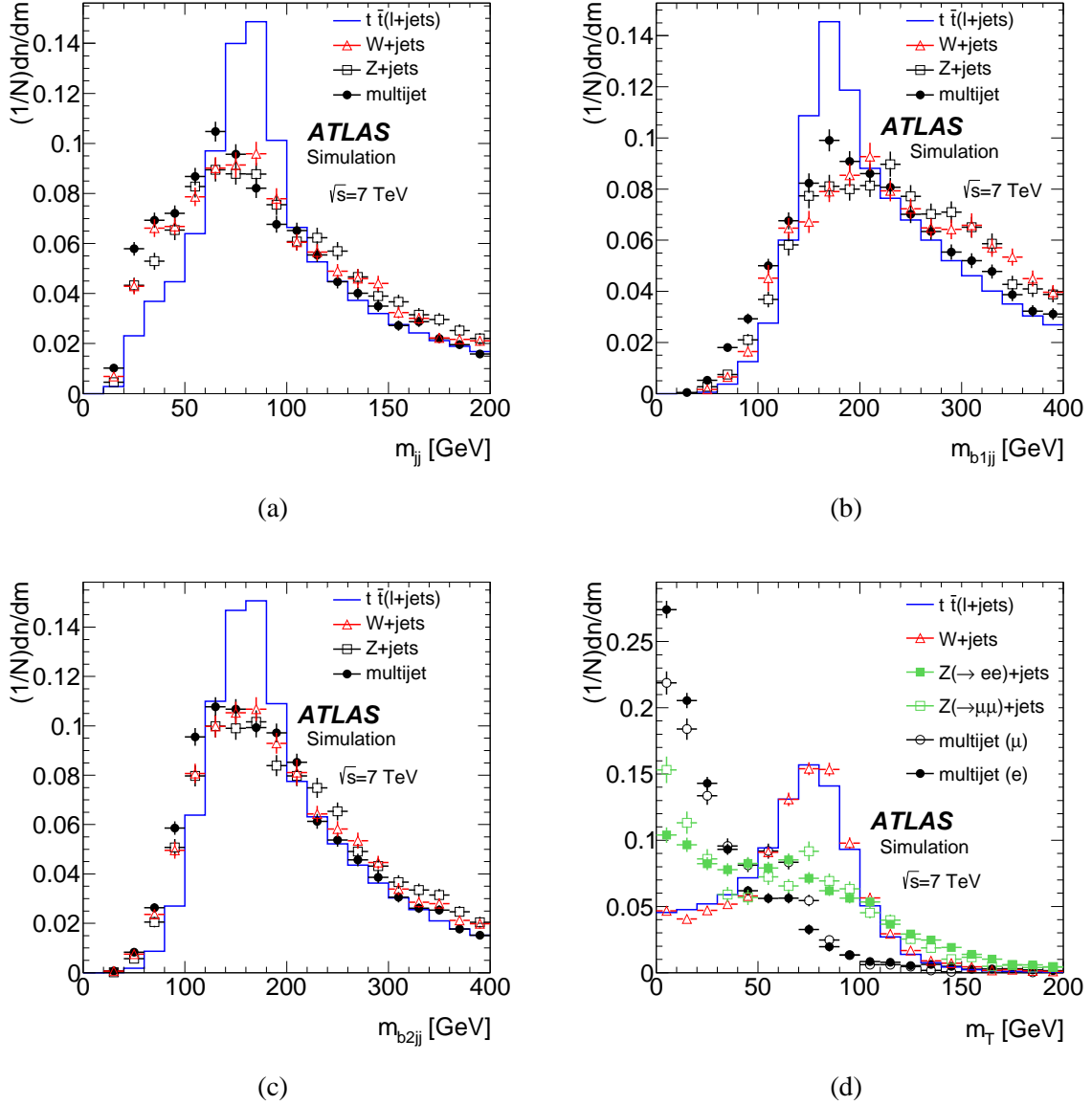


Figure 1: (a) Invariant mass of two highest- p_T jets not designated as b -jets (m_{jj}), (b) and (c) invariant masses of jets designated as b -jets and the jets used for m_{jj} , (m_{b1jj}) and (m_{b2jj}), where $b1$ stands for the leading b -jet and $b2$ for the subleading b -jet, and (d) transverse mass of lepton and E_T^{miss} (m_T). The distributions have been normalized and show distributions for $t\bar{t} \rightarrow \ell+jets$, $Z(\rightarrow \ell\ell)+jets$, $W(\rightarrow \ell\nu)+jets$ MC events and multijet events populating the $\ell+jets$ channels. The e and μ channels have been merged together in the m_{jj} , m_{b1jj} and m_{b2jj} distributions. They are kept separate in the m_T distributions except for $t\bar{t}$ and $W+jets$. Events are required to have exactly one isolated e or μ , $E_T^{\text{miss}} > 30$ GeV, at least four jets, and at least one b -tagged jet.

and the data after applying scale factors (SF) based on comparing data and simulation as a function of the Z boson p_T and the jet multiplicity. The small expected $t\bar{t}$ contribution is subtracted from the data distributions. The Kolmogorov-Smirnov goodness-of-fit test (KS) value in each plot indicates how well

the shape of the data distribution is described by the ALPGEN MC simulation.⁴ Since there is no noticeable difference between the shapes of the W +jets and Z +jets templates, as shown in Fig. 1, one can conclude that both MC templates can reproduce reasonably well the distributions expected in the data. The number of selected Z +jets events is also predicted well by the simulation.

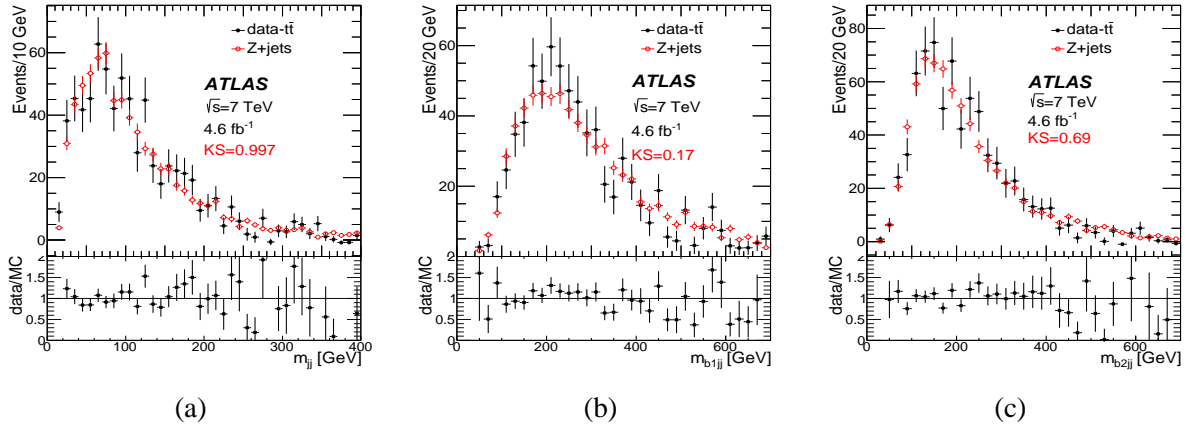


Figure 2: (a) Invariant mass of two highest- p_T jets not designated as b -jets (m_{jj}), (b) and (c) invariant masses of jets designated as b -jets and the jets used for m_{jj} , (m_{b1jj}) and (m_{b2jj}), where $b1$ stands for the leading b -jet and $b2$ for the subleading b -jet, and (d) transverse mass of lepton and E_T^{miss} (m_T). The distributions show ALPGEN MC for a control sample of $Z(\rightarrow \ell\ell)$ +jets events selected by requiring $70 < m_{\ell\ell} < 110$ GeV ($m_{\ell\ell}$ is the invariant mass of the two leptons), $E_T^{\text{miss}} > 30$ GeV, at least four jets, and at least one of them b -tagged, compared to the data after subtracting the expected $t\bar{t}$ contribution. KS is the value of the Kolmogorov-Smirnov goodness-of-fit test.

6.2 Fits to mass distributions

As shown in Sec. 6.1 the three invariant masses constructed from jets do not discriminate between the various backgrounds, while the signal from $t\bar{t}$ is quite distinct. The only distribution that is different for each background is the transverse mass. In particular, the transverse mass clearly distinguishes final states with intrinsic E_T^{miss} , i.e. those with a W boson decaying to a lepton and neutrino, from those where E_T^{miss} is due to mismeasurements. The dominant processes without sizable intrinsic E_T^{miss} are multijet and Z +jets. The transverse mass distributions for those two processes are different. However, they contribute little in $m_T > 40$ GeV so most of the separation comes from the region below 40 GeV. As shown in Fig. 2, the ALPGEN Z +jets simulation predicts the shape and the number of Z +jets events well, so the choice is made to normalize the number of Z +jets events to that predicted by the simulation. The number of single top events is similarly normalized from MC simulation. The amount of multijet background is obtained from the fit to the data using the templates derived from nonisolated lepton samples. The other free parameters are the total number of W +jets events and the total number of $t\bar{t}$ events. The fractional contributions for the various $t\bar{t}$ channels are obtained using MC events. To ensure that events are not used more than once, two sets of data are fitted: $E_T^{\text{miss}} < 30$ GeV (set 1) and $E_T^{\text{miss}} > 30$ GeV (set 2). Set 1 is used to fit the m_T distributions and helps determine the multijet background. Set 2 is used to fit the three jet mass distributions. Both sets are fit simultaneously with three parameters: the total number of multijet events, the total number of W +jets events and the total number of $t\bar{t}$ events.

⁴ KS is calculated with the function supplied by ROOT for comparing the compatibility of two histograms [44].

The variables m_{b1jj} and m_{b2jj} are strongly correlated with m_{jj} . To exploit the fact that the correlations are very different in $t\bar{t}$ and the background, the fits are done simultaneously in $6 \times 6 \times 6$ bins of m_{jj} , m_{b1jj} and m_{b2jj} for a total of 216 bins. Of those, 30 bins have zero events since they are kinematically not possible. The ranges and bin sizes are chosen so that all bins used for fitting are populated by more than 10 events. That limits the range of m_T to $m_T < 120$ GeV, m_{jj} to $m_{jj} < 250$ GeV, m_{b1jj} to $m_{b1jj} < 450$ GeV, and m_{b2jj} to $m_{b2jj} < 450$ GeV.

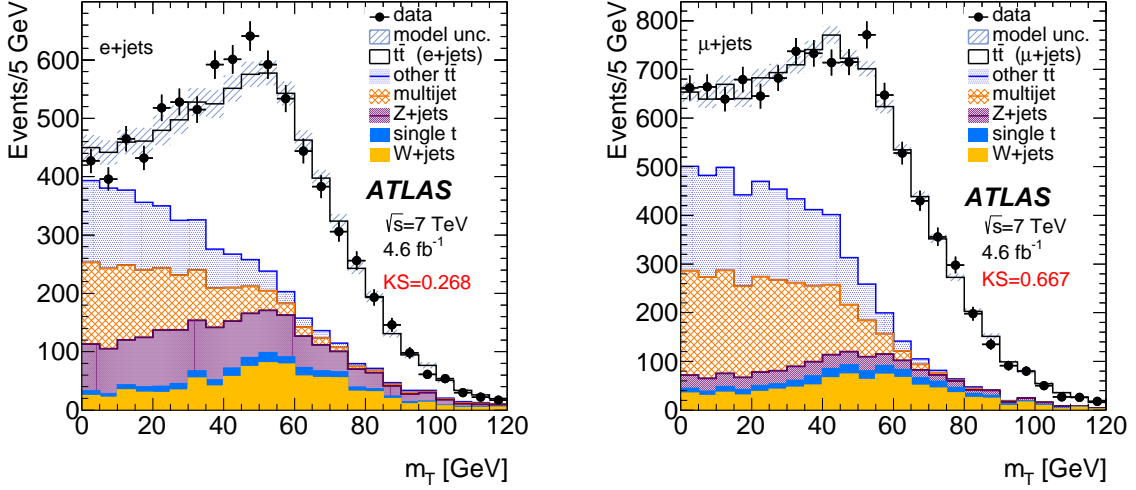


Figure 3: Transverse mass of lepton and E_T^{miss} (m_T) distributions used in the fits. Events are required to have exactly one isolated e or μ , $E_T^{\text{miss}} < 30$ GeV, at least four jets, and at least one b -tag. The model uncertainty (model unc.) is the sum in quadrature of the statistical uncertainties of the templates used in the fits. KS is the value of the Kolmogorov-Smirnov goodness-of-fit test.

The m_T distributions for events with $E_T^{\text{miss}} < 30$ GeV, used in the fits, are shown in Fig. 3. Table 1 shows the predicted contributions from each channel, combining events with $E_T^{\text{miss}} < 30$ GeV and $E_T^{\text{miss}} > 30$ GeV. Figure 4 shows that the fits describe well the full e +jets and μ +jets event distributions of m_{jj} , m_{b1jj} and m_{b2jj} after requiring $E_T^{\text{miss}} > 30$ GeV. Figure 5 shows the m_T distribution for events with $E_T^{\text{miss}} > 30$ GeV compared with the predicted contributions, which agree well with the data.

Noticeable features from these fits are as follows:

- The largest backgrounds originate in W +jets (15%) and other $t\bar{t}$ channels (8.5%); the rest add up to 12% (multijets 5.3%, Z +jets 3.9%, and single top 3.0%).
- The numbers of $t\bar{t}$ and W +jets events obtained by fitting are in good agreement with those predicted by the SM.

Table 1: Results from fitting e +jets and μ +jets mass distributions from ℓ +jets events requiring exactly one isolated lepton (e or μ), at least four jets, and at least one b -tag. The uncertainties quoted here are from the fits and do not include systematic uncertainties. The Z+jets contribution is normalized to the MC expectation. In addition to MC statistical uncertainty, it includes the uncertainty from the scale factors applied to the simulation in order to match the jet multiplicity and the Z boson p_T dependence to that observed in the data. The single top and diboson contributions are normalized to MC predictions, include only MC statistical uncertainty and the SM cross section uncertainty. The (MC) rows give the numbers expected from MC simulation. The χ^2/ndf row gives the χ^2 and degrees of freedom of the fits.

Channel	e +jets	μ +jets
$t\bar{t} \rightarrow \ell$ +jets	19710 \pm 280	25090 \pm 310
(MC)	(18966 \pm 31)	(24233 \pm 34)
$t\bar{t}$ (other)	2674 \pm 30	3393 \pm 30
(MC)	(2577 \pm 11)	(3277 \pm 16)
W +jets	4800 \pm 500	5600 \pm 500
(MC)	(4140 \pm 70)	(5850 \pm 90)
Z+jets (MC)	1900 \pm 500	790 \pm 200
Single top (MC)	910 \pm 70	1170 \pm 80
Diboson (MC)	5.0 \pm 0.2	6.1 \pm 0.2
Multijet	1000 \pm 120	2800 \pm 140
Total background	11333 \pm 700	13700 \pm 600
Signal+background	31000 \pm 800	38800 \pm 700
Data	30733	40414
χ^2/ndf	188/207	218/207

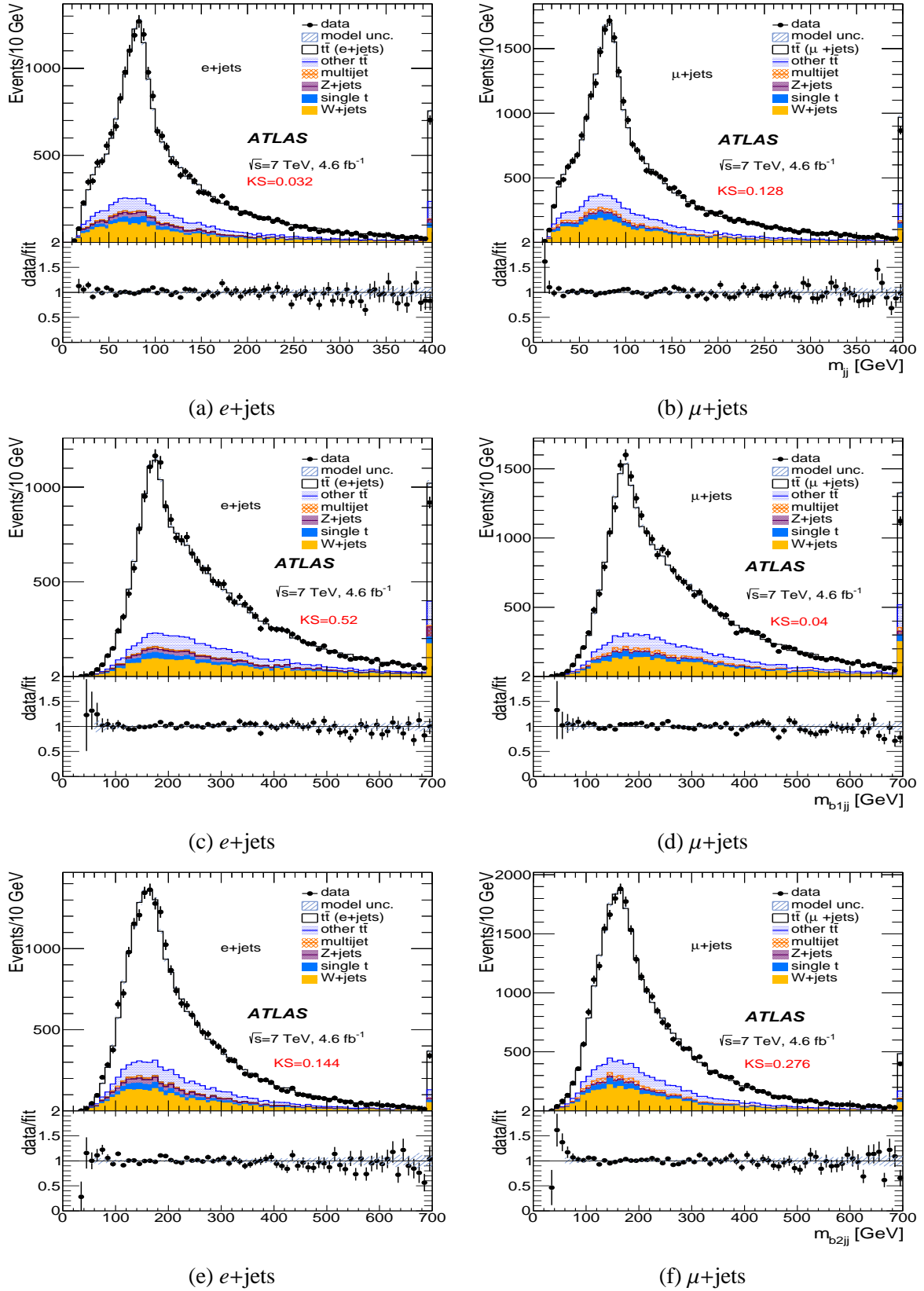


Figure 4: Distributions in data compared to the SM expectations after fitting the following distributions: (a,b) the invariant mass of two highest- p_T jets not designated as b -jets; (c,d) the invariant mass of the leading jet designated as b -jet and the jets used for m_{jj} (m_{b1jj}), and (e,f) the invariant mass of the second jet designated as a b -jet and the two jets used for m_{jj} (m_{b2ij}). The distributions are shown for events with isolated leptons, at least four jets, at least one b -tag, and $E_T^{\text{miss}} > 30$ GeV, with the $e+jets$ and $\mu+jets$ channels separated. The last bin shows the overflow. The ratio plots show the result of dividing the data points by the model expectation. The model uncertainty (model unc.) is the sum in quadrature of the statistical uncertainties of the templates used in the fits. KS is the value of the Kolmogorov-Smirnov goodness-of-fit test.

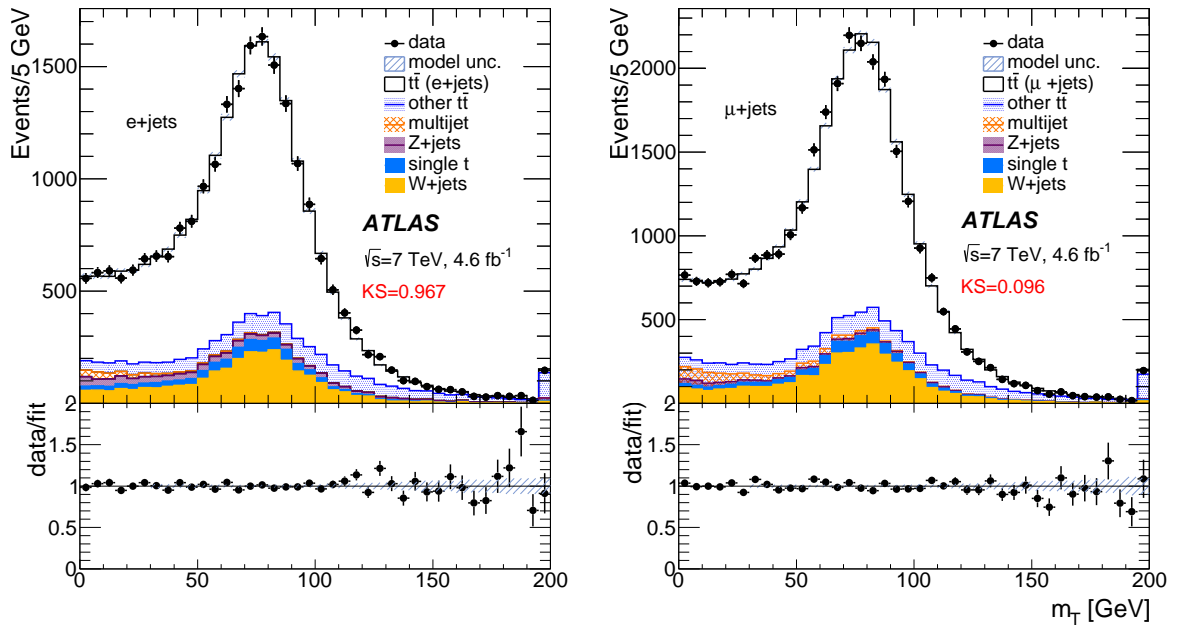


Figure 5: The transverse mass of lepton and E_T^{miss} (m_T) distributions for events with isolated leptons, at least four jets, at least one b -tag and $E_T^{\text{miss}} > 30$ GeV in the e +jets and μ +jets channels. The last bin shows the overflow. The ratio plots show the result of dividing the data points by the model expectation. The model uncertainty (model unc.) is the sum in quadrature of the statistical uncertainties of the templates used in the fits. KS is the value of the Kolmogorov-Smirnov goodness-of-fit test.

7 Dilepton + jets channel

The number of $t\bar{t} \rightarrow \ell\ell'+\text{jets}$ events in the data is extracted by fitting two dilepton invariant mass distributions: one with $30 < E_T^{\text{miss}} < 60$ GeV and the other with $E_T^{\text{miss}} > 60$ GeV. The most significant background to the $t\bar{t} \rightarrow \ell\ell'+\text{jets}$ channels after requiring $E_T^{\text{miss}} > 30$ GeV and at least one b -tagged jet comes from the $Z(\rightarrow \ell\ell')+\text{jets}$, with a smaller contribution from single top production (4%). Since the E_T^{miss} distribution falls more rapidly for the $Z+\text{jets}$ background than for the $t\bar{t}$ signal process separating it into two E_T^{miss} bins improves the sensitivity of the fit for separating the two processes. Backgrounds from dibosons and jets misidentified as isolated leptons (mainly from $W+\text{jets}$ with leptons from heavy-quark semileptonic decays or an isolated charged hadron misidentified as a lepton, together denoted as nonprompt leptons) amount to 1.0% of the events. The background from nonprompt isolated leptons is estimated from the number of data events with lepton pairs with the same charge after subtracting a very small expected contribution from diboson processes. The invariant mass distributions are fitted with three templates: one derived from a $t\bar{t}$ MC sample, one from a $Z+\text{jets}$ MC sample, and one summed over all other contributions. Only the amounts contributed by $t\bar{t}$ and $Z+\text{jets}$ are allowed to vary. The Z boson background in the $e\mu+\text{jets}$ channel from the $Z(\rightarrow \tau\tau \rightarrow e\mu)+X$ channel is too small to be extracted by a fit, so $m_{e\mu}$ is fitted only for the number of $t\bar{t}$ events in the data while the background is fixed. The fits in the $\ell\ell$ channel are performed over a mass range from 40 GeV to 250 GeV and in the $e\mu$ channel over a mass range from 10 GeV to 250 GeV. Figures 6 and 7 show that the $m_{\ell\ell'}$ and E_T^{miss} distributions are well described in all dilepton channels. Results of the fits are given in Table 2.

Table 2: Results from fitting $\ell\ell'$ invariant mass distributions using two E_T^{miss} regions from $\ell\ell'+\text{jets}$ events requiring two isolated leptons (e or μ), $E_T^{\text{miss}} > 30$ GeV, at least two jets, and at least one b -tag. The numbers of events are after summing events from both E_T^{miss} regions $E_T^{\text{miss}} < 60$ GeV and $E_T^{\text{miss}} > 60$ GeV. The uncertainties are from the fits and do not include systematic uncertainties. The single top and diboson contributions are normalized to the SM predictions and include only the MC statistical uncertainty and the uncertainty on the SM cross section. The (MC) rows give the numbers expected from MC simulation.

Channel	$\mu\mu+\text{jets}$	$ee+\text{jets}$	$e\mu+\text{jets}$
$t\bar{t}$	2890± 80	1000±40	2640±50
(MC)	(2536± 11)	(903± 6)	(2420±11)
$Z+\text{jets}$	1380± 50	379±11	13± 4
(MC)	(1267± 8)	(385±11)	(13± 4)
Single top (MC)	86± 8	36± 7	98± 9
Diboson (MC)	22± 1	8.1±0.5	3.3±0.3
Fake leptons	17± 10	17± 8	19±10
Total background	1430± 50	442±15	136±12
Signal+background	4400±100	1440±40	2770±80
Data	4102	1447	2848
χ^2/ndf	35/34	31/34	58/49

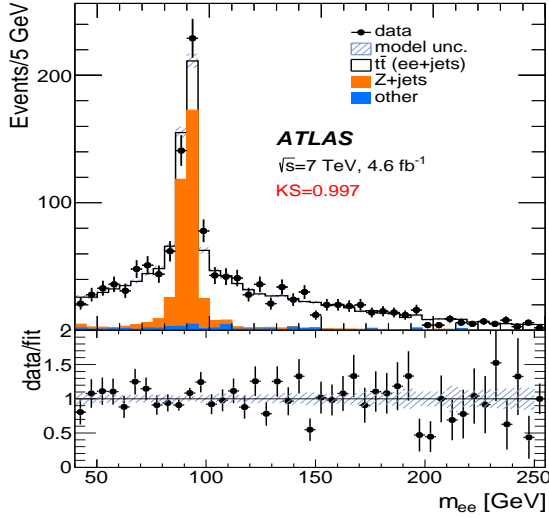
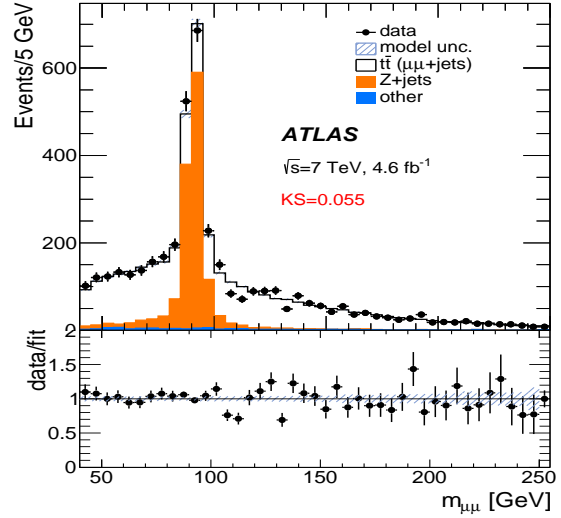
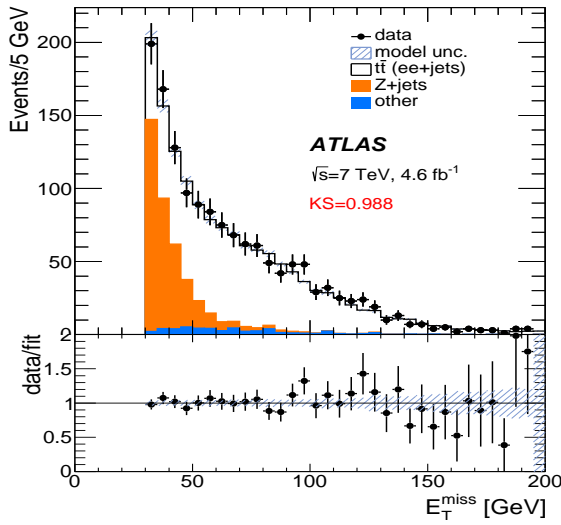
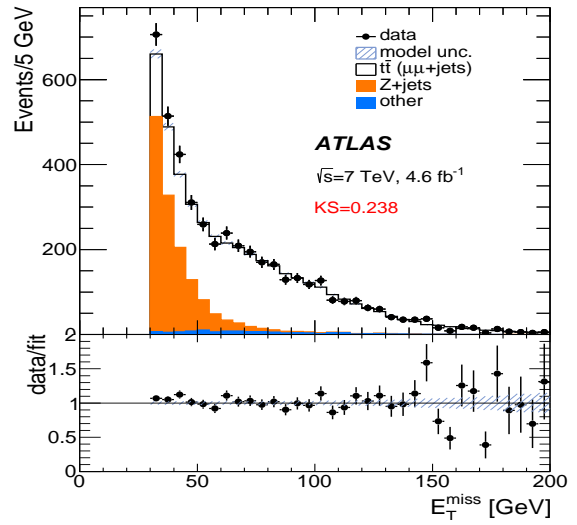
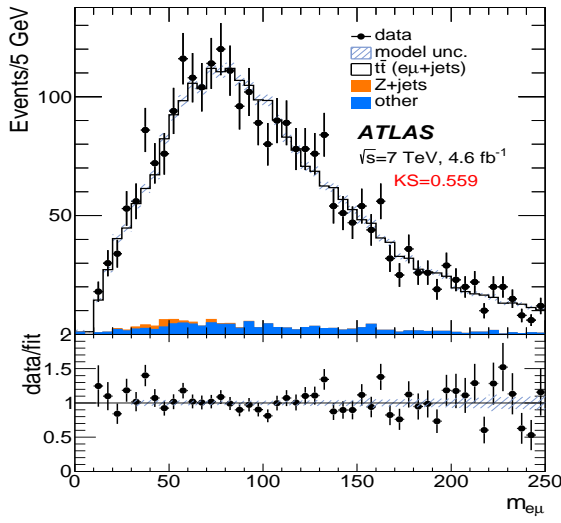
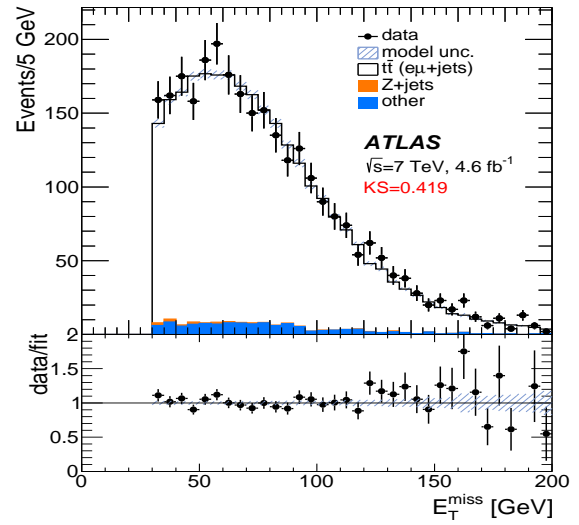
(a) $ee+jets$ (b) $\mu\mu+jets$ (c) $ee+jets$ (d) $\mu\mu+jets$

Figure 6: Dilepton invariant masses (a) m_{ee} , (b) $m_{\mu\mu}$, and E_T^{miss} distributions for events with two isolated leptons, $E_T^{\text{miss}} > 30$ GeV, at least two jets, and at least one b -tag in the (c) $ee+jets$ and (d) $\mu\mu+jets$ channels. The Z+jet entries include a small contribution from $Z \rightarrow \tau^+ \tau^-$ with both τ leptons decaying to e or μ . The ratio plots show the result of dividing the data points by the fit. The model uncertainty (model unc.) is the sum in quadrature of the statistical uncertainties of the templates used in the fits. KS is the value of the Kolmogorov-Smirnov goodness-of-fit test.



(a)



(b)

Figure 7: (a) Invariant mass of electron and muon ($m_{e\mu}$) and (b) E_T^{miss} distributions for $e\mu$ events after requiring one isolated e and one isolated μ , $E_T^{\text{miss}} > 30$ GeV, at least two jets, and at least one b -tag. The ratio plots show the result of dividing the data points by the fit. The model uncertainty (model unc.) is the sum in quadrature of the statistical uncertainties of the templates used in the fits. KS is the value of the Kolmogorov-Smirnov goodness-of-fit test.

8 Lepton+ τ_{had} +jets channel

Unlike the single-lepton + jets and dilepton channels the background in the $\ell\tau_{\text{had}}$ +jets channel is not small and is dominated by contributions from other $t\bar{t}$ channels. Thus, invariant masses and other kinematic variables are not sufficiently sensitive to separate signal and background. In this case a BDT multivariate discriminant, named BDT_j , is used to separate τ leptons from jets identified as τ candidates (see Sec. 5). Compared to the previous ATLAS measurement with this channel [13], the present analysis uses only one-prong τ decays and is based on a larger data sample with a different background model to reduce the statistical uncertainty on the background prediction.

8.1 Tau background templates

In order to separate the contribution of processes with τ leptons (signal) from those with jets misidentified as τ (fake τ) the BDT_j distributions of selected events are fitted with templates for fake τ distributions derived from data and true τ lepton distributions derived from MC simulation. Control data samples to obtain templates of jets misidentified as τ candidates are selected with the following requirements:

- exactly one isolated electron with $p_{\text{T}}^e > 25$ GeV and no identified muons for the $e + \tau$ channel;
- or exactly one isolated muon with $p_{\text{T}}^\mu > 20$ GeV and no identified electrons for the $\mu + \tau$ channel;
- and no additional muons with $p_{\text{T}} > 4$ GeV;
- and $40 \text{ GeV} < m_{\text{T}}(\ell, E_{\text{T}}^{\text{miss}}) < 100 \text{ GeV}$;
- and exactly one τ candidate and at most one additional jet.

There are two mutually exclusive control samples:

The $W+1$ -jet sample contains a lepton, one jet misidentified as a τ candidate and no additional jets. The $W+2$ -jets sample contains a lepton and exactly two jets with the lower p_{T} jet misidentified as a τ candidate.

The control samples are divided into two subsamples, one with τ and ℓ having the opposite-sign charges (OS), and the other with τ and ℓ having the same-sign charges (SS). The $W + 1$ -jet sample is rich in jets originating from quark hadronization (quark jets) while the $W + 2$ -jets sample has a high percentage of jets originating from gluon hadronization (gluon jets) as determined from MC studies. One can extract the distributions of gluon jets misidentified as τ candidates since the number of gluon jets in OS and SS samples must be the same because they are not correlated with the charge of the lepton. Fake τ template shapes depend on the jet type. Those from light-quark jets peak at higher BDT_j values than those from gluon jets. The signal contributes only to OS events. Therefore, the BDT_j distributions of OS events are fitted with a pair of background templates, whose linear combination equals the sum of the OS light-quark and gluon jets identified as τ candidates, and a signal τ template. MC studies show that requiring τ candidates that have only one associated charged particle strongly suppresses jets originating from heavy quarks (c -jets, b -jets). The b -jets are further suppressed by excluding τ candidates that are tagged as b -jets. The BDT_j template from remaining c -jets identified as τ candidates is similar to the light-quark template. The signal template is constructed by summing the expected contribution of any channel that has a real τ lepton or a lepton misidentified as a τ lepton.

In the $W + 2$ -jets sample the lower- p_T jet has a high probability of coming from final- or initial-state radiation and thus a high probability of being a gluon jet. In the following, OS1 (SS1) stands for the τ fake BDT_j distribution obtained from OS (SS) $W + 1$ -jet data sets and OS2 (SS2) represent the equivalent distribution for $W + 2$ -jets. Figures 8(a) and 8(b) show the OS and OS-SS distributions normalized to compare the shapes. It can be seen that there are significant differences between OS1 and OS2, but if one subtracts the SS distribution from the OS distribution (OS-SS) the shapes are in good agreement. The distributions are a sum of light-quark jets and gluon jets, and can be described by the following equations:

$$\text{OS1} = a_1 \cdot \text{OS}_q + b_1 \cdot G, \quad (1)$$

$$\text{SS1} = c_1 \cdot \text{SS}_q + b_1 \cdot G, \quad (2)$$

$$\text{OS2} = a_2 \cdot \text{OS}_q + b_2 \cdot G, \quad (3)$$

$$\text{SS2} = c_2 \cdot \text{SS}_q + b_2 \cdot G, \quad (4)$$

where OS_q (SS_q) is a function describing the shape of the distribution of light-quark jets contributing to OS (SS) and G is the corresponding function for gluon jets. The observation that the OS1–SS1 and OS2–SS2 distributions have the same shape leads to the conclusion that $a_1/c_1 = a_2/c_2$ for any E_T as the E_T of τ candidates from $W + 2$ -jets are significantly lower than those from $W + 1$ -jet. Using the above equations, one can extract the G function from the OS and SS distributions separately, i.e.

$$K \cdot G = (R \cdot \text{OS2} - \text{OS1}), \quad (5)$$

$$K \cdot G = (R \cdot \text{SS2} - \text{SS1}), \quad (6)$$

where R is the ratio of the total number of OS1–SS1 events to OS2–SS2 events and $K = R \cdot b_2 - b_1$ is an unknown constant that must be the same whether SS or OS is used to extract G . Figure 8(c) shows the extracted $K \cdot G$ distributions for τ candidates. It is seen that the OS and SS distributions are fully consistent with each other and can be summed to reduce the statistical uncertainties.

In principle any background BDT_j distribution can be described by a linear combination of G and OS1 distributions. Furthermore, the BDT_j distributions depend on E_T of the τ candidates, which differs from sample to sample. The E_T dependence of the BDT_j is taken into account by fitting separate E_T regions with templates derived for those regions weighted to reproduce the E_T distributions of the expected background. The OS1 sample has a small (2%) number of τ leptons from dibosons and $Z \rightarrow \tau^+ \tau^-$ final states that have no impact on the fits to $\ell\tau_{\text{had}} + \text{jets}$ BDT_j data distributions whether or not they are subtracted from the OS1 template.

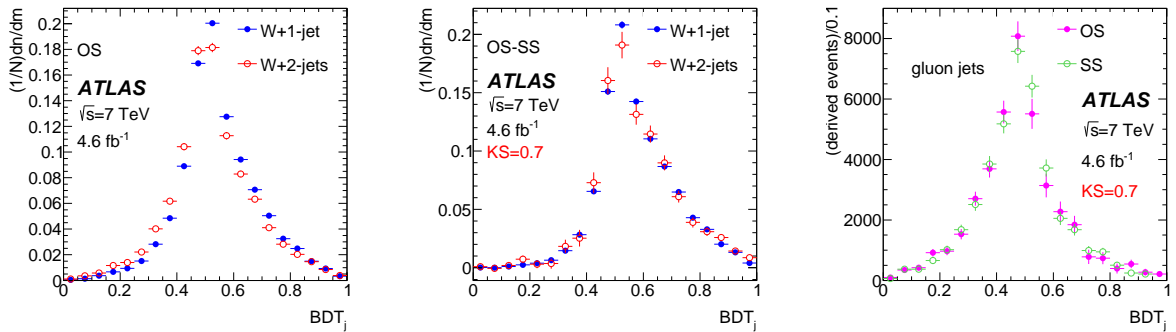


Figure 8: Normalized distributions of the output of the boosted decision tree used to discriminate τ leptons from jets misidentified as τ s, BDT_j , for τ candidates from $W + 1\text{-jet}$ and $W + 2\text{-jets}$ samples for leptons with opposite sign (OS), the distribution of opposite-sign leptons with the same-sign lepton distribution subtracted (OS–SS), and the extracted BDT_j distributions ($K \cdot G$, see text) for gluon jets misidentified as τ candidates is shown.

8.2 Signal extraction by fitting to BDT_j shape

The final background normalization and signal measurement are established through fitting templates to the data. There are various classes of background:

1. from processes with an isolated ℓ where a jet is misidentified as a τ candidate;
2. from processes other than $t\bar{t}$ that have τ leptons and an isolated ℓ ;
3. from processes with two isolated ℓ where one ℓ is misidentified as a τ candidate;
4. from multijet processes where both ℓ and τ are from one jet misidentified as an isolated ℓ and another as a τ candidate.

The dominant background to the $t\bar{t} \rightarrow \ell\tau_{\text{had}}+\text{jets}$ channel comes from the $t\bar{t} \rightarrow \ell+\text{jets}$ channel with one jet misidentified as a τ candidate (class 1). The only powerful suppression technique for that background is τ identification, thus the best variable is the BDT_j score, described with the τ candidate selection in Sec. 5. Background of classes 1 and 4 is taken into account using templates consisting of light-quark jet τ fakes and gluon jet τ fakes derived from enriched $W+\text{jets}$ data samples as described in Sec. 8.1.

The signal BDT_j template is derived from MC τ candidates that are matched to a τ lepton or a lepton from MC events that satisfy the event selection (classes 2 and 3). The class 2 processes contributing to the signal template are: $t\bar{t} \rightarrow \ell\tau+\text{jets}$, $Z(\rightarrow \tau^+\tau^-)+\text{jets}$, and small contributions from single top and diboson events. The main backgrounds of class 3 are $Z \rightarrow e^+e^-$ and $t\bar{t}$ events. Most electrons are removed by the BDT_e cut (see Sec. 5); the few that remain are indistinguishable from τ leptons. There is an even smaller number of muons overlapping with τ candidates that are not removed by the muon veto and are also indistinguishable from τ leptons. In these cases, the τ candidates are added to the signal template. The efficiency for electrons and muons misidentified as τ candidates is determined by studying $Z \rightarrow \ell^+\ell^-$ events. Based on these studies the estimated contribution from class 3 background to the signal template is 2.8%. The total contribution from class 2 and class 3 backgrounds ($Z+\text{jets}$, $t\bar{t} \rightarrow \ell\ell+\text{jets}$, single top and dibosons) to the signal template is 15%. Table 3 shows the detailed composition of the signal templates.

Table 3: Composition of signal template: all events from MC simulation with a true τ , e or μ matched to the τ candidate. The number of events are normalized to the number expected from simulation. Regions 1 and 2 are $20 \text{ GeV} \leq E_T^r \leq 35 \text{ GeV}$ and $35 \text{ GeV} \leq E_T^r \leq 100 \text{ GeV}$ respectively. The uncertainties represent the statistical uncertainties of the MC samples.

Channel	Region 1	Region 2
$t\bar{t} \rightarrow \ell\tau_{\text{had}}+\text{jets}$	611.5 ± 5.4	621.4 ± 5.4
$t\bar{t} \rightarrow \ell\ell+\text{jets}$	13.0 ± 0.7	13.0 ± 0.7
$Z + \text{jets}$	54.5 ± 3.3	45.3 ± 3.0
Single top	23.6 ± 2.3	27.1 ± 2.4
Dibosons	1.5 ± 0.2	2.2 ± 0.3
Total	705.2 ± 6.8	709.5 ± 6.8

With these background templates and MC signal template (S), a χ^2 fit is performed with parameters to set the normalization of each template: $a \cdot \text{OS1} + b \cdot G + c \cdot S$. The combined e and μ channel results are obtained by fitting to the sum of the distributions. Comparisons of the template shapes of the e and μ channel show they are identical within the uncertainties.

Two different E_T regions, $20 \text{ GeV} \leq E_T^r \leq 35 \text{ GeV}$ and $35 \text{ GeV} \leq E_T^r \leq 100 \text{ GeV}$, are chosen such that each region has the same number of expected signal events. Three parameters are used to fit both regions simultaneously: the fraction of τ candidates in each E_T region that are gluon jets and the total fraction of signal. In the fit the sum of signal and background must add up to the number of observed events in each E_T region and the amount of signal in the two regions is constrained by the ratio predicted from MC simulation.

8.3 Fit results

The three-parameter fit was applied to MC samples to establish whether it can extract the known signal without bias. The MC samples are made with events from $t\bar{t}$, $W+\text{jets}$, $Z+\text{jets}$, single top and diboson final states satisfying the data selection criteria. The MC samples were split into two, one used as the data to fit and the other to generate the templates for the fit. Figure 9 shows these MC fit results after correcting the background templates derived from $W+\text{jets}$ to account for the different E_T distribution of the τ candidates in the expected background to $t\bar{t} \rightarrow \ell\tau_{\text{had}}+\text{jets}$. The model uncertainty shown in Figure 9 corresponds to the uncertainty of the templates in the fits to the data and used for ensemble tests. The ensemble tests show that no bias is introduced by the fitting procedure. The μ and e channels are combined by adding together the distributions of both channels. The data BDT_j distributions can have multiple entries for an event as all τ candidates are considered. This has no impact on the $t\bar{t} \rightarrow \ell\tau_{\text{had}}+\text{jets}$ signal as there is only one τ lepton decaying to hadrons in that channel.

The results of fitting the data are summarized in Table 4. N_S^{Fitted} is the number of signal template events. $N_{t\bar{t}}^{\text{Fitted}}$ is the number of observed $t\bar{t} \rightarrow \ell\tau+\text{jets}$ events, obtained by subtracting the contributions from class 2 and class 3 backgrounds (see Sec. 8.2) from N_S^{Fitted} . The number of expected ($N_{t\bar{t}}^{\text{MC}}$) is in good

agreement with $N_{\bar{t}t}^{\text{Fitted}}$. Figure 10 shows the final results using these μ and e channel combined templates.

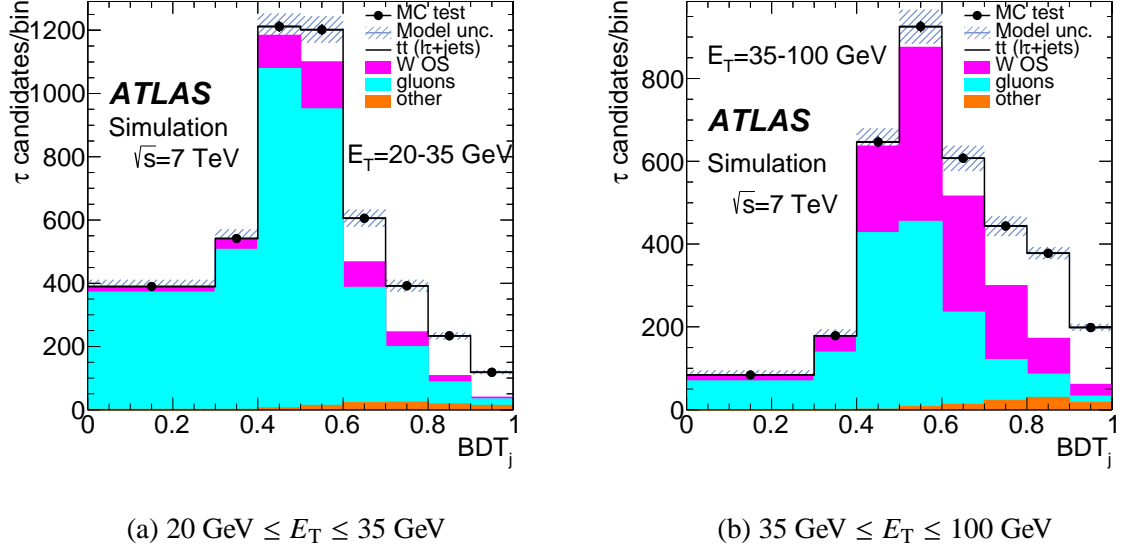


Figure 9: Fitted distributions of the τ -jet discriminant BDT_j MC using corrected background templates for two E_T regions. The model uncertainty is the uncertainty of the templates used in the fits to the data.

Table 4: Numbers of events expected from MC simulation and fit results to the BDT_j distribution using background and signal templates as described in Sec. 8.1. $N_{\bar{t}t}^{\text{MC}}$ is the expected number of $\bar{t}t \rightarrow \ell\tau_{\text{had}}+\text{jets}$ events for a cross section of 177 pb. $B_{\text{non } \bar{t}t \tau}$ is the number of τ leptons expected from sources other than $\bar{t}t \rightarrow \ell\tau_{\text{had}}+\text{jets}$. B_{lepton} is the expected number of leptons misidentified as τ leptons. N_S^{Fitted} is the number of events extracted with the signal template (S , see text) and $N_{\bar{t}t}^{\text{Fitted}} = N_S^{\text{Fitted}} - B_{\text{non } \bar{t}t \tau} - B_{\text{lepton}}$

	$N_{\bar{t}t}^{\text{MC}}$	$B_{\text{non } \bar{t}t \tau}$	B_{lepton}	N_S^{Fitted}	$N_{\bar{t}t}^{\text{Fitted}}$
$20 < E_T^\tau < 35 \text{ GeV}$	611 ± 5	76.2 ± 3.5	17.1 ± 1.1	N/A	N/A
$35 < E_T^\tau < 100 \text{ GeV}$	621 ± 5	69.5 ± 3.3	17.6 ± 1.1	N/A	N/A
Combined E_T^τ bins	1232 ± 8	146 ± 5	34.8 ± 1.5	1460 ± 60 ($\chi^2/\text{ndf} = 0.69$)	1280 ± 60

Jets misidentified as τ leptons come mostly from $\bar{t}t \rightarrow \ell+\text{jets}$ and from $W+\text{jets}$. Thus the m_T distributions should show a Jacobian peak from a W decay. The $\bar{t}t \rightarrow \ell\tau_{\text{had}}+\text{jets}$ events have additional neutrinos, which produce a broader m_T distribution. Figure 11 shows the distributions from events selected with $\text{BDT}_j < 0.6$, which are mostly background, and for events selected with $\text{BDT}_j > 0.7$ where the ratio of signal to all background is 2:1. The plots include the predicted distributions using the normalizations based on the fits to the BDT_j distributions. The amount of $Z \rightarrow \tau\tau$ is normalized to the MC prediction. The data are well reproduced in all cases.

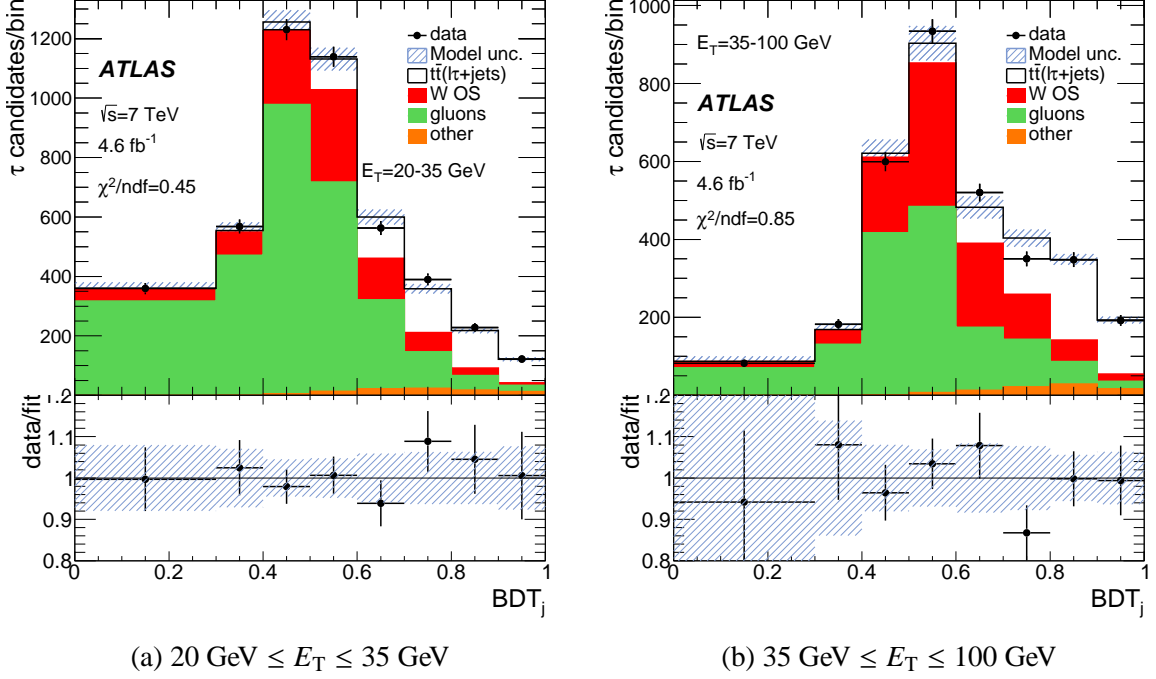


Figure 10: Fitted distributions of the τ -jet discriminant BDT_j in data using corrected background templates for (a) $20 \text{ GeV} \leq E_T \leq 35 \text{ GeV}$ and (b) $35 \text{ GeV} \leq E_T \leq 100 \text{ GeV}$. The model uncertainty is the statistical uncertainty of the templates used in the fits.

9 Measuring Cross Section and Branching Ratios

In the SM 100% of the top quark decays have one W boson and a quark. Therefore the top quark branching ratios into channels with leptons and jets are determined by the W decay branching ratios that have been measured with 0.3% precision (assuming lepton universality) [15] and are predicted by the SM with an uncertainty of order 0.1%. It is possible to derive the branching ratios into all decay modes using the number of $t\bar{t}$ events extracted in the previous sections assuming that the top quark branching ratios to leptons and jets add up to 100%. Any deviation from the W branching ratios would be an indication of some process not predicted by the SM. The following observed quantities are defined (where $\mathcal{A}_{ch} \cdot \epsilon_{ch}$ is the geometric detector acceptance times the efficiency of channel ch):

- $N_{\mu j} = (\text{observed number of } t\bar{t} \rightarrow \mu + \text{jets}) / \mathcal{A}_{\mu j} \cdot \epsilon_{\mu j}$,
- $N_{ej} = (\text{observed number of } t\bar{t} \rightarrow e + \text{jets}) / \mathcal{A}_{ej} \cdot \epsilon_{ej}$,
- $N_{\mu\mu} = (\text{observed number of } t\bar{t} \rightarrow \mu + \mu + \text{jets}) / \mathcal{A}_{\mu\mu} \cdot \epsilon_{\mu\mu}$,
- $N_{ee} = (\text{observed number of } t\bar{t} \rightarrow e + e + \text{jets}) / \mathcal{A}_{ee} \cdot \epsilon_{ee}$,
- $N_{e\mu} = (\text{observed number of } t\bar{t} \rightarrow e + \mu + \text{jets}) / \mathcal{A}_{e\mu} \cdot \epsilon_{e\mu}$,
- $N_{\ell\tau} = (\text{observed number of } t\bar{t} \rightarrow \ell + \tau_{\text{had}} + \text{jets}) / \mathcal{A}_{\ell\tau} \cdot \epsilon_{\ell\tau}$,
- $N_{\ell j} = N_{\mu j} + N_{ej}$,

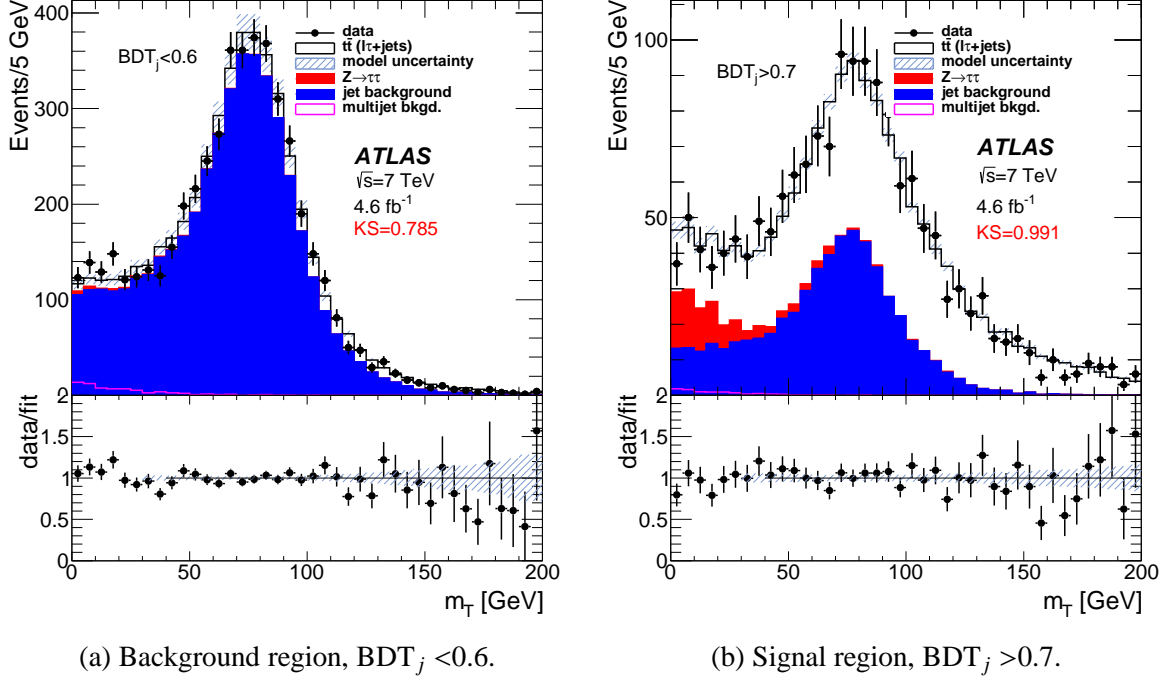


Figure 11: Transverse mass distributions (m_T) of $t\bar{t} \rightarrow \ell\tau_{\text{had}}+\text{jets}$ events. The black points are data, the solid histograms the prediction based on the fits to the BDT_j distributions. The jet background is the sum of all channels with jets misidentified as τ candidates normalized to the amount obtained from the fits to BDT_j distributions. The multijet background is the estimated contribution from non- $t\bar{t}$ multijet processes and is included in the jet background. The model uncertainty is the statistical uncertainty of the templates used in the fits. KS is the value of the Kolmogorov-Smirnov goodness-of-fit test.

- $N_{\ell\ell} = N_{\mu\mu} + N_{ee} + N_{e\mu}$.

The following notation is used for the top quark branching ratios:

- B_μ : top quark branching ratio to $\mu\nu_\mu(\nu_\tau) + X$,
- B_e : top quark branching ratio to $e\nu_e(\nu_\tau) + X$,
- B_τ : top quark branching ratio to $\tau\nu_\tau + X$, with the τ lepton decaying hadronically
- B_j : top quark branching ratio to jets,
- B_ℓ : $B_\mu + B_e$.

The branching ratios B_μ and B_e include events with leptonic τ decays.

With these definitions the following relations hold:

$$N_{\ell j} = 2\sigma_{t\bar{t}} \cdot B_\ell \cdot B_j \cdot \mathcal{L}, \quad (7)$$

$$N_{\ell\ell} = \sigma_{t\bar{t}} \cdot B_\ell^2 \cdot \mathcal{L}, \quad (8)$$

$$N_{\ell\tau} = 2\sigma_{t\bar{t}} \cdot B_\ell \cdot B_\tau \cdot \mathcal{L}, \quad (9)$$

$$B_j + B_\ell + B_\tau = 1, \quad (10)$$

where $\sigma_{t\bar{t}}$ is the cross section for $t\bar{t}$ pair production and \mathcal{L} is the integrated luminosity. These four equations with four unknowns can be solved to obtain:

$$B_j = N_{\ell j}/(N_{\ell j} + 2N_{\ell\ell} + N_{\ell\tau}), \quad (11)$$

$$B_\ell = 2N_{\ell\ell}/(N_{\ell j} + 2N_{\ell\ell} + N_{\ell\tau}), \quad (12)$$

$$B_\tau = N_{\ell\tau}/(N_{\ell j} + 2N_{\ell\ell} + N_{\ell\tau}), \quad (13)$$

$$\sigma_{t\bar{t}} \cdot \mathcal{L} = (N_{\ell j} + 2N_{\ell\ell} + N_{\ell\tau})^2/4N_{\ell\ell}. \quad (14)$$

From the numbers of $t\bar{t}$ events given in Tables 1–4 and the acceptances given in Table 5 the values are obtained for $N_{\ell x}$ and given in Table 6. The $N_{\ell x}$ are in units of events/pb⁻¹.

After solving for B_ℓ one can solve for B_e and B_μ using ratios in the dilepton and the single-lepton channel:

$$B_{\mu(e)} = 2N_{\mu\mu(ee)} \cdot B_j/N_{\mu(e)j} \equiv a, \quad (15)$$

$$B_{\mu(e)} = B_\ell \cdot \sqrt{N_{\mu\mu(ee)}/N_{\ell\ell}} \equiv b. \quad (16)$$

The best values are obtained by minimizing

$$\chi^2 = ([B_{\mu(e)} - a]/\delta a)^2 + ([B_{\mu(e)} - b]/\delta b)^2, \quad (17)$$

where δa and δb are the a and b uncertainties.

Table 5: The acceptance \times efficiency ($\mathcal{A}_{ch} \cdot \epsilon_{ch}$) of each channel used to extract the number of $t\bar{t}$ events after all selections. The $\mathcal{A}_{ch} \cdot \epsilon_{ch}$ are calculated by taking the ratio of fully reconstructed MC events to MC generated events. The uncertainties represent the statistical uncertainties of the MC samples.

	e +jets	μ +jets	ee +jets	$\mu\mu$ +jets	$e\mu$ +jets	$\ell\tau$ +jets
$\mathcal{A}_{ch} \cdot \epsilon_{ch}(\%)$	14.02±0.02	17.88±0.02	7.09±0.04	19.74±0.08	9.50±0.04	4.36±0.02

Table 6: Measured number of events/ pb^{-1} for each channel and the number predicted by the SM. Data uncertainties are statistical only. The SM uncertainty is calculated using the theoretical uncertainty of the NNLO+NNLL calculation of the cross section.

	N_{ej}	$N_{\mu j}$	N_{ee}	$N_{\mu\mu}$	$N_{e\mu}$	$N_{\ell\tau}$
	$N_{\ell j}$		$N_{\ell\ell}$			
Measured	30.62 ± 0.26	30.57 ± 0.29	3.06 ± 0.12	3.19 ± 0.10	6.06 ± 0.12	6.39 ± 0.30
	61.19 ± 0.40		12.31 ± 0.20			
SM	30.40 ± 1.2	30.40 ± 1.2	2.86 ± 0.11	2.86 ± 0.11	5.72 ± 0.20	6.39 ± 0.25
	60.64 ± 2.4		10.95 ± 0.44			

10 Systematic Uncertainties

Several sources of experimental and theoretical systematic uncertainty are considered. Lepton trigger, reconstruction and selection efficiencies are assessed in data and MC simulation by comparing the $Z \rightarrow \ell^+ \ell^-$ events selected with the same object criteria as used for the $t\bar{t}$ analyses. Scale factors are applied to MC samples when calculating acceptances to account for any differences between predicted and observed efficiencies. The scale factors are evaluated by comparing the observed efficiencies with those determined with simulated Z boson events. Systematic uncertainties on these scale factors are evaluated by varying the selection of events used in the efficiency measurements and by checking the stability of the measurements over the course of data taking. The modeling of the lepton momentum scale and resolution is studied with reconstructed invariant mass distributions of $Z \rightarrow \ell^+ \ell^-$ candidate events, and these distributions are used to adjust the simulation accordingly [36, 37].

The jet energy scale (JES), jet energy resolution (JER), and their uncertainties are derived by combining information from test-beam data, LHC collision data and simulation. For jets within the acceptance, the JES uncertainty varies in the range 4%–8% as a function of jet p_T and η [39]. The b -tagging efficiency and its uncertainty is determined using a sample of jets containing muons [40]. The effect of all these variations on the final result is evaluated by varying each source of systematic uncertainty by $\pm 1\sigma$ in the MC-derived templates and fitting all the distributions with the new templates.

The uncertainty in the kinematic distributions of the $t\bar{t}$ signal events gives rise to systematic uncertainties in the signal acceptance, with contributions from the choice of generator, the modeling of initial- and final-state radiation (ISR/FSR) and the choice of PDF set. The generator uncertainty is evaluated by comparing the MC@NLO and ALPGEN [29] predictions with those of POWHEG [20] interfaced to either HERWIG or PYTHIA. The PDF uncertainty is evaluated following the PDF4LHC recommendation [45]. An event-by-event weighting is applied to a default MC@NLO sample that uses the central value of CT10 [28], MSTW2008 [46] and NNPDF2.0 [47, 48] sets are taken to estimate the systematic uncertainty due to the PDF. The uncertainty due to ISR/FSR is evaluated using the ALPGEN generator interfaced to the PYTHIA shower model, and by varying the parameters controlling ISR and FSR in a range consistent with experimental data [49]. The dominant uncertainty in this category of systematic uncertainties is the modeling of ISR/FSR. In addition there is an uncertainty in the W +jets MC simulation due to the uncertainty in the heavy flavor component of the jets. The systematic uncertainty from single top MC simulation has a negligible impact on the overall systematic uncertainty.

The τ identification uncertainty is derived from a template fit to the BDT_j distribution from an enriched $Z \rightarrow \tau^+\tau^-$ data sample selected with the same μ and τ candidate requirements as the sample for this analysis, but with fewer than two jets and $m_T < 20$ GeV to remove W +jets events. The background templates are the W +1-jet OS and the gluon template used in the fit to the $t\bar{t}$ data sample. The signal template is the BDT_j distribution from $Z \rightarrow \tau^+\tau^-$ MC events. The uncertainty includes the statistical uncertainty of the data samples, the uncertainty in the Z inclusive cross section measured by ATLAS [50] (excluding luminosity uncertainty) and jet energy scale uncertainty. The signal template shape uncertainty, estimated from fits to the $Z \rightarrow \tau^+\tau^-$ data sample, is found to be negligible. The uncertainty on the number of misidentified electrons ($< 0.5\%$), determined from an enriched $Z \rightarrow e^+e^-$ data sample, is included. In addition there is an uncertainty in the correction applied to the τ background templates derived from W +jets data to account for the different E_T distribution of the τ candidates in the expected background to $t\bar{t} \rightarrow \ell\tau_{\text{had}}+\text{jets}$.

The calculated systematic uncertainties for the inclusive cross section measured with the $\ell\tau_{\text{had}}+\text{jet}$ channel are given in Table 7. Table 8 gives the systematic uncertainties estimated when combining all channels. The uncertainty on the measured integrated luminosity is estimated to be 1.8% [51]. As expected the systematic uncertainties are substantially larger in the measurement of the cross section based on the $\ell\tau_{\text{had}}+\text{jets}$ channel alone than in the combination of all channels. The largest uncertainty in the combined cross-section measurement and in the branching ratio measurements is due to the JES uncertainty, followed by the MC generator and the uncertainty in the heavy-flavor component of W +jets. The uncertainties on the measured branching ratios are significantly smaller than on the measured inclusive cross section, as expected due to cancellations. B_τ has a larger systematic uncertainty than the other branching ratios due to uncertainties on τ identification that do not cancel in the ratios.

Table 7: Absolute systematic uncertainties, in pb, for the cross-section measurements with the $t\bar{t} \rightarrow \ell\tau_{\text{had}}+\text{jets}$ channel. The e and μ uncertainties are the sum in quadrature of trigger, reconstruction and selection efficiency uncertainties. The τ identification uncertainty includes electrons misidentified as τ leptons.

	Absolute uncertainties [pb]
μ uncertainty	1.7
e uncertainty	3.0
Jet energy scale	-5.5 / +6.8
Jet energy resolution	1.5
ISR/FSR	12.3
MC generator	10.1
PDF	0.6
b -tag	-8.3 / +10.0
τ identification	8.0
τ background correction	5.6
Total	-22/+23
Luminosity	3.3

Table 8: Relative systematic uncertainties (%) for cross section and branching ratio measurements. The systematic uncertainties for B_e and B_μ (not shown) are 100% correlated with the B_ℓ uncertainties and of the same size. The e and μ uncertainties are the sum in quadrature of trigger, reconstruction and selection efficiency uncertainties. The MC generator uncertainty is the difference between POWHEG interfaced with PYTHIA and ALPGEN interfaced with HERWIG. HF stands for heavy-flavor.

	$\sigma_{\bar{t}t}$	B_j	B_ℓ	B_τ
μ uncertainty	1.3	0.15	0.6	0.5
e uncertainty	1.1	0.15	0.5	0.5
Jet energy scale	-6.9/ + 4.9	-1.6/ + 1.4	-1.9/ + 2.7	-3.8/ + 4.3
Jet energy resolution	1.2	0.3	0.8	0.7
ISR/FSR	2.0	0.3	1.3	4.0
MC generator	3.6	0.6	0.8	1.9
PDF	2.9	0.3	0.1	0.3
b -tag	-1.3/ + 5.0	0.3	1.0	1.5
τ identification	0.5	0.15	1.1	3.5
τ background correction	0.2	<0.1	<0.1	2.5
W +jets HF content	-4.1/ + 2.7	-1.0/ + 0.7	-1.1/ + 2.3	-1.3/ + 2.1
Total	-9.7/ + 9.2	-2.1/ + 1.8	-3.4/ + 4.2	-7.1/ + 7.6
Luminosity	1.8	<0.1	<0.1	<0.1

11 Results

The inclusive $t\bar{t}$ cross section using only the $\ell\tau_{\text{had}}+\text{jets}$ channel is derived from the number of observed $t\bar{t} \rightarrow \ell\tau+\text{jets}$ events given in Table 4 (Sec. 8.3):

$$\sigma_{t\bar{t}} = 183 \pm 9 \text{ (stat.)} \pm 23 \text{ (syst.)} \pm 3 \text{ (lumi.) pb}$$

This result is consistent with the previous ATLAS measurement, 186 ± 25 pb [13]. This measurement differs from the earlier one in that it uses only τ s decaying into one charged hadron and a different background model to reduce the systematic uncertainties in the branching ratios. The results from combining all channels to extract the top quark branching ratios are given in Table 9. The measured cross section of 178 ± 17 pb is in good agreement with those obtained by ATLAS for individual channels [52–54]. The selection criteria for this measurement were optimized for the $t\bar{t} \rightarrow \ell\tau_{\text{had}}+\text{jets}$ channel, which has the largest uncertainty, and then applied uniformly to all channels, ensuring no event overlap between them to exploit cancellation of systematic uncertainties in the ratios. This reduces the systematic uncertainties in the branching ratio measurements but it is not optimal for a cross-section measurement combining all channels. The systematic uncertainty on the inclusive cross section obtained by combining the samples used for this measurement is larger than the best ATLAS inclusive cross-section measurement [54], which achieved much smaller uncertainties because it was designed to minimize the systematic uncertainties related to jets, including the b-tagging efficiency and the jet energy scale. All cross-section measurements are in good agreement with the NNLO+NNLL theoretical prediction $177.3 \pm 9.0^{+4.6}_{-6.0}$ pb (calculated for a top mass of 172.5 GeV [24, 55]).

The branching ratios into leptons and jets are in good agreement with the SM prediction that the top quark decays 100% to $W+\text{quark}$. The precision of the measurements ranges from 2.3% for B_j to 7.6% for B_τ . The B_e and B_μ include the leptonic decay of τ leptons while B_τ includes only the hadronic decays of τ leptons. There is no evidence for any non-SM top quark decay or for any non-SM process contribution that could affect these measurements. For example, the measured branching ratio B_τ will vary by more than the observed uncertainty if the branching ratio $\tilde{t} \rightarrow b\nu_\tau\tilde{\tau}$ times the $t\bar{t}$ production cross section ($\sigma_{t\bar{t}}$) is greater than 3% of $\sigma_{t\bar{t}}$. The predicted $\sigma_{\tilde{t}\tilde{\tau}}$ depends on \tilde{t} mass ($m_{\tilde{t}}$); it is equal to $\sigma_{t\bar{t}}$ for $m_{\tilde{t}} = 120$ GeV and 12% of $\sigma_{t\bar{t}}$ for $m_{\tilde{t}} = 180$ GeV [56].

12 Conclusion

The inclusive cross section for producing $t\bar{t}$ pairs in pp collisions at a center-of-mass energy of $\sqrt{s} = 7$ TeV at the LHC has been measured with the ATLAS detector and an integrated luminosity of 4.6 fb^{-1} using the $\ell\tau_{\text{had}}+\text{jets}$ channel alone, as $\sigma_{t\bar{t}} = 183 \pm 23$ pb, and as a single parameter to fit the channels $\ell+\text{jets}$, $\ell\ell+\text{jets}$ and $\ell\tau_{\text{had}}+\text{jets}$, to be 178 ± 17 pb. These are in agreement with all other cross-section measurements obtained by ATLAS and CMS. All cross-section measurements are fully compatible with the NNLO+NNLL theoretical prediction. Top quark branching ratios have also been measured and found to be in good agreement with branching ratios predicted by the SM. The precision ranges from 2.3% for the decays to jets to 7.6% for the decays to $\tau\nu+\text{jet}$. There is no evidence for any non-SM process affecting these branching ratios.

Table 9: Measured cross section (pb) and top quark branching ratios (%) including statistical and systematic uncertainties without imposing lepton universality. The top quark branching ratios add up to 100.2% because of rounding precision. The uncertainty on the SM prediction for the cross section is the uncertainty in the NNLO+NNLL theoretical calculation [24, 55]. The SM branching ratios are the predicted W branching ratios. The LEP measurements represent the W branching ratios obtained by combining results for ALEPH, DELPHI, L3 and OPAL collaborations imposing lepton universality [15]. The LEP entries B_e and B_μ include the τ leptonic decays that have been subtracted from B_τ .

	Measured (top quark)	SM	LEP (W)
$\sigma_{t\bar{t}}$	178 ± 3 (stat.) ± 16 (syst.) ± 3 (lumi.) pb	$177.3 \pm 9.0^{+4.6}_{-6.0}$ pb	
B_j	66.5 ± 0.4 (stat.) ± 1.3 (syst.)	67.51 ± 0.07	67.48 ± 0.28
B_e	13.3 ± 0.4 (stat.) ± 0.5 (syst.)	12.72 ± 0.01	12.70 ± 0.20
B_μ	13.4 ± 0.3 (stat.) ± 0.5 (syst.)	12.72 ± 0.01	12.60 ± 0.18
B_τ	7.0 ± 0.3 (stat.) ± 0.5 (syst.)	7.05 ± 0.01	7.20 ± 0.13

We thank CERN for the very successful operation of the LHC, as well as the support staff from our institutions without whom ATLAS could not be operated efficiently.

We acknowledge the support of ANPCyT, Argentina; YerPhI, Armenia; ARC, Australia; BMWFW and FWF, Austria; ANAS, Azerbaijan; SSTC, Belarus; CNPq and FAPESP, Brazil; NSERC, NRC and CFI, Canada; CERN; CONICYT, Chile; CAS, MOST and NSFC, China; COLCIENCIAS, Colombia; MSMT CR, MPO CR and VSC CR, Czech Republic; DNRF, DNSRC and Lundbeck Foundation, Denmark; EPLANET, ERC and NSRF, European Union; IN2P3-CNRS, CEA-DSM/IRFU, France; GNSF, Georgia; BMBF, DFG, HGF, MPG and AvH Foundation, Germany; GSRT and NSRF, Greece; RGC, Hong Kong SAR, China; ISF, MINERVA, GIF, I-CORE and Benoziyo Center, Israel; INFN, Italy; MEXT and JSPS, Japan; CNRST, Morocco; FOM and NWO, Netherlands; BRF and RCN, Norway; MNiSW and NCN, Poland; GRICES and FCT, Portugal; MNE/IFA, Romania; MES of Russia and NRC KI, Russian Federation; JINR; MSTD, Serbia; MSSR, Slovakia; ARRS and MIZŠ, Slovenia; DST/NRF, South Africa; MINECO, Spain; SRC and Wallenberg Foundation, Sweden; SER, SNSF and Cantons of Bern and Geneva, Switzerland; NSC, Taiwan; TAEK, Turkey; STFC, the Royal Society and Leverhulme Trust, United Kingdom; DOE and NSF, United States of America.

The crucial computing support from all WLCG partners is acknowledged gratefully, in particular from CERN and the ATLAS Tier-1 facilities at TRIUMF (Canada), NDGF (Denmark, Norway, Sweden), CC-IN2P3 (France), KIT/GridKA (Germany), INFN-CNAF (Italy), NL-T1 (Netherlands), PIC (Spain), ASGC (Taiwan), RAL (UK) and BNL (USA) and in the Tier-2 facilities worldwide.

References

- [1] CMS Collaboration, Phys. Lett. B **736**, 33 (2014).
- [2] ATLAS Collaboration, Phys. Rev. D **90**, 112006 (2014).
- [3] CMS Collaboration, J. High Energy Phys. **06** (2014) 090.
- [4] T.Aaltonen *et al.* (CDF and D0 Collaborations), [arXiv:hep-ex/1503.05027](https://arxiv.org/abs/hep-ex/1503.05027).
- [5] H.Baer, C.H.Chen, M.Drees, F. Paige, X.Tata, Phys. Rev. Lett. **79**, 986 (1997).
- [6] T.Aaltonen *et al.*, CDF Collaboration, Phys. Rev. Lett. **103**, 101803 (2009).
- [7] V.M.Abazov *et al.*, D0 Collaboration, Phys. Lett. B **682**, 278 (2009).
- [8] V.M.Abazov *et al.*, D0 Collaboration, Phys. Rev. D **80**, 071102 (2009).
- [9] ATLAS Collaboration, Eur. Phys. J. C **73**,2465 (2013).
- [10] ATLAS Collaboration, J. High Energy Phys. **03** (2015) 088.
- [11] CMS Collaboration, J. High Energy Phys. **07** (2012) 143.
- [12] G.F.Giudice and R.Rattazi, Phys. Rep. **322**, 419 (1999).
- [13] ATLAS Collaboration, Phys. Lett. B **717**, 89 (2012).
- [14] CMS Collaboration, Phys. Rev. D **85**, 112007 (2012).
- [15] ALEPH, DELPHI, L3 and OPAL Collaborations and LEP Electroweak Working group, [arXiv:hep-ex/0612034](https://arxiv.org/abs/hep-ex/0612034).
- [16] K.G.Chetyrkin, J.H.Kuhn and A.Kwiatowski, Phys. Rep. **277**, 189 (1996).
- [17] B.P.Roe *et al.*, Nucl. Instrum. Meth. Phys., Sect. A **543** (2005) 577.
- [18] ATLAS Collaboration, JINST **3**, S08003 (2008).
- [19] S. Frixione, P.Nason and C.Oleari, **11** (2007) 070.
- [20] S.Alioli, P.Nason, C.Oleari and E.Re, **06** (2010) 043.
- [21] T.Sjostrand *et al.*, J. High Energy Phys. **05** (2006) 026.
- [22] P.Z.Skands, Phys. Rev. D **82**, 074018 (2010).
- [23] P.M.Nadolsky *et al.*, Phys. Rev. D **78**, 013004 (2008).
- [24] M.Czakon, P.Fiedler and A.Mitov, Physical Review Letters **110**, 252004 (2013).
- [25] S.Frixione, E.Laenen and B.R.Webber, **03** J. High Energy Phys. (2006) 092.
- [26] G.Corcella *et al.*, **01** J. High Energy Phys. (2001) 010.
- [27] J.M.Butterworth *et al.*, Zeit. für Phys. C **72**, 637 (1996).
- [28] H.L.Lai *et al.*, Phys. Rev. D **82**, 074024 (2010).
- [29] M.L.Mangano *et al.*, J. High Energy Phys. **07** (2003) 001.

- [30] J.Pumplin *et al.*, J. High Energy Phys. **07** (2002) 012.
- [31] J.Alwall *et al.*, Eur. Phys. J. C **53**, 473 (2008).
- [32] A.Sherstnev and R.S.Thorne, Eur. Phys. J. C **55**, 553 (2008).
- [33] N.Davidson *et al.*, Comput. Phys. Commun. **183**, 821 (2012).
- [34] S.Agostinelli *et al.*, Nucl. Instrum. Meth. Phys., Sect. A **506**, 250 (2003).
- [35] ATLAS Collaboration, Eur. Phys. J. C **70**, 823 (2010).
- [36] ATLAS Collaboration, Eur. Phys. J. C **74**, 3130 (2014).
- [37] ATLAS Collaboration, Eur. Phys. J. C **74**, 2941 (2014).
- [38] M.Cacciari, G.P.Salam and G.Soyez, J. High Energy Phys. **04** (2008) 063.
- [39] ATLAS Collaboration, Eur. Phys. J. C **75**, 17 (2015).
- [40] ATLAS Collaboration, ATLAS-CONF-2012-043, <https://cdsweb.cern.ch/record/1435197>.
- [41] C.Issever, K.Borras and D.Wegener, Nucl. Instrum. Meth. Phys., Sect. A **545**, 803 (2005).
- [42] ATLAS Collaboration, Eur. Phys. J. C **73**, 23004 (2013).
- [43] ATLAS Collaboration, Eur. Phys. J. C **75**, 303 (2015).
- [44] R.Brun *et al.*, <https://root.cern.ch/root/html526/TH1.html/#TH1:KolmogorovTest>.
- [45] M.Botje *et al.*, [arXiv:hep-ph/1101.0538](https://arxiv.org/abs/hep-ph/1101.0538).
- [46] A.Martin, W.Stirling, R.Thorne and G.Watt, Eur. Phys. J. C **63**, 189 (2009).
- [47] R.D.Ball *et al.*, Nucl. Phys. B **809**, 1 (2009).
- [48] R.D.Ball *et al.*, Nucl.Phys B **823**, 195 (2009).
- [49] ATLAS Collaboration, Eur. Phys. J. C **72**, 2043 (2012).
- [50] ATLAS Collaboration, Phys. Rev. D **85**, 072004 (2012).
- [51] ATLAS collaboration, Eur. Phys. J. C **73**, 2518 (2013).
- [52] ATLAS Collaboration, Phys. Lett. B **711**, 244 (2012).
- [53] ATLAS Collaboration, J. High Energy Phys. **05** (2012) 059.
- [54] ATLAS Collaboration, Eur. Phys. J. C **74**, 3109 (2014).
- [55] M.Czakon and A.Mitov, Comp. Phys. Comm. **182**, 2930 (2014).
- [56] W.Beenakker *et al.* J. High Energy Phys. **08** (2010) 098.

ATLAS Collaboration

G. Aad⁸⁵, B. Abbott¹¹³, J. Abdallah¹⁵¹, O. Abdinov¹¹, R. Aben¹⁰⁷, M. Abolins⁹⁰, O.S. AbouZeid¹⁵⁸, H. Abramowicz¹⁵³, H. Abreu¹⁵², R. Abreu³⁰, Y. Abulaiti^{146a,146b}, B.S. Acharya^{164a,164b,a}, L. Adamczyk^{38a}, D.L. Adams²⁵, J. Adelman¹⁰⁸, S. Adomeit¹⁰⁰, T. Adye¹³¹, A.A. Affolder⁷⁴, T. Agatonovic-Jovin¹³, J.A. Aguilar-Saavedra^{126a,126f}, S.P. Ahlen²², F. Ahmadov^{65,b}, G. Aielli^{133a,133b}, H. Akerstedt^{146a,146b}, T.P.A. Åkesson⁸¹, G. Akimoto¹⁵⁵, A.V. Akimov⁹⁶, G.L. Alberghi^{20a,20b}, J. Albert¹⁶⁹, S. Albrand⁵⁵, M.J. Alconada Verzini⁷¹, M. Aleksa³⁰, I.N. Aleksandrov⁶⁵, C. Alexa^{26a}, G. Alexander¹⁵³, T. Alexopoulos¹⁰, M. Alhroob¹¹³, G. Alimonti^{91a}, L. Alio⁸⁵, J. Alison³¹, S.P. Alkire³⁵, B.M.M. Allbrooke¹⁸, P.P. Allport⁷⁴, A. Aloisio^{104a,104b}, A. Alonso³⁶, F. Alonso⁷¹, C. Alpigiani⁷⁶, A. Altheimer³⁵, B. Alvarez Gonzalez³⁰, D. Álvarez Piqueras¹⁶⁷, M.G. Alviggi^{104a,104b}, B.T. Amadio¹⁵, K. Amako⁶⁶, Y. Amaral Coutinho^{24a}, C. Amelung²³, D. Amidei⁸⁹, S.P. Amor Dos Santos^{126a,126c}, A. Amorim^{126a,126b}, S. Amoroso⁴⁸, N. Amram¹⁵³, G. Amundsen²³, C. Anastopoulos¹³⁹, L.S. Ancu⁴⁹, N. Andari³⁰, T. Andeen³⁵, C.F. Anders^{58b}, G. Anders³⁰, J.K. Anders⁷⁴, K.J. Anderson³¹, A. Andreazza^{91a,91b}, V. Andrei^{58a}, S. Angelidakis⁹, I. Angelozzi¹⁰⁷, P. Anger⁴⁴, A. Angerami³⁵, F. Anghinolfi³⁰, A.V. Anisenkov^{109,c}, N. Anjos¹², A. Annovi^{124a,124b}, M. Antonelli⁴⁷, A. Antonov⁹⁸, J. Antos^{144b}, F. Anulli^{132a}, M. Aoki⁶⁶, L. Aperio Bella¹⁸, G. Arabidze⁹⁰, Y. Arai⁶⁶, J.P. Araque^{126a}, A.T.H. Arce⁴⁵, F.A. Arduh⁷¹, J-F. Arguin⁹⁵, S. Argyropoulos⁴², M. Arik^{19a}, A.J. Armbruster³⁰, O. Arnaez³⁰, V. Arnal⁸², H. Arnold⁴⁸, M. Arratia²⁸, O. Arslan²¹, A. Artamonov⁹⁷, G. Artoni²³, S. Asai¹⁵⁵, N. Asbah⁴², A. Ashkenazi¹⁵³, B. Åsman^{146a,146b}, L. Asquith¹⁴⁹, K. Assamagan²⁵, R. Astalos^{144a}, M. Atkinson¹⁶⁵, N.B. Atlay¹⁴¹, B. Auerbach⁶, K. Augsten¹²⁸, M. Aurousseau^{145b}, G. Avolio³⁰, B. Axen¹⁵, M.K. Ayoub¹¹⁷, G. Azuelos^{95,d}, M.A. Baak³⁰, A.E. Baas^{58a}, C. Bacci^{134a,134b}, H. Bachacou¹³⁶, K. Bachas¹⁵⁴, M. Backes³⁰, M. Backhaus³⁰, P. Bagiacchi^{132a,132b}, P. Bagnaia^{132a,132b}, Y. Bai^{33a}, T. Bain³⁵, J.T. Baines¹³¹, O.K. Baker¹⁷⁶, P. Balek¹²⁹, T. Balestri¹⁴⁸, F. Balli⁸⁴, E. Banas³⁹, Sw. Banerjee¹⁷³, A.A.E. Bannoura¹⁷⁵, H.S. Bansil¹⁸, L. Barak³⁰, E.L. Barberio⁸⁸, D. Barberis^{50a,50b}, M. Barbero⁸⁵, T. Barillari¹⁰¹, M. Barisonzi^{164a,164b}, T. Barklow¹⁴³, N. Barlow²⁸, S.L. Barnes⁸⁴, B.M. Barnett¹³¹, R.M. Barnett¹⁵, Z. Barnovska⁵, A. Baroncelli^{134a}, G. Barone⁴⁹, A.J. Barr¹²⁰, F. Barreiro⁸², J. Barreiro Guimarães da Costa⁵⁷, R. Bartoldus¹⁴³, A.E. Barton⁷², P. Bartos^{144a}, A. Basalae¹²³, A. Bassalat¹¹⁷, A. Basye¹⁶⁵, R.L. Bates⁵³, S.J. Batista¹⁵⁸, J.R. Batley²⁸, M. Battaglia¹³⁷, M. Bauce^{132a,132b}, F. Bauer¹³⁶, H.S. Bawa^{143,e}, J.B. Beacham¹¹¹, M.D. Beattie⁷², T. Beau⁸⁰, P.H. Beauchemin¹⁶¹, R. Beccherle^{124a,124b}, P. Bechtel²¹, H.P. Beck^{17,f}, K. Becker¹²⁰, M. Becker⁸³, S. Becker¹⁰⁰, M. Beckingham¹⁷⁰, C. Becot¹¹⁷, A.J. Beddall^{19c}, A. Beddall^{19c}, V.A. Bednyakov⁶⁵, C.P. Bee¹⁴⁸, L.J. Beamster¹⁰⁷, T.A. Beermann¹⁷⁵, M. Beger²⁵, J.K. Behr¹²⁰, C. Belanger-Champagne⁸⁷, W.H. Bell⁴⁹, G. Bella¹⁵³, L. Bellagamba^{20a}, A. Bellerive²⁹, M. Bellomo⁸⁶, K. Belotskiy⁹⁸, O. Beltramello³⁰, O. Benary¹⁵³, D. Bencheikroun^{135a}, M. Bender¹⁰⁰, K. Bendtz^{146a,146b}, N. Benekos¹⁰, Y. Benhammou¹⁵³, E. Benhar Noccioli⁴⁹, J.A. Benitez Garcia^{159b}, D.P. Benjamin⁴⁵, J.R. Bensinger²³, S. Bentvelsen¹⁰⁷, L. Beresford¹²⁰, M. Beretta⁴⁷, D. Berge¹⁰⁷, E. Bergeaas Kuutmann¹⁶⁶, N. Berger⁵, F. Berghaus¹⁶⁹, J. Beringer¹⁵, C. Bernard²², N.R. Bernard⁸⁶, C. Bernius¹¹⁰, F.U. Bernlochner²¹, T. Berry⁷⁷, P. Berta¹²⁹, C. Bertella⁸³, G. Bertoli^{146a,146b}, F. Bertolucci^{124a,124b}, C. Bertsche¹¹³, D. Bertsche¹¹³, M.I. Besana^{91a}, G.J. Besjes¹⁰⁶, O. Bessidskaia Bylund^{146a,146b}, M. Bessner⁴², N. Besson¹³⁶, C. Betancourt⁴⁸, S. Bethke¹⁰¹, A.J. Bevan⁷⁶, W. Bhimji⁴⁶, R.M. Bianchi¹²⁵, L. Bianchini²³, M. Bianco³⁰, O. Biebel¹⁰⁰, D. Biedermann¹⁶, S.P. Bieniek⁷⁸, M. Biglietti^{134a}, J. Bilbao De Mendizabal⁴⁹, H. Bilokon⁴⁷, M. Bindi⁵⁴, S. Binet¹¹⁷, A. Bingul^{19c}, C. Bini^{132a,132b}, C.W. Black¹⁵⁰, J.E. Black¹⁴³, K.M. Black²², D. Blackburn¹³⁸, R.E. Blair⁶, J.-B. Blanchard¹³⁶, J.E. Blanco⁷⁷, T. Blazek^{144a}, I. Bloch⁴², C. Blocker²³, W. Blum^{83,*}, U. Blumenschein⁵⁴, G.J. Bobbink¹⁰⁷, V.S. Bobrovnikov^{109,c}, S.S. Bocchetta⁸¹, A. Bocci⁴⁵, C. Bock¹⁰⁰, M. Boehler⁴⁸,

J.A. Bogaerts³⁰, D. Bogavac¹³, A.G. Bogdanchikov¹⁰⁹, C. Bohm^{146a}, V. Boisvert⁷⁷, T. Bold^{38a},
 V. Boldea^{26a}, A.S. Boldyrev⁹⁹, M. Bomben⁸⁰, M. Bona⁷⁶, M. Boonekamp¹³⁶, A. Borisov¹³⁰,
 G. Borissov⁷², S. Borroni⁴², J. Bortfeldt¹⁰⁰, V. Bortolotto^{60a,60b,60c}, K. Bos¹⁰⁷, D. Boscherini^{20a},
 M. Bosman¹², J. Boudreau¹²⁵, J. Bouffard², E.V. Bouhova-Thacker⁷², D. Boumediene³⁴,
 C. Bourdarios¹¹⁷, N. Bousson¹¹⁴, A. Boveia³⁰, J. Boyd³⁰, I.R. Boyko⁶⁵, I. Bozic¹³, J. Bracinik¹⁸,
 A. Brandt⁸, G. Brandt⁵⁴, O. Brandt^{58a}, U. Bratzler¹⁵⁶, B. Brau⁸⁶, J.E. Brau¹¹⁶, H.M. Braun^{175,*},
 S.F. Brazzale^{164a,164c}, W.D. Breaden Madden⁵³, K. Brendlinger¹²², A.J. Brennan⁸⁸, L. Brenner¹⁰⁷,
 R. Brenner¹⁶⁶, S. Bressler¹⁷², K. Bristow^{145c}, T.M. Bristow⁴⁶, D. Britton⁵³, D. Britzger⁴²,
 F.M. Brochu²⁸, I. Brock²¹, R. Brock⁹⁰, J. Bronner¹⁰¹, G. Brooijmans³⁵, T. Brooks⁷⁷, W.K. Brooks^{32b},
 J. Brosamer¹⁵, E. Brost¹¹⁶, J. Brown⁵⁵, P.A. Bruckman de Renstrom³⁹, D. Bruncko^{144b}, R. Bruneliere⁴⁸,
 A. Bruni^{20a}, G. Bruni^{20a}, M. Bruschi^{20a}, N. Bruscinio²¹, L. Bryngemark⁸¹, T. Buanes¹⁴, Q. Buat¹⁴²,
 P. Buchholz¹⁴¹, A.G. Buckley⁵³, S.I. Buda^{26a}, I.A. Budagov⁶⁵, F. Buehrer⁴⁸, L. Bugge¹¹⁹,
 M.K. Bugge¹¹⁹, O. Bulekov⁹⁸, D. Bullock⁸, H. Burckhart³⁰, S. Burdin⁷⁴, B. Burghgrave¹⁰⁸, S. Burke¹³¹,
 I. Burmeister⁴³, E. Busato³⁴, D. Büscher⁴⁸, V. Büscher⁸³, P. Bussey⁵³, J.M. Butler²², A.I. Butt³,
 C.M. Buttar⁵³, J.M. Butterworth⁷⁸, P. Butti¹⁰⁷, W. Buttinger²⁵, A. Buzatu⁵³, A.R. Buzykaev^{109,c},
 S. Cabrera Urbán¹⁶⁷, D. Caforio¹²⁸, V.M. Cairo^{37a,37b}, O. Cakir^{4a}, P. Calafiura¹⁵, A. Calandri¹³⁶,
 G. Calderini⁸⁰, P. Calfayan¹⁰⁰, L.P. Caloba^{24a}, D. Calvet³⁴, S. Calvet³⁴, R. Camacho Toro³¹,
 S. Camarda⁴², P. Camarri^{133a,133b}, D. Cameron¹¹⁹, R. Caminal Armadans¹⁶⁵, S. Campana³⁰,
 M. Campanelli⁷⁸, A. Campoverde¹⁴⁸, V. Canale^{104a,104b}, A. Canepa^{159a}, M. Cano Bret⁷⁶, J. Cantero⁸²,
 R. Cantrill^{126a}, T. Cao⁴⁰, M.D.M. Capeans Garrido³⁰, I. Caprini^{26a}, M. Caprini^{26a}, M. Capua^{37a,37b},
 R. Caputo⁸³, R. Cardarelli^{133a}, F. Cardillo⁴⁸, T. Carli³⁰, G. Carlino^{104a}, L. Carminati^{91a,91b}, S. Caron¹⁰⁶,
 E. Carquin^{32a}, G.D. Carrillo-Montoya⁸, J.R. Carter²⁸, J. Carvalho^{126a,126c}, D. Casadei⁷⁸, M.P. Casado¹²,
 M. Casolino¹², E. Castaneda-Miranda^{145b}, A. Castelli¹⁰⁷, V. Castillo Gimenez¹⁶⁷, N.F. Castro^{126a,g},
 P. Catastini⁵⁷, A. Catinaccio³⁰, J.R. Catmore¹¹⁹, A. Cattai³⁰, J. Caudron⁸³, V. Cavaliere¹⁶⁵, D. Cavalli^{91a},
 M. Cavalli-Sforza¹², V. Cavasinni^{124a,124b}, F. Ceradini^{134a,134b}, B.C. Cerio⁴⁵, K. Cerny¹²⁹,
 A.S. Cerqueira^{24b}, A. Cerri¹⁴⁹, L. Cerrito⁷⁶, F. Cerutti¹⁵, M. Cerv³⁰, A. Cervelli¹⁷, S.A. Cetin^{19b},
 A. Chafaq^{135a}, D. Chakraborty¹⁰⁸, I. Chalupkova¹²⁹, P. Chang¹⁶⁵, B. Chapleau⁸⁷, J.D. Chapman²⁸,
 D.G. Charlton¹⁸, C.C. Chau¹⁵⁸, C.A. Chavez Barajas¹⁴⁹, S. Cheatham¹⁵², A. Chegwidden⁹⁰,
 S. Chekanov⁶, S.V. Chekulaev^{159a}, G.A. Chelkov^{65,h}, M.A. Chelstowska⁸⁹, C. Chen⁶⁴, H. Chen²⁵,
 K. Chen¹⁴⁸, L. Chen^{33d,i}, S. Chen^{33c}, X. Chen^{33f}, Y. Chen⁶⁷, H.C. Cheng⁸⁹, Y. Cheng³¹, A. Cheplakov⁶⁵,
 E. Cheremushkina¹³⁰, R. Cherkaoui El Moursli^{135e}, V. Chernyatin^{25,*}, E. Cheu⁷, L. Chevalier¹³⁶,
 V. Chiarella⁴⁷, J.T. Childers⁶, G. Chiodini^{73a}, A.S. Chisholm¹⁸, R.T. Chislett⁷⁸, A. Chitan^{26a},
 M.V. Chizhov⁶⁵, K. Choi⁶¹, S. Chouridou⁹, B.K.B. Chow¹⁰⁰, V. Christodoulou⁷⁸,
 D. Chromek-Burckhart³⁰, J. Chudoba¹²⁷, A.J. Chuinard⁸⁷, J.J. Chwastowski³⁹, L. Chytka¹¹⁵,
 G. Ciapetti^{132a,132b}, A.K. Ciftci^{4a}, D. Cinca⁵³, V. Cindro⁷⁵, I.A. Cioara²¹, A. Ciocio¹⁵, Z.H. Citron¹⁷²,
 M. Ciubancan^{26a}, A. Clark⁴⁹, B.L. Clark⁵⁷, P.J. Clark⁴⁶, R.N. Clarke¹⁵, W. Cleland¹²⁵,
 C. Clement^{146a,146b}, Y. Coadou⁸⁵, M. Cobal^{164a,164c}, A. Coccaro¹³⁸, J. Cochran⁶⁴, L. Coffey²³,
 J.G. Cogan¹⁴³, B. Cole³⁵, S. Cole¹⁰⁸, A.P. Colijn¹⁰⁷, J. Collot⁵⁵, T. Colombo^{58c}, G. Compostella¹⁰¹,
 P. Conde Muiño^{126a,126b}, E. Coniavitis⁴⁸, S.H. Connell^{145b}, I.A. Connelly⁷⁷, S.M. Consonni^{91a,91b},
 V. Consorti⁴⁸, S. Constantinescu^{26a}, C. Conta^{121a,121b}, G. Conti³⁰, F. Conventi^{104a,j}, M. Cooke¹⁵,
 B.D. Cooper⁷⁸, A.M. Cooper-Sarkar¹²⁰, T. Cornelissen¹⁷⁵, M. Corradi^{20a}, F. Corriveau^{87,k},
 A. Corso-Radu¹⁶³, A. Cortes-Gonzalez¹², G. Cortiana¹⁰¹, G. Costa^{91a}, M.J. Costa¹⁶⁷, D. Costanzo¹³⁹,
 D. Côte⁸, G. Cottin²⁸, G. Cowan⁷⁷, B.E. Cox⁸⁴, K. Cranmer¹¹⁰, G. Cree²⁹, S. Crépe-Renaudin⁵⁵,
 F. Crescioli⁸⁰, W.A. Cribbs^{146a,146b}, M. Crispin Ortuzar¹²⁰, M. Cristinziani²¹, V. Croft¹⁰⁶,
 G. Crosetti^{37a,37b}, T. Cuhadar Donszelmann¹³⁹, J. Cummings¹⁷⁶, M. Curatolo⁴⁷, C. Cuthbert¹⁵⁰,
 H. Czirr¹⁴¹, P. Czodrowski³, S. D'Auria⁵³, M. D'Onofrio⁷⁴, M.J. Da Cunha Sargedas De Sousa^{126a,126b},
 C. Da Via⁸⁴, W. Dabrowski^{38a}, A. Dafinca¹²⁰, T. Dai⁸⁹, O. Dale¹⁴, F. Dallaire⁹⁵, C. Dallapiccola⁸⁶,

M. Dam³⁶, J.R. Dandoy³¹, N.P. Dang⁴⁸, A.C. Daniells¹⁸, M. Danninger¹⁶⁸, M. Dano Hoffmann¹³⁶,
V. Dao⁴⁸, G. Darbo^{50a}, S. Darmora⁸, J. Dassoulas³, A. Dattagupta⁶¹, W. Davey²¹, C. David¹⁶⁹,
T. Davidek¹²⁹, E. Davies^{120,l}, M. Davies¹⁵³, P. Davison⁷⁸, Y. Davygora^{58a}, E. Dawe⁸⁸, I. Dawson¹³⁹,
R.K. Daya-Ishmukhametova⁸⁶, K. De⁸, R. de Asmundis^{104a}, S. De Castro^{20a,20b}, S. De Cecco⁸⁰,
N. De Groot¹⁰⁶, P. de Jong¹⁰⁷, H. De la Torre⁸², F. De Lorenzi⁶⁴, L. De Nooij¹⁰⁷, D. De Pedis^{132a},
A. De Salvo^{132a}, U. De Sanctis¹⁴⁹, A. De Santo¹⁴⁹, J.B. De Vivie De Regie¹¹⁷, W.J. Dearnaley⁷²,
R. Debbe²⁵, C. Debenedetti¹³⁷, D.V. Dedovich⁶⁵, I. Deigaard¹⁰⁷, J. Del Peso⁸², T. Del Prete^{124a,124b},
D. Delgove¹¹⁷, F. Deliot¹³⁶, C.M. Delitzsch⁴⁹, M. Deliyergiyev⁷⁵, A. Dell'Acqua³⁰, L. Dell'Asta²²,
M. Dell'Orso^{124a,124b}, M. Della Pietra^{104a,j}, D. della Volpe⁴⁹, M. Delmastro⁵, P.A. Delsart⁵⁵,
C. Deluca¹⁰⁷, D.A. DeMarco¹⁵⁸, S. Demers¹⁷⁶, M. Demichev⁶⁵, A. Demilly⁸⁰, S.P. Denisov¹³⁰,
D. Derendarz³⁹, J.E. Derkaoui^{135d}, F. Derue⁸⁰, P. Dervan⁷⁴, K. Desch²¹, C. Deterre⁴², P.O. Deviveiros³⁰,
A. Dewhurst¹³¹, S. Dhaliwal²³, A. Di Ciaccio^{133a,133b}, L. Di Ciaccio⁵, A. Di Domenico^{132a,132b},
C. Di Donato^{104a,104b}, A. Di Girolamo³⁰, B. Di Girolamo³⁰, A. Di Mattia¹⁵², B. Di Micco^{134a,134b},
R. Di Nardo⁴⁷, A. Di Simone⁴⁸, R. Di Sipio¹⁵⁸, D. Di Valentino²⁹, C. Diaconu⁸⁵, M. Diamond¹⁵⁸,
F.A. Dias⁴⁶, M.A. Diaz^{32a}, E.B. Diehl⁸⁹, J. Dietrich¹⁶, S. Diglio⁸⁵, A. Dimitrievska¹³, J. Dingfelder²¹,
P. Dita^{26a}, S. Dita^{26a}, F. Dittus³⁰, F. Djama⁸⁵, T. Djobava^{51b}, J.I. Djuvland^{58a}, M.A.B. do Vale^{24c},
D. Dobos³⁰, M. Dobre^{26a}, C. Doglioni⁴⁹, T. Dohmae¹⁵⁵, J. Dolejsi¹²⁹, Z. Dolezal¹²⁹,
B.A. Dolgoshein^{98,*}, M. Donadelli^{24d}, S. Donati^{124a,124b}, P. Dondero^{121a,121b}, J. Donini³⁴, J. Dopke¹³¹,
A. Doria^{104a}, M.T. Dova⁷¹, A.T. Doyle⁵³, E. Drechsler⁵⁴, M. Dris¹⁰, E. Dubreuil³⁴, E. Duchovni¹⁷²,
G. Duckeck¹⁰⁰, O.A. Ducu^{26a,85}, D. Duda¹⁷⁵, A. Dudarev³⁰, L. Duflot¹¹⁷, L. Duguid⁷⁷, M. Dührssen³⁰,
M. Dunford^{58a}, H. Duran Yildiz^{4a}, M. Düren⁵², A. Durglishvili^{51b}, D. Duschinger⁴⁴, M. Dyndal^{38a},
C. Eckardt⁴², K.M. Ecker¹⁰¹, R.C. Edgar⁸⁹, W. Edson², N.C. Edwards⁴⁶, W. Ehrenfeld²¹, T. Eifert³⁰,
G. Eigen¹⁴, K. Einsweiler¹⁵, T. Ekelof¹⁶⁶, M. El Kacimi^{135c}, M. Ellert¹⁶⁶, S. Elles⁵, F. Ellinghaus⁸³,
A.A. Elliot¹⁶⁹, N. Ellis³⁰, J. Elmsheuser¹⁰⁰, M. Elsing³⁰, D. Emelianov¹³¹, Y. Enari¹⁵⁵, O.C. Endner⁸³,
M. Endo¹¹⁸, J. Erdmann⁴³, A. Ereditato¹⁷, G. Ernis¹⁷⁵, J. Ernst², M. Ernst²⁵, S. Errede¹⁶⁵, E. Ertel⁸³,
M. Escalier¹¹⁷, H. Esch⁴³, C. Escobar¹²⁵, B. Esposito⁴⁷, A.I. Etiennev¹³⁶, E. Etzion¹⁵³, H. Evans⁶¹,
A. Ezhilov¹²³, L. Fabbri^{20a,20b}, G. Facini³¹, R.M. Fakhruddinov¹³⁰, S. Falciano^{132a}, R.J. Falla⁷⁸,
J. Faltova¹²⁹, Y. Fang^{33a}, M. Fanti^{91a,91b}, A. Farbin⁸, A. Farilla^{134a}, T. Farooque¹², S. Farrell¹⁵,
S.M. Farrington¹⁷⁰, P. Farthouat³⁰, F. Fassi^{135e}, P. Fassnacht³⁰, D. Fassouliotis⁹, M. Fauci Giannelli⁷⁷,
A. Favareto^{50a,50b}, L. Fayard¹¹⁷, P. Federic^{144a}, O.L. Fedin^{123,m}, W. Fedorko¹⁶⁸, S. Feigl³⁰,
L. Feligioni⁸⁵, C. Feng^{33d}, E.J. Feng⁶, H. Feng⁸⁹, A.B. Fenyuk¹³⁰, L. Feremenga⁸,
P. Fernandez Martinez¹⁶⁷, S. Fernandez Perez³⁰, J. Ferrando⁵³, A. Ferrari¹⁶⁶, P. Ferrari¹⁰⁷, R. Ferrari^{121a},
D.E. Ferreira de Lima⁵³, A. Ferrer¹⁶⁷, D. Ferrere⁴⁹, C. Ferretti⁸⁹, A. Ferretto Parodi^{50a,50b},
M. Fiascaris³¹, F. Fiedler⁸³, A. Filipčič⁷⁵, M. Filipuzzi⁴², F. Filthaut¹⁰⁶, M. Fincke-Keeler¹⁶⁹,
K.D. Finelli¹⁵⁰, M.C.N. Fiolhais^{126a,126c}, L. Fiorini¹⁶⁷, A. Firan⁴⁰, A. Fischer², C. Fischer¹²,
J. Fischer¹⁷⁵, W.C. Fisher⁹⁰, E.A. Fitzgerald²³, N. Flaschel⁴², I. Fleck¹⁴¹, P. Fleischmann⁸⁹,
S. Fleischmann¹⁷⁵, G.T. Fletcher¹³⁹, G. Fletcher⁷⁶, R.R.M. Fletcher¹²², T. Flick¹⁷⁵, A. Floderus⁸¹,
L.R. Flores Castillo^{60a}, M.J. Flowerdew¹⁰¹, A. Formica¹³⁶, A. Forti⁸⁴, D. Fournier¹¹⁷, H. Fox⁷²,
S. Fracchia¹², P. Francavilla⁸⁰, M. Franchini^{20a,20b}, D. Francis³⁰, L. Franconi¹¹⁹, M. Franklin⁵⁷,
M. Frate¹⁶³, M. Fraternali^{121a,121b}, D. Freeborn⁷⁸, S.T. French²⁸, F. Friedrich⁴⁴, D. Froidevaux³⁰,
J.A. Frost¹²⁰, C. Fukunaga¹⁵⁶, E. Fullana Torregrosa⁸³, B.G. Fulsom¹⁴³, J. Fuster¹⁶⁷, C. Gabaldon⁵⁵,
O. Gabizon¹⁷⁵, A. Gabrielli^{20a,20b}, A. Gabrielli^{132a,132b}, S. Gadatsch¹⁰⁷, S. Gadomski⁴⁹,
G. Gagliardi^{50a,50b}, P. Gagnon⁶¹, C. Galea¹⁰⁶, B. Galhardo^{126a,126c}, E.J. Gallas¹²⁰, B.J. Gallop¹³¹,
P. Gallus¹²⁸, G. Galster³⁶, K.K. Gan¹¹¹, J. Gao^{33b,85}, Y. Gao⁴⁶, Y.S. Gao^{143,e}, F.M. Garay Walls⁴⁶,
F. Garbers¹⁷⁶, C. García¹⁶⁷, J.E. García Navarro¹⁶⁷, M. Garcia-Sciveres¹⁵, R.W. Gardner³¹,
N. Garelli¹⁴³, V. Garonne¹¹⁹, C. Gatti⁴⁷, A. Gaudiello^{50a,50b}, G. Gaudio^{121a}, B. Gaur¹⁴¹, L. Gauthier⁹⁵,
P. Gauzzi^{132a,132b}, I.L. Gavrilenko⁹⁶, C. Gay¹⁶⁸, G. Gaycken²¹, E.N. Gazis¹⁰, P. Ge^{33d}, Z. Gece¹⁶⁸,

C.N.P. Gee¹³¹, D.A.A. Geerts¹⁰⁷, Ch. Geich-Gimbel²¹, M.P. Geisler^{58a}, C. Gemme^{50a}, M.H. Genest⁵⁵, S. Gentile^{132a,132b}, M. George⁵⁴, S. George⁷⁷, D. Gerbaudo¹⁶³, A. Gershon¹⁵³, H. Ghazlane^{135b}, B. Giacobbe^{20a}, S. Giagu^{132a,132b}, V. Giangiobbe¹², P. Giannetti^{124a,124b}, B. Gibbard²⁵, S.M. Gibson⁷⁷, M. Gilchriese¹⁵, T.P.S. Gillam²⁸, D. Gillberg³⁰, G. Gilles³⁴, D.M. Gingrich^{3,d}, N. Giokaris⁹, M.P. Giordani^{164a,164c}, F.M. Giorgi^{20a}, F.M. Giorgi¹⁶, P.F. Giraud¹³⁶, P. Giromini⁴⁷, D. Giugni^{91a}, C. Giuliani⁴⁸, M. Giulini^{58b}, B.K. Gjelsten¹¹⁹, S. Gkaitatzis¹⁵⁴, I. Gkialas¹⁵⁴, E.L. Gkoukousis¹¹⁷, L.K. Gladilin⁹⁹, C. Glasman⁸², J. Glatzer³⁰, P.C.F. Glaysher⁴⁶, A. Glazov⁴², M. Goblirsch-Kolb¹⁰¹, J.R. Goddard⁷⁶, J. Godlewski³⁹, S. Goldfarb⁸⁹, T. Golling⁴⁹, D. Golubkov¹³⁰, A. Gomes^{126a,126b,126d}, R. Gonçalo^{126a}, J. Goncalves Pinto Firmino Da Costa¹³⁶, L. Gonella²¹, S. González de la Hoz¹⁶⁷, G. Gonzalez Parra¹², S. Gonzalez-Sevilla⁴⁹, L. Goossens³⁰, P.A. Gorbounov⁹⁷, H.A. Gordon²⁵, I. Gorelov¹⁰⁵, B. Gorini³⁰, E. Gorini^{73a,73b}, A. Gorišek⁷⁵, E. Gornicki³⁹, A.T. Goshaw⁴⁵, C. Gössling⁴³, M.I. Gostkin⁶⁵, D. Goujdami^{135c}, A.G. Goussiou¹³⁸, N. Govender^{145b}, E. Gozani¹⁵², H.M.X. Grabas¹³⁷, L. Graber⁵⁴, I. Grabowska-Bold^{38a}, P. Grafström^{20a,20b}, K.-J. Grahm⁴², J. Gramling⁴⁹, E. Gramstad¹¹⁹, S. Grancagnolo¹⁶, V. Grassi¹⁴⁸, V. Gratchev¹²³, H.M. Gray³⁰, E. Graziani^{134a}, Z.D. Greenwood^{79,n}, K. Gregersen⁷⁸, I.M. Gregor⁴², P. Grenier¹⁴³, J. Griffiths⁸, A.A. Grillo¹³⁷, K. Grimm⁷², S. Grinstein^{12,o}, Ph. Gris³⁴, J.-F. Grivaz¹¹⁷, J.P. Grohs⁴⁴, A. Grohsjean⁴², E. Gross¹⁷², J. Grosse-Knetter⁵⁴, G.C. Grossi⁷⁹, Z.J. Grout¹⁴⁹, L. Guan^{33b}, J. Guenther¹²⁸, F. Guescini⁴⁹, D. Guest¹⁷⁶, O. Gueta¹⁵³, E. Guido^{50a,50b}, T. Guillemin¹¹⁷, S. Guindon², U. Gul⁵³, C. Gumpert⁴⁴, J. Guo^{33e}, Y. Guo^{33b}, S. Gupta¹²⁰, G. Gustavino^{132a,132b}, P. Gutierrez¹¹³, N.G. Gutierrez Ortiz⁵³, C. Gutsche⁴⁴, C. Guyot¹³⁶, C. Gwenlan¹²⁰, C.B. Gwilliam⁷⁴, A. Haas¹¹⁰, C. Haber¹⁵, H.K. Hadavand⁸, N. Haddad^{135e}, P. Haefner²¹, S. Hageböck²¹, Z. Hajduk³⁹, H. Hakobyan¹⁷⁷, M. Haleem⁴², J. Haley¹¹⁴, D. Hall¹²⁰, G. Halladjian⁹⁰, G.D. Hallowell⁸⁵, K. Hamacher¹⁷⁵, P. Hamal¹¹⁵, K. Hamano¹⁶⁹, M. Hamer⁵⁴, A. Hamilton^{145a}, G.N. Hamity^{145c}, P.G. Hamnett⁴², L. Han^{33b}, K. Hanagaki¹¹⁸, K. Hanawa¹⁵⁵, M. Hance¹⁵, P. Hanke^{58a}, R. Hanna¹³⁶, J.B. Hansen³⁶, J.D. Hansen³⁶, M.C. Hansen²¹, P.H. Hansen³⁶, K. Hara¹⁶⁰, A.S. Hard¹⁷³, T. Harenberg¹⁷⁵, F. Hariri¹¹⁷, S. Harkusha⁹², R.D. Harrington⁴⁶, P.F. Harrison¹⁷⁰, F. Hartjes¹⁰⁷, M. Hasegawa⁶⁷, S. Hasegawa¹⁰³, Y. Hasegawa¹⁴⁰, A. Hasib¹¹³, S. Hassani¹³⁶, S. Haug¹⁷, R. Hauser⁹⁰, L. Hauswald⁴⁴, M. Havranek¹²⁷, C.M. Hawkes¹⁸, R.J. Hawkins³⁰, A.D. Hawkins⁸¹, T. Hayashi¹⁶⁰, D. Hayden⁹⁰, C.P. Hays¹²⁰, J.M. Hays⁷⁶, H.S. Hayward⁷⁴, S.J. Haywood¹³¹, S.J. Head¹⁸, T. Heck⁸³, V. Hedberg⁸¹, L. Heelan⁸, S. Heim¹²², T. Heim¹⁷⁵, B. Heinemann¹⁵, L. Heinrich¹¹⁰, J. Hejbal¹²⁷, L. Helary²², S. Hellman^{146a,146b}, D. Hellmich²¹, C. Helsen³⁰, J. Henderson¹²⁰, R.C.W. Henderson⁷², Y. Heng¹⁷³, C. Hengler⁴², A. Henrichs¹⁷⁶, A.M. Henriques Correia³⁰, S. Henrot-Versille¹¹⁷, G.H. Herbert¹⁶, Y. Hernández Jiménez¹⁶⁷, R. Herrberg-Schubert¹⁶, G. Herten⁴⁸, R. Hertenberger¹⁰⁰, L. Hervas³⁰, G.G. Hesketh⁷⁸, N.P. Hesse¹⁰⁷, J.W. Hetherly⁴⁰, R. Hickling⁷⁶, E. Higón-Rodríguez¹⁶⁷, E. Hill¹⁶⁹, J.C. Hill²⁸, K.H. Hiller⁴², S.J. Hillier¹⁸, I. Hinchliffe¹⁵, E. Hines¹²², R.R. Hinman¹⁵, M. Hirose¹⁵⁷, D. Hirschbuehl¹⁷⁵, J. Hobbs¹⁴⁸, N. Hod¹⁰⁷, M.C. Hodgkinson¹³⁹, P. Hodgson¹³⁹, A. Hoecker³⁰, M.R. Hoferkamp¹⁰⁵, F. Hoenic¹⁰⁰, M. Hohlfeld⁸³, D. Hohn²¹, T.R. Holmes¹⁵, M. Homann⁴³, T.M. Hong¹²⁵, L. Hooft van Huysduyten¹¹⁰, W.H. Hopkins¹¹⁶, Y. Horii¹⁰³, A.J. Horton¹⁴², J.-Y. Hostachy⁵⁵, S. Hou¹⁵¹, A. Hoummada^{135a}, J. Howard¹²⁰, J. Howarth⁴², M. Hrabovsky¹¹⁵, I. Hristova¹⁶, J. Hrivnac¹¹⁷, T. Hryn'ova⁵, A. Hrynevich⁹³, C. Hsu^{145c}, P.J. Hsu^{151,p}, S.-C. Hsu¹³⁸, D. Hu³⁵, Q. Hu^{33b}, X. Hu⁸⁹, Y. Huang⁴², Z. Hubacek³⁰, F. Hubaut⁸⁵, F. Huegging²¹, T.B. Huffman¹²⁰, E.W. Hughes³⁵, G. Hughes⁷², M. Huhtinen³⁰, T.A. Hülsing⁸³, N. Huseynov^{65,b}, J. Huston⁹⁰, J. Huth⁵⁷, G. Iacobucci⁴⁹, G. Iakovidis²⁵, I. Ibragimov¹⁴¹, L. Iconomidou-Fayard¹¹⁷, E. Ideal¹⁷⁶, Z. Idrissi^{135e}, P. Iengo³⁰, O. Igonkina¹⁰⁷, T. Iizawa¹⁷¹, Y. Ikegami⁶⁶, K. Ikematsu¹⁴¹, M. Ikeno⁶⁶, Y. Ilchenko^{31,q}, D. Iliadis¹⁵⁴, N. Ilic¹⁴³, Y. Inamaru⁶⁷, T. Ince¹⁰¹, G. Introzzi^{121a,121b}, P. Ioannou⁹, M. Iodice^{134a}, K. Iordanidou³⁵, V. Ippolito⁵⁷, A. Irlles Quiles¹⁶⁷, C. Isaksson¹⁶⁶, M. Ishino⁶⁸, M. Ishitsuka¹⁵⁷, R. Ishmukhametov¹¹¹, C. Issever¹²⁰, S. Istin^{19a}, J.M. Iturbe Ponce⁸⁴, R. Iuppa^{133a,133b}, J. Ivarsson⁸¹, W. Iwanski³⁹, H. Iwasaki⁶⁶, J.M. Izen⁴¹, V. Izzo^{104a}, S. Jabbar³,

B. Jackson¹²², M. Jackson⁷⁴, P. Jackson¹, M.R. Jaekel³⁰, V. Jain², K. Jakobs⁴⁸, S. Jakobsen³⁰,
 T. Jakoubek¹²⁷, J. Jakubek¹²⁸, D.O. Jamin¹¹⁴, D.K. Jana⁷⁹, E. Jansen⁷⁸, R.W. Jansky⁶², J. Janssen²¹,
 M. Janus¹⁷⁰, G. Jarlskog⁸¹, N. Javadov^{65,b}, T. Javůrek⁴⁸, L. Jeanty¹⁵, J. Jejelava^{51a,r}, G.-Y. Jeng¹⁵⁰,
 D. Jennens⁸⁸, P. Jenni^{48,s}, J. Jentzsch⁴³, C. Jeske¹⁷⁰, S. Jézéquel⁵, H. Ji¹⁷³, J. Jia¹⁴⁸, Y. Jiang^{33b},
 S. Jiggins⁷⁸, J. Jimenez Pena¹⁶⁷, S. Jin^{33a}, A. Jinaru^{26a}, O. Jinnouchi¹⁵⁷, M.D. Joergensen³⁶,
 P. Johansson¹³⁹, K.A. Johns⁷, K. Jon-And^{146a,146b}, G. Jones¹⁷⁰, R.W.L. Jones⁷², T.J. Jones⁷⁴,
 J. Jongmanns^{58a}, P.M. Jorge^{126a,126b}, K.D. Joshi⁸⁴, J. Jovicevic^{159a}, X. Ju¹⁷³, C.A. Jung⁴³, P. Jussel⁶²,
 A. Juste Rozas^{12,o}, M. Kaci¹⁶⁷, A. Kaczmarek³⁹, M. Kado¹¹⁷, H. Kagan¹¹¹, M. Kagan¹⁴³, S.J. Kahn⁸⁵,
 E. Kajomovitz⁴⁵, C.W. Kalderon¹²⁰, S. Kama⁴⁰, A. Kamenshchikov¹³⁰, N. Kanaya¹⁵⁵, M. Kaneda³⁰,
 S. Kaneti²⁸, V.A. Kantserov⁹⁸, J. Kanzaki⁶⁶, B. Kaplan¹¹⁰, A. Kapliy³¹, D. Kar⁵³, K. Karakostas¹⁰,
 A. Karamaoun³, N. Karastathis^{10,107}, M.J. Kareem⁵⁴, M. Karnevskiy⁸³, S.N. Karpov⁶⁵, Z.M. Karpova⁶⁵,
 K. Karthik¹¹⁰, V. Kartvelishvili⁷², A.N. Karyukhin¹³⁰, L. Kashif¹⁷³, R.D. Kass¹¹¹, A. Kastanas¹⁴,
 Y. Kataoka¹⁵⁵, A. Katre⁴⁹, J. Katzy⁴², K. Kawagoe⁷⁰, T. Kawamoto¹⁵⁵, G. Kawamura⁵⁴, S. Kazama¹⁵⁵,
 V.F. Kazanin^{109,c}, M.Y. Kazarinov⁶⁵, R. Keeler¹⁶⁹, R. Kehoe⁴⁰, J.S. Keller⁴², J.J. Kempster⁷⁷,
 H. Keoshkerian⁸⁴, O. Kepka¹²⁷, B.P. Kerševan⁷⁵, S. Kersten¹⁷⁵, R.A. Keyes⁸⁷, F. Khalil-zada¹¹,
 H. Khandanyan^{146a,146b}, A. Khanov¹¹⁴, A.G. Kharlamov^{109,c}, T.J. Khoo²⁸, V. Khovanskiy⁹⁷,
 E. Khramov⁶⁵, J. Khubua^{51b,t}, H.Y. Kim⁸, H. Kim^{146a,146b}, S.H. Kim¹⁶⁰, Y. Kim³¹, N. Kimura¹⁵⁴,
 O.M. Kind¹⁶, B.T. King⁷⁴, M. King¹⁶⁷, S.B. King¹⁶⁸, J. Kirk¹³¹, A.E. Kiryunin¹⁰¹, T. Kishimoto⁶⁷,
 D. Kisielewska^{38a}, F. Kiss⁴⁸, K. Kiuchi¹⁶⁰, O. Kivernyk¹³⁶, E. Kladiva^{144b}, M.H. Klein³⁵, M. Klein⁷⁴,
 U. Klein⁷⁴, K. Kleinknecht⁸³, P. Klimek^{146a,146b}, A. Klimentov²⁵, R. Klingenberg⁴³, J.A. Klinger¹³⁹,
 T. Klioutchnikova³⁰, E.-E. Kluge^{58a}, P. Kluit¹⁰⁷, S. Kluth¹⁰¹, E. Kneringer⁶², E.B.F.G. Knoop⁸⁵,
 A. Knue⁵³, A. Kobayashi¹⁵⁵, D. Kobayashi¹⁵⁷, T. Kobayashi¹⁵⁵, M. Kobel⁴⁴, M. Kocian¹⁴³, P. Kodys¹²⁹,
 T. Koffas²⁹, E. Koffeman¹⁰⁷, L.A. Kogan¹²⁰, S. Kohlmann¹⁷⁵, Z. Kohout¹²⁸, T. Kohriki⁶⁶, T. Koi¹⁴³,
 H. Kolanoski¹⁶, I. Koletsou⁵, A.A. Komar^{96,*}, Y. Komori¹⁵⁵, T. Kondo⁶⁶, N. Kondrashova⁴²,
 K. Köneke⁴⁸, A.C. König¹⁰⁶, S. König⁸³, T. Kono^{66,u}, R. Konoplich^{110,v}, N. Konstantinidis⁷⁸,
 R. Kopeliansky¹⁵², S. Koperny^{38a}, L. Köpke⁸³, A.K. Kopp⁴⁸, K. Korcyl³⁹, K. Kordas¹⁵⁴, A. Korn⁷⁸,
 A.A. Korol^{109,c}, I. Korolkov¹², E.V. Korolkova¹³⁹, O. Kortner¹⁰¹, S. Kortner¹⁰¹, T. Kosek¹²⁹,
 V.V. Kostyukhin²¹, V.M. Kotov⁶⁵, A. Kotwal⁴⁵, A. Kourkouveli-Charalampidi¹⁵⁴, C. Kourkouvelis⁹,
 V. Kouskoura²⁵, A. Koutsman^{159a}, R. Kowalewski¹⁶⁹, T.Z. Kowalski^{38a}, W. Kozanecki¹³⁶,
 A.S. Kozhin¹³⁰, V.A. Kramarenko⁹⁹, G. Kramberger⁷⁵, D. Krasnopevtsev⁹⁸, M.W. Krasny⁸⁰,
 A. Krasznahorkay³⁰, J.K. Kraus²¹, A. Kravchenko²⁵, S. Kreiss¹¹⁰, M. Kretz^{58c}, J. Kretzschmar⁷⁴,
 K. Kreutzfeldt⁵², P. Krieger¹⁵⁸, K. Krizka³¹, K. Kroeninger⁴³, H. Kroha¹⁰¹, J. Kroll¹²², J. Kroseberg²¹,
 J. Krstic¹³, U. Kruchonak⁶⁵, H. Krüger²¹, N. Krumnack⁶⁴, Z.V. Krumshcheyn⁶⁵, A. Kruse¹⁷³,
 M.C. Kruse⁴⁵, M. Kruskal²², T. Kubota⁸⁸, H. Kucuk⁷⁸, S. Kuday^{4c}, S. Kuehn⁴⁸, A. Kugel^{58c},
 F. Kuger¹⁷⁴, A. Kuhl¹³⁷, T. Kuhl⁴², V. Kukhtin⁶⁵, Y. Kulchitsky⁹², S. Kuleshov^{32b}, M. Kuna^{132a,132b},
 T. Kunigo⁶⁸, A. Kupco¹²⁷, H. Kurashige⁶⁷, Y.A. Kurochkin⁹², R. Kurumida⁶⁷, V. Kus¹²⁷,
 E.S. Kuwertz¹⁶⁹, M. Kuze¹⁵⁷, J. Kvita¹¹⁵, T. Kwan¹⁶⁹, D. Kyriazopoulos¹³⁹, A. La Rosa⁴⁹,
 J.L. La Rosa Navarro^{24d}, L. La Rotonda^{37a,37b}, C. Lacasta¹⁶⁷, F. Lacava^{132a,132b}, J. Lacey²⁹, H. Lacker¹⁶,
 D. Lacour⁸⁰, V.R. Lacuesta¹⁶⁷, E. Ladygin⁶⁵, R. Lafaye⁵, B. Laforge⁸⁰, T. Lagouri¹⁷⁶, S. Lai⁴⁸,
 L. Lambourne⁷⁸, S. Lammers⁶¹, C.L. Lampen⁷, W. Lampl⁷, E. Lançon¹³⁶, U. Landgraf⁴⁸,
 M.P.J. Landon⁷⁶, V.S. Lang^{58a}, J.C. Lange¹², A.J. Lankford¹⁶³, F. Lanni²⁵, K. Lantzsch³⁰, A. Lanza^{121a},
 S. Laplace⁸⁰, C. Lapoire³⁰, J.F. Laporte¹³⁶, T. Lari^{91a}, F. Lasagni Manghi^{20a,20b}, M. Lassnig³⁰,
 P. Laurelli⁴⁷, W. Lavrijsen¹⁵, A.T. Law¹³⁷, P. Laycock⁷⁴, T. Lazovich⁵⁷, O. Le Dortz⁸⁰, E. Le Guirriec⁸⁵,
 E. Le Menedeu¹², M. LeBlanc¹⁶⁹, T. LeCompte⁶, F. Ledroit-Guillon⁵⁵, C.A. Lee^{145b}, S.C. Lee¹⁵¹,
 L. Lee¹, G. Lefebvre⁸⁰, M. Lefebvre¹⁶⁹, F. Legger¹⁰⁰, C. Leggett¹⁵, A. Lehan⁷⁴, G. Lehmann Miotto³⁰,
 X. Lei⁷, W.A. Leight²⁹, A. Leisos^{154,w}, A.G. Leister¹⁷⁶, M.A.L. Leite^{24d}, R. Leitner¹²⁹, D. Lellouch¹⁷²,
 B. Lemmer⁵⁴, K.J.C. Leney⁷⁸, T. Lenz²¹, B. Lenzi³⁰, R. Leone⁷, S. Leone^{124a,124b}, C. Leonidopoulos⁴⁶,

S. Leontsinis¹⁰, C. Leroy⁹⁵, C.G. Lester²⁸, M. Levchenko¹²³, J. Levêque⁵, D. Levin⁸⁹, L.J. Levinson¹⁷²,
 M. Levy¹⁸, A. Lewis¹²⁰, A.M. Leyko²¹, M. Leyton⁴¹, B. Li^{33b,x}, H. Li¹⁴⁸, H.L. Li³¹, L. Li⁴⁵, L. Li^{33e},
 S. Li⁴⁵, Y. Li^{33c,y}, Z. Liang¹³⁷, H. Liao³⁴, B. Liberti^{133a}, A. Liblong¹⁵⁸, P. Lichard³⁰, K. Lie¹⁶⁵,
 J. Liebal²¹, W. Liebig¹⁴, C. Limbach²¹, A. Limosani¹⁵⁰, S.C. Lin^{151,z}, T.H. Lin⁸³, F. Linde¹⁰⁷,
 B.E. Lindquist¹⁴⁸, J.T. Linnemann⁹⁰, E. Lipeles¹²², A. Lipniacka¹⁴, M. Lisovyi^{58b}, T.M. Liss¹⁶⁵,
 D. Lissauer²⁵, A. Lister¹⁶⁸, A.M. Litke¹³⁷, B. Liu^{151,aa}, D. Liu¹⁵¹, H. Liu⁸⁹, J. Liu⁸⁵, J.B. Liu^{33b},
 K. Liu⁸⁵, L. Liu¹⁶⁵, M. Liu⁴⁵, M. Liu^{33b}, Y. Liu^{33b}, M. Livan^{121a,121b}, A. Lleres⁵⁵, J. Llorente Merino⁸²,
 S.L. Lloyd⁷⁶, F. Lo Sterzo¹⁵¹, E. Lobodzinska⁴², P. Loch⁷, W.S. Lockman¹³⁷, F.K. Loebinger⁸⁴,
 A.E. Loevschall-Jensen³⁶, A. Loginov¹⁷⁶, T. Lohse¹⁶, K. Lohwasser⁴², M. Lokajicek¹²⁷, B.A. Long²²,
 J.D. Long⁸⁹, R.E. Long⁷², K.A. Looper¹¹¹, L. Lopes^{126a}, D. Lopez Mateos⁵⁷, B. Lopez Paredes¹³⁹,
 I. Lopez Paz¹², J. Lorenz¹⁰⁰, N. Lorenzo Martinez⁶¹, M. Losada¹⁶², P. Loscutoff¹⁵, P.J. Lösel¹⁰⁰,
 X. Lou^{33a}, A. Lounis¹¹⁷, J. Love⁶, P.A. Love⁷², N. Lu⁸⁹, H.J. Lubatti¹³⁸, C. Luci^{132a,132b}, A. Lucotte⁵⁵,
 F. Luehring⁶¹, W. Lukas⁶², L. Luminari^{132a}, O. Lundberg^{146a,146b}, B. Lund-Jensen¹⁴⁷, D. Lynn²⁵,
 R. Lysak¹²⁷, E. Lytken⁸¹, H. Ma²⁵, L.L. Ma^{33d}, G. Maccarrone⁴⁷, A. Macchiolo¹⁰¹, C.M. Macdonald¹³⁹,
 J. Machado Miguens^{122,126b}, D. Macina³⁰, D. Madaffari⁸⁵, R. Madar³⁴, H.J. Maddocks⁷², W.F. Mader⁴⁴,
 A. Madsen¹⁶⁶, S. Maeland¹⁴, T. Maeno²⁵, A. Maevskiy⁹⁹, E. Magradze⁵⁴, K. Mahboubi⁴⁸,
 J. Mahlstedt¹⁰⁷, C. Maiani¹³⁶, C. Maidantchik^{24a}, A.A. Maier¹⁰¹, T. Maier¹⁰⁰, A. Maio^{126a,126b,126d},
 S. Majewski¹¹⁶, Y. Makida⁶⁶, N. Makovec¹¹⁷, B. Malaescu⁸⁰, Pa. Malecki³⁹, V.P. Maleev¹²³, F. Malek⁵⁵,
 U. Mallik⁶³, D. Malon⁶, C. Malone¹⁴³, S. Maltezos¹⁰, V.M. Malyshev¹⁰⁹, S. Malyukov³⁰, J. Mamuzic⁴²,
 G. Mancini⁴⁷, B. Mandelli³⁰, L. Mandelli^{91a}, I. Mandić⁷⁵, R. Mandrysch⁶³, J. Maneira^{126a,126b},
 A. Manfredini¹⁰¹, L. Manhaes de Andrade Filho^{24b}, J. Manjarres Ramos^{159b}, A. Mann¹⁰⁰,
 P.M. Manning¹³⁷, A. Manousakis-Katsikakis⁹, B. Mansoulié¹³⁶, R. Mantifel⁸⁷, M. Mantoani⁵⁴,
 L. Mapelli³⁰, L. March^{145c}, G. Marchiori⁸⁰, M. Marcisovsky¹²⁷, C.P. Marino¹⁶⁹, M. Marjanovic¹³,
 D.E. Marley⁸⁹, F. Marroquim^{24a}, S.P. Marsden⁸⁴, Z. Marshall¹⁵, L.F. Marti¹⁷, S. Marti-Garcia¹⁶⁷,
 B. Martin⁹⁰, T.A. Martin¹⁷⁰, V.J. Martin⁴⁶, B. Martin dit Latour¹⁴, M. Martinez^{12,o}, S. Martin-Haugh¹³¹,
 V.S. Martoiu^{26a}, A.C. Martyniuk⁷⁸, M. Marx¹³⁸, F. Marzano^{132a}, A. Marzin³⁰, L. Masetti⁸³,
 T. Mashimo¹⁵⁵, R. Mashinistov⁹⁶, J. Masik⁸⁴, A.L. Maslennikov^{109,c}, I. Massa^{20a,20b}, L. Massa^{20a,20b},
 N. Massol⁵, P. Mastrandrea¹⁴⁸, A. Mastroberardino^{37a,37b}, T. Masubuchi¹⁵⁵, P. Mättig¹⁷⁵, J. Mattmann⁸³,
 J. Maurer^{26a}, S.J. Maxfield⁷⁴, D.A. Maximov^{109,c}, R. Mazini¹⁵¹, S.M. Mazza^{91a,91b},
 L. Mazzaferro^{133a,133b}, G. Mc Goldrick¹⁵⁸, S.P. Mc Kee⁸⁹, A. McCarn⁸⁹, R.L. McCarthy¹⁴⁸,
 T.G. McCarthy²⁹, N.A. McCubbin¹³¹, K.W. McFarlane^{56,*}, J.A. McFayden⁷⁸, G. Mchedlidze⁵⁴,
 S.J. McMahon¹³¹, R.A. McPherson^{169,k}, M. Medinnis⁴², S. Meehan^{145a}, S. Mehlhase¹⁰⁰, A. Mehta⁷⁴,
 K. Meier^{58a}, C. Meineck¹⁰⁰, B. Meirose⁴¹, B.R. Mellado Garcia^{145c}, F. Meloni¹⁷, A. Mengarelli^{20a,20b},
 S. Menke¹⁰¹, E. Meoni¹⁶¹, K.M. Mercurio⁵⁷, S. Mergelmeyer²¹, P. Mermoud⁴⁹, L. Merola^{104a,104b},
 C. Meroni^{91a}, F.S. Merritt³¹, A. Messina^{132a,132b}, J. Metcalfe²⁵, A.S. Mete¹⁶³, C. Meyer⁸³, C. Meyer¹²²,
 J-P. Meyer¹³⁶, J. Meyer¹⁰⁷, R.P. Middleton¹³¹, S. Miglioranza^{164a,164c}, L. Mijović²¹, G. Mikenberg¹⁷²,
 M. Mikestikova¹²⁷, M. Mikuž⁷⁵, M. Milesi⁸⁸, A. Milic³⁰, D.W. Miller³¹, C. Mills⁴⁶, A. Milov¹⁷²,
 D.A. Milstead^{146a,146b}, A.A. Minaenko¹³⁰, Y. Minami¹⁵⁵, I.A. Minashvili⁶⁵, A.I. Mincer¹¹⁰,
 B. Mindur^{38a}, M. Mineev⁶⁵, Y. Ming¹⁷³, L.M. Mir¹², T. Mitani¹⁷¹, J. Mitrevski¹⁰⁰, V.A. Mitsou¹⁶⁷,
 A. Miucci⁴⁹, P.S. Miyagawa¹³⁹, J.U. Mjörnmark⁸¹, T. Moa^{146a,146b}, K. Mochizuki⁸⁵, S. Mohapatra³⁵,
 W. Mohr⁴⁸, S. Molander^{146a,146b}, R. Moles-Valls¹⁶⁷, K. Mönig⁴², C. Monini⁵⁵, J. Monk³⁶, E. Monnier⁸⁵,
 J. Montejo Berlingen¹², F. Monticelli⁷¹, S. Monzani^{132a,132b}, R.W. Moore³, N. Morange¹¹⁷,
 D. Moreno¹⁶², M. Moreno Llácer⁵⁴, P. Morettini^{50a}, M. Morgenstern⁴⁴, M. Morii⁵⁷, M. Morinaga¹⁵⁵,
 V. Morisbak¹¹⁹, S. Moritz⁸³, A.K. Morley¹⁴⁷, G. Mornacchi³⁰, J.D. Morris⁷⁶, S.S. Mortensen³⁶,
 A. Morton⁵³, L. Morvaj¹⁰³, M. Mosidze^{51b}, J. Moss¹¹¹, K. Motohashi¹⁵⁷, R. Mount¹⁴³, E. Mountricha²⁵,
 S.V. Mouraviev^{96,*}, E.J.W. Moyse⁸⁶, S. Muanza⁸⁵, R.D. Mudd¹⁸, F. Mueller¹⁰¹, J. Mueller¹²⁵,
 K. Mueller²¹, R.S.P. Mueller¹⁰⁰, T. Mueller²⁸, D. Muenstermann⁴⁹, P. Mullen⁵³, G.A. Mullier¹⁷,

Y. Munwes¹⁵³, J.A. Murillo Quijada¹⁸, W.J. Murray^{170,131}, H. Musheghyan⁵⁴, E. Musto¹⁵²,
 A.G. Myagkov^{130.ab}, M. Myska¹²⁸, O. Nackenhorst⁵⁴, J. Nadal⁵⁴, K. Nagai¹²⁰, R. Nagai¹⁵⁷, Y. Nagai⁸⁵,
 K. Nagano⁶⁶, A. Nagarkar¹¹¹, Y. Nagasaka⁵⁹, K. Nagata¹⁶⁰, M. Nagel¹⁰¹, E. Nagy⁸⁵, A.M. Nairz³⁰,
 Y. Nakahama³⁰, K. Nakamura⁶⁶, T. Nakamura¹⁵⁵, I. Nakano¹¹², H. Namasivayam⁴¹,
 R.F. Naranjo Garcia⁴², R. Narayan³¹, T. Naumann⁴², G. Navarro¹⁶², R. Nayyar⁷, H.A. Neal⁸⁹,
 P.Yu. Nechaeva⁹⁶, T.J. Neep⁸⁴, P.D. Nef¹⁴³, A. Negri^{121a,121b}, M. Negrini^{20a}, S. Nektarijevic¹⁰⁶,
 C. Nellist¹¹⁷, A. Nelson¹⁶³, S. Nemecek¹²⁷, P. Nemethy¹¹⁰, A.A. Nepomuceno^{24a}, M. Nessi^{30.ac},
 M.S. Neubauer¹⁶⁵, M. Neumann¹⁷⁵, R.M. Neves¹¹⁰, P. Nevski²⁵, P.R. Newman¹⁸, D.H. Nguyen⁶,
 R.B. Nickerson¹²⁰, R. Nicolaidou¹³⁶, B. Nicquevert³⁰, J. Nielsen¹³⁷, N. Nikiforou³⁵, A. Nikiforov¹⁶,
 V. Nikolaenko^{130.ab}, I. Nikolic-Audit⁸⁰, K. Nikolopoulos¹⁸, J.K. Nilsen¹¹⁹, P. Nilsson²⁵, Y. Ninomiya¹⁵⁵,
 A. Nisati^{132a}, R. Nisius¹⁰¹, T. Nobe¹⁵⁷, M. Nomachi¹¹⁸, I. Nomidis²⁹, T. Nooney⁷⁶, S. Norberg¹¹³,
 M. Nordberg³⁰, O. Novgorodova⁴⁴, S. Nowak¹⁰¹, M. Nozaki⁶⁶, L. Nozka¹¹⁵, K. Ntekas¹⁰,
 G. Nunes Hanninger⁸⁸, T. Nunnemann¹⁰⁰, E. Nurse⁷⁸, F. Nuti⁸⁸, B.J. O'Brien⁴⁶, F. O'grady⁷,
 D.C. O'Neil¹⁴², V. O'Shea⁵³, F.G. Oakham^{29.d}, H. Oberlack¹⁰¹, T. Obermann²¹, J. Ocariz⁸⁰, A. Ochi⁶⁷,
 I. Ochoa⁷⁸, J.P. Ochoa-Ricoux^{32a}, S. Oda⁷⁰, S. Odaka⁶⁶, H. Ogren⁶¹, A. Oh⁸⁴, S.H. Oh⁴⁵, C.C. Ohm¹⁵,
 H. Ohman¹⁶⁶, H. Oide³⁰, W. Okamura¹¹⁸, H. Okawa¹⁶⁰, Y. Okumura³¹, T. Okuyama¹⁵⁵, A. Olariu^{26a},
 S.A. Olivares Pino⁴⁶, D. Oliveira Damazio²⁵, E. Oliver Garcia¹⁶⁷, A. Olszewski³⁹, J. Olszowska³⁹,
 A. Onofre^{126a,126e}, P.U.E. Onyisi^{31.g}, C.J. Oram^{159a}, M.J. Oreglia³¹, Y. Oren¹⁵³, D. Orestano^{134a,134b},
 N. Orlando¹⁵⁴, C. Oropeza Barrera⁵³, R.S. Orr¹⁵⁸, B. Osculati^{50a,50b}, R. Ospanov⁸⁴,
 G. Otero y Garzon²⁷, H. Otono⁷⁰, M. Ouchrif^{135d}, E.A. Ouellette¹⁶⁹, F. Ould-Saada¹¹⁹, A. Ouraou¹³⁶,
 K.P. Oussoren¹⁰⁷, Q. Ouyang^{33a}, A. Ovcharova¹⁵, M. Owen⁵³, R.E. Owen¹⁸, V.E. Ozcan^{19a}, N. Ozturk⁸,
 K. Pachal¹⁴², A. Pacheco Pages¹², C. Padilla Aranda¹², M. Pagáčová⁴⁸, S. Pagan Griso¹⁵, E. Paganis¹³⁹,
 C. Pahl¹⁰¹, F. Paige²⁵, P. Pais⁸⁶, K. Pajchel¹¹⁹, G. Palacino^{159b}, S. Palestini³⁰, M. Palka^{38b}, D. Pallin³⁴,
 A. Palma^{126a,126b}, Y.B. Pan¹⁷³, E. Panagiotopoulou¹⁰, C.E. Pandini⁸⁰, J.G. Panduro Vazquez⁷⁷,
 P. Pani^{146a,146b}, S. Panitkin²⁵, D. Pantea^{26a}, L. Paolozzi⁴⁹, Th.D. Papadopoulou¹⁰, K. Papageorgiou¹⁵⁴,
 A. Paramonov⁶, D. Paredes Hernandez¹⁵⁴, M.A. Parker²⁸, K.A. Parker¹³⁹, F. Parodi^{50a,50b},
 J.A. Parsons³⁵, U. Parzefall⁴⁸, E. Pasqualucci^{132a}, S. Passaggio^{50a}, F. Pastore^{134a,134b,*}, Fr. Pastore⁷⁷,
 G. Pásztor²⁹, S. Pataria¹⁷⁵, N.D. Patel¹⁵⁰, J.R. Pater⁸⁴, T. Pauly³⁰, J. Pearce¹⁶⁹, B. Pearson¹¹³,
 L.E. Pedersen³⁶, M. Pedersen¹¹⁹, S. Pedraza Lopez¹⁶⁷, R. Pedro^{126a,126b}, S.V. Peleganchuk^{109.c},
 D. Pelikan¹⁶⁶, O. Penc¹²⁷, H. Peng^{33b}, B. Penning³¹, J. Penwell⁶¹, D.V. Perepelitsa²⁵,
 E. Perez Codina^{159a}, M.T. Pérez García-Estañ¹⁶⁷, L. Perini^{91a,91b}, H. Pernegger³⁰, S. Perrella^{104a,104b},
 R. Peschke⁴², V.D. Peshekhonov⁶⁵, K. Peters³⁰, R.F.Y. Peters⁸⁴, B.A. Petersen³⁰, T.C. Petersen³⁶,
 E. Petit⁴², A. Petridis^{146a,146b}, C. Petridou¹⁵⁴, E. Petrolo^{132a}, F. Petrucci^{134a,134b}, N.E. Pettersson¹⁵⁷,
 R. Pezoa^{32b}, P.W. Phillips¹³¹, G. Piacquadio¹⁴³, E. Pianori¹⁷⁰, A. Picazio⁴⁹, E. Piccaro⁷⁶,
 M. Piccinini^{20a,20b}, M.A. Pickering¹²⁰, R. Piegaia²⁷, D.T. Pignotti¹¹¹, J.E. Pilcher³¹, A.D. Pilkington⁸⁴,
 J. Pina^{126a,126b,126d}, M. Pinamonti^{164a,164c.ad}, J.L. Pinfold³, A. Pingel³⁶, B. Pinto^{126a}, S. Pires⁸⁰,
 H. Pirumov⁴², M. Pitt¹⁷², C. Pizio^{91a,91b}, L. Plazak^{144a}, M.-A. Pleier²⁵, V. Pleskot¹²⁹, E. Plotnikova⁶⁵,
 P. Plucinski^{146a,146b}, D. Pluth⁶⁴, R. Poettgen^{146a,146b}, L. Poggioli¹¹⁷, D. Pohl²¹, G. Polesello^{121a},
 A. Poley⁴², A. Policicchio^{37a,37b}, R. Polifka¹⁵⁸, A. Polini^{20a}, C.S. Pollard⁵³, V. Polychronakos²⁵,
 K. Pommès³⁰, L. Pontecorvo^{132a}, B.G. Pope⁹⁰, G.A. Popeneciu^{26b}, D.S. Popovic¹³, A. Poppleton³⁰,
 S. Pospisil¹²⁸, K. Potamianos¹⁵, I.N. Potrap⁶⁵, C.J. Potter¹⁴⁹, C.T. Potter¹¹⁶, G. Poulard³⁰, J. Poveda³⁰,
 V. Pozdnyakov⁶⁵, P. Pralavorio⁸⁵, A. Pranko¹⁵, S. Prasad³⁰, S. Prell⁶⁴, D. Price⁸⁴, L.E. Price⁶,
 M. Primavera^{73a}, S. Prince⁸⁷, M. Proissl⁴⁶, K. Prokofiev^{60c}, F. Prokoshin^{32b}, E. Protopapadaki¹³⁶,
 S. Protopopescu²⁵, J. Proudfoot⁶, M. Przybycien^{38a}, E. Ptacek¹¹⁶, D. Puddu^{134a,134b}, E. Pueschel⁸⁶,
 D. Puldon¹⁴⁸, M. Purohit^{25.ae}, P. Puzo¹¹⁷, J. Qian⁸⁹, G. Qin⁵³, Y. Qin⁸⁴, A. Quadt⁵⁴, D.R. Quarrie¹⁵,
 W.B. Quayle^{164a,164b}, M. Queitsch-Maitland⁸⁴, D. Quilty⁵³, S. Raddum¹¹⁹, V. Radeka²⁵, V. Radescu⁴²,
 S.K. Radhakrishnan¹⁴⁸, P. Radloff¹¹⁶, P. Rados⁸⁸, F. Ragusa^{91a,91b}, G. Rahal¹⁷⁸, S. Rajagopalan²⁵,

M. Rammensee³⁰, C. Rangel-Smith¹⁶⁶, F. Rauscher¹⁰⁰, S. Rave⁸³, T. Ravenscroft⁵³, M. Raymond³⁰,
A.L. Read¹¹⁹, N.P. Readioff⁷⁴, D.M. Rebutzi^{121a,121b}, A. Redelbach¹⁷⁴, G. Redlinger²⁵, R. Reece¹³⁷,
K. Reeves⁴¹, L. Rehnisch¹⁶, H. Reisin²⁷, M. Relich¹⁶³, C. Rembser³⁰, H. Ren^{33a}, A. Renaud¹¹⁷,
M. Rescigno^{132a}, S. Resconi^{91a}, O.L. Rezanova^{109,c}, P. Reznicek¹²⁹, R. Rezvani⁹⁵, R. Richter¹⁰¹,
S. Richter⁷⁸, E. Richter-Was^{38b}, O. Ricken²¹, M. Ridel⁸⁰, P. Rieck¹⁶, C.J. Riegel¹⁷⁵, J. Rieger⁵⁴,
M. Rijssenbeek¹⁴⁸, A. Rimoldi^{121a,121b}, L. Rinaldi^{20a}, B. Ristić⁴⁹, E. Ritsch³⁰, I. Riu¹²,
F. Rizatdinova¹¹⁴, E. Rizvi⁷⁶, S.H. Robertson^{87,k}, A. Robichaud-Veronneau⁸⁷, D. Robinson²⁸,
J.E.M. Robinson⁸⁴, A. Robson⁵³, C. Roda^{124a,124b}, S. Roe³⁰, O. Røhne¹¹⁹, S. Rolli¹⁶¹, A. Romaniouk⁹⁸,
M. Romano^{20a,20b}, S.M. Romano Saez³⁴, E. Romero Adam¹⁶⁷, N. Rompotis¹³⁸, M. Ronzani⁴⁸,
L. Roos⁸⁰, E. Ros¹⁶⁷, S. Rosati^{132a}, K. Rosbach⁴⁸, P. Rose¹³⁷, P.L. Rosendahl¹⁴, O. Rosenthal¹⁴¹,
V. Rossetti^{146a,146b}, E. Rossi^{104a,104b}, L.P. Rossi^{50a}, R. Rosten¹³⁸, M. Rotaru^{26a}, I. Roth¹⁷²,
J. Rothberg¹³⁸, D. Rousseau¹¹⁷, C.R. Royon¹³⁶, A. Rozanov⁸⁵, Y. Rozen¹⁵², X. Ruan^{145c}, F. Rubbo¹⁴³,
I. Rubinskiy⁴², V.I. Rud⁹⁹, C. Rudolph⁴⁴, M.S. Rudolph¹⁵⁸, F. Rühr⁴⁸, A. Ruiz-Martinez³⁰,
Z. Rurikova⁴⁸, N.A. Rusakovich⁶⁵, A. Ruschke¹⁰⁰, H.L. Russell¹³⁸, J.P. Rutherford⁷, N. Ruthmann⁴⁸,
Y.F. Ryabov¹²³, M. Rybar¹²⁹, G. Rybkin¹¹⁷, N.C. Ryder¹²⁰, A.F. Saavedra¹⁵⁰, G. Sabato¹⁰⁷,
S. Sacerdoti²⁷, A. Saddique³, H.F.-W. Sadrozinski¹³⁷, R. Sadykov⁶⁵, F. Safai Tehrani^{132a},
M. Saimpert¹³⁶, H. Sakamoto¹⁵⁵, Y. Sakurai¹⁷¹, G. Salamanna^{134a,134b}, A. Salamon^{133a}, M. Saleem¹¹³,
D. Salek¹⁰⁷, P.H. Sales De Bruin¹³⁸, D. Salihagic¹⁰¹, A. Salnikov¹⁴³, J. Salt¹⁶⁷, D. Salvatore^{37a,37b},
F. Salvatore¹⁴⁹, A. Salvucci¹⁰⁶, A. Salzburger³⁰, D. Sampsonidis¹⁵⁴, A. Sanchez^{104a,104b}, J. Sánchez¹⁶⁷,
V. Sanchez Martinez¹⁶⁷, H. Sandaker¹⁴, R.L. Sandbach⁷⁶, H.G. Sander⁸³, M.P. Sanders¹⁰⁰,
M. Sandhoff¹⁷⁵, C. Sandoval¹⁶², R. Sandstroem¹⁰¹, D.P.C. Sankey¹³¹, M. Sannino^{50a,50b}, A. Sansoni⁴⁷,
C. Santoni³⁴, R. Santonico^{133a,133b}, H. Santos^{126a}, I. Santoyo Castillo¹⁴⁹, K. Sapp¹²⁵, A. Sapronov⁶⁵,
J.G. Saraiva^{126a,126d}, B. Sarrazin²¹, O. Sasaki⁶⁶, Y. Sasaki¹⁵⁵, K. Sato¹⁶⁰, G. Sauvage^{5,*}, E. Sauvan⁵,
G. Savage⁷⁷, P. Savard^{158,d}, C. Sawyer¹³¹, L. Sawyer^{79,n}, J. Saxon³¹, C. Sbarra^{20a}, A. Sbrizzi^{20a,20b},
T. Scanlon⁷⁸, D.A. Scannicchio¹⁶³, M. Scarcella¹⁵⁰, V. Scarfone^{37a,37b}, J. Schaarschmidt¹⁷²,
P. Schacht¹⁰¹, D. Schaefer³⁰, R. Schaefer⁴², J. Schaeffer⁸³, S. Schaepe²¹, S. Schaezel^{58b}, U. Schäfer⁸³,
A.C. Schaffer¹¹⁷, D. Schaile¹⁰⁰, R.D. Schamberger¹⁴⁸, V. Scharf^{58a}, V.A. Schegelsky¹²³, D. Scheirich¹²⁹,
M. Schernau¹⁶³, C. Schiavi^{50a,50b}, C. Schillo⁴⁸, M. Schioppa^{37a,37b}, S. Schlenker³⁰, E. Schmidt⁴⁸,
K. Schmieden³⁰, C. Schmitt⁸³, S. Schmitt^{58b}, S. Schmitt⁴², B. Schneider^{159a}, Y.J. Schnellbach⁷⁴,
U. Schnoor⁴⁴, L. Schoeffel¹³⁶, A. Schoening^{58b}, B.D. Schoenrock⁹⁰, E. Schopf²¹,
A.L.S. Schorlemmer⁵⁴, M. Schott⁸³, D. Schouten^{159a}, J. Schovancova⁸, S. Schramm¹⁵⁸, M. Schreyer¹⁷⁴,
C. Schroeder⁸³, N. Schuh⁸³, M.J. Schultens²¹, H.-C. Schultz-Coulon^{58a}, H. Schulz¹⁶, M. Schumacher⁴⁸,
B.A. Schumm¹³⁷, Ph. Schune¹³⁶, C. Schwanenberger⁸⁴, A. Schwartzman¹⁴³, T.A. Schwarz⁸⁹,
Ph. Schwegler¹⁰¹, Ph. Schwemling¹³⁶, R. Schwienhorst⁹⁰, J. Schwindling¹³⁶, T. Schwindt²¹,
F.G. Sciacca¹⁷, E. Scifo¹¹⁷, G. Sciolla²³, F. Scuri^{124a,124b}, F. Scutti²¹, J. Searcy⁸⁹, G. Sedov⁴²,
E. Sedykh¹²³, P. Seema²¹, S.C. Seidel¹⁰⁵, A. Seiden¹³⁷, F. Seifert¹²⁸, J.M. Seixas^{24a}, G. Sekhniaidze^{104a},
K. Sekhon⁸⁹, S.J. Sekula⁴⁰, D.M. Seliverstov^{123,*}, N. Semprini-Cesari^{20a,20b}, C. Serfon³⁰, L. Serin¹¹⁷,
L. Serkin^{164a,164b}, T. Serre⁸⁵, M. Sessa^{134a,134b}, R. Seuster^{159a}, H. Severini¹¹³, T. Sfiligoj⁷⁵, F. Sforza³⁰,
A. Sfyrla³⁰, E. Shabalina⁵⁴, M. Shamim¹¹⁶, L.Y. Shan^{33a}, R. Shang¹⁶⁵, J.T. Shank²², M. Shapiro¹⁵,
P.B. Shatalov⁹⁷, K. Shaw^{164a,164b}, S.M. Shaw⁸⁴, A. Shcherbakova^{146a,146b}, C.Y. Shehu¹⁴⁹, P. Sherwood⁷⁸,
L. Shi^{151,af}, S. Shimizu⁶⁷, C.O. Shimmin¹⁶³, M. Shimojima¹⁰², M. Shiyakova⁶⁵, A. Shmeleva⁹⁶,
D. Shoaleh Saadi⁹⁵, M.J. Shochet³¹, S. Shojaii^{91a,91b}, S. Shrestha¹¹¹, E. Shulga⁹⁸, M.A. Shupe⁷,
S. Shushkevich⁴², P. Sicho¹²⁷, O. Sidiropoulou¹⁷⁴, D. Sidorov¹¹⁴, A. Sidoti^{20a,20b}, F. Siegert⁴⁴,
Dj. Sijacki¹³, J. Silva^{126a,126d}, Y. Silver¹⁵³, S.B. Silverstein^{146a}, V. Simak¹²⁸, O. Simard⁵, Lj. Simic¹³,
S. Simion¹¹⁷, E. Simioni⁸³, B. Simmons⁷⁸, D. Simon³⁴, R. Simoniello^{91a,91b}, P. Sinervo¹⁵⁸,
N.B. Sinev¹¹⁶, G. Siragusa¹⁷⁴, A.N. Sisakyan^{65,*}, S.Yu. Sivoklov⁹⁹, J. Sjölin^{146a,146b}, T.B. Sjørnsen¹⁴,
M.B. Skinner⁷², H.P. Skottowe⁵⁷, P. Skubic¹¹³, M. Slater¹⁸, T. Slavicek¹²⁸, M. Slawinska¹⁰⁷,

K. Sliwa¹⁶¹, V. Smakhtin¹⁷², B.H. Smart⁴⁶, L. Smestad¹⁴, S.Yu. Smirnov⁹⁸, Y. Smirnov⁹⁸,
 L.N. Smirnova^{99.ag}, O. Smirnova⁸¹, M.N.K. Smith³⁵, R.W. Smith³⁵, M. Smizanska⁷², K. Smolek¹²⁸,
 A.A. Snesarev⁹⁶, G. Snidero⁷⁶, S. Snyder²⁵, R. Sobie^{169.k}, F. Socher⁴⁴, A. Soffer¹⁵³, D.A. Soh^{151.af},
 C.A. Solans³⁰, M. Solar¹²⁸, J. Solc¹²⁸, E.Yu. Soldatov⁹⁸, U. Soldevila¹⁶⁷, A.A. Solodkov¹³⁰,
 A. Soloshenko⁶⁵, O.V. Solovyanov¹³⁰, V. Solovyev¹²³, P. Sommer⁴⁸, H.Y. Song^{33b}, N. Soni¹, A. Sood¹⁵,
 A. Sopczak¹²⁸, B. Sopko¹²⁸, V. Sopko¹²⁸, V. Sorin¹², D. Sosa^{58b}, M. Sosebee⁸,
 C.L. Sotiropoulou^{124a,124b}, R. Soualah^{164a,164c}, A.M. Soukharev^{109.c}, D. South⁴², B.C. Sowden⁷⁷,
 S. Spagnolo^{73a,73b}, M. Spalla^{124a,124b}, F. Spanò⁷⁷, W.R. Spearman⁵⁷, F. Spettel¹⁰¹, R. Spighi^{20a},
 G. Spigo³⁰, L.A. Spiller⁸⁸, M. Spousta¹²⁹, T. Spreitzer¹⁵⁸, R.D. St. Denis^{53,*}, S. Staerz⁴⁴, J. Stahlman¹²²,
 R. Stamen^{58a}, S. Stamm¹⁶, E. Stanecka³⁹, C. Stanescu^{134a}, M. Stanescu-Bellu⁴², M.M. Stanitzki⁴²,
 S. Stapnes¹¹⁹, E.A. Starchenko¹³⁰, J. Stark⁵⁵, P. Staroba¹²⁷, P. Starovoitov⁴², R. Staszewski³⁹,
 P. Stavina^{144a,*}, P. Steinberg²⁵, B. Stelzer¹⁴², H.J. Stelzer³⁰, O. Stelzer-Chilton^{159a}, H. Stenzel⁵²,
 S. Stern¹⁰¹, G.A. Stewart⁵³, J.A. Stillings²¹, M.C. Stockton⁸⁷, M. Stoebe⁸⁷, G. Stoicea^{26a}, P. Stolte⁵⁴,
 S. Stonjek¹⁰¹, A.R. Stradling⁸, A. Straessner⁴⁴, M.E. Stramaglia¹⁷, J. Strandberg¹⁴⁷,
 S. Strandberg^{146a,146b}, A. Strandlie¹¹⁹, E. Strauss¹⁴³, M. Strauss¹¹³, P. Strizenec^{144b}, R. Ströhmer¹⁷⁴,
 D.M. Strom¹¹⁶, R. Stroynowski⁴⁰, A. Strubig¹⁰⁶, S.A. Stucci¹⁷, B. Stugu¹⁴, N.A. Styles⁴², D. Su¹⁴³,
 J. Su¹²⁵, R. Subramaniam⁷⁹, A. Succurro¹², Y. Sugaya¹¹⁸, C. Suhr¹⁰⁸, M. Suk¹²⁸, V.V. Sulin⁹⁶,
 S. Sultansoy^{4d}, T. Sumida⁶⁸, S. Sun⁵⁷, X. Sun^{33a}, J.E. Sundermann⁴⁸, K. Suruliz¹⁴⁹, G. Susinno^{37a,37b},
 M.R. Sutton¹⁴⁹, S. Suzuki⁶⁶, Y. Suzuki⁶⁶, M. Svatos¹²⁷, S. Swedish¹⁶⁸, M. Swiatlowski¹⁴³, I. Sykora^{144a},
 T. Sykora¹²⁹, D. Ta⁹⁰, C. Taccini^{134a,134b}, K. Tackmann⁴², J. Taenzer¹⁵⁸, A. Taffard¹⁶³, R. Tafirout^{159a},
 N. Taiblum¹⁵³, H. Takai²⁵, R. Takashima⁶⁹, H. Takeda⁶⁷, T. Takeshita¹⁴⁰, Y. Takubo⁶⁶, M. Talby⁸⁵,
 A.A. Talyshev^{109.c}, J.Y.C. Tam¹⁷⁴, K.G. Tan⁸⁸, J. Tanaka¹⁵⁵, R. Tanaka¹¹⁷, S. Tanaka⁶⁶,
 B.B. Tannenwald¹¹¹, N. Tannoury²¹, S. Tapprogge⁸³, S. Tarem¹⁵², F. Tarrade²⁹, G.F. Tartarelli^{91a},
 P. Tas¹²⁹, M. Tasevsky¹²⁷, T. Tashiro⁶⁸, E. Tassi^{37a,37b}, A. Tavares Delgado^{126a,126b}, Y. Tayalati^{135d},
 F.E. Taylor⁹⁴, G.N. Taylor⁸⁸, W. Taylor^{159b}, F.A. Teischinger³⁰, M. Teixeira Dias Castanheira⁷⁶,
 P. Teixeira-Dias⁷⁷, K.K. Temming⁴⁸, H. Ten Kate³⁰, P.K. Teng¹⁵¹, J.J. Teoh¹¹⁸, F. Tepel¹⁷⁵, S. Terada⁶⁶,
 K. Terashi¹⁵⁵, J. Terron⁸², S. Terzo¹⁰¹, M. Testa⁴⁷, R.J. Teuscher^{158,k}, J. Therhaag²¹,
 T. Thevenaux-Pelzer³⁴, J.P. Thomas¹⁸, J. Thomas-Wilsker⁷⁷, E.N. Thompson³⁵, P.D. Thompson¹⁸,
 R.J. Thompson⁸⁴, A.S. Thompson⁵³, L.A. Thomsen¹⁷⁶, E. Thomson¹²², M. Thomson²⁸, R.P. Thun^{89,*},
 M.J. Tibbets¹⁵, R.E. Ticse Torres⁸⁵, V.O. Tikhomirov^{96.ah}, Yu.A. Tikhonov^{109.c}, S. Timoshenko⁹⁸,
 E. Tiouchichine⁸⁵, P. Tipton¹⁷⁶, S. Tisserant⁸⁵, T. Todorov^{5,*}, S. Todorova-Nova¹²⁹, J. Tojo⁷⁰,
 S. Tokár^{144a}, K. Tokushuku⁶⁶, K. Tollefson⁹⁰, E. Tolley⁵⁷, L. Tomlinson⁸⁴, M. Tomoto¹⁰³,
 L. Tompkins^{143.ai}, K. Toms¹⁰⁵, E. Torrence¹¹⁶, H. Torres¹⁴², E. Torrón Pastor¹⁶⁷, J. Toth^{85.aj},
 F. Touchard⁸⁵, D.R. Tovey¹³⁹, T. Trefzger¹⁷⁴, L. Tremblet³⁰, A. Tricoli³⁰, I.M. Trigger^{159a},
 S. Trincaz-Duvoid⁸⁰, M.F. Tripiana¹², W. Trischuk¹⁵⁸, B. Trocmé⁵⁵, C. Troncon^{91a},
 M. Trottier-McDonald¹⁵, M. Trovatelli¹⁶⁹, P. True⁹⁰, L. Truong^{164a,164c}, M. Trzebinski³⁹, A. Trzupek³⁹,
 C. Tsarouchas³⁰, J.C-L. Tseng¹²⁰, P.V. Tsiarehka⁹², D. Tsionou¹⁵⁴, G. Tsipolitis¹⁰, N. Tsirintanis⁹,
 S. Tsiskaridze¹², V. Tsiskaridze⁴⁸, E.G. Tskhadadze^{51a}, I.I. Tsukerman⁹⁷, V. Tsulaia¹⁵, S. Tsuno⁶⁶,
 D. Tsybychev¹⁴⁸, A. Tudorache^{26a}, V. Tudorache^{26a}, A.N. Tuna¹²², S.A. Tupputi^{20a,20b},
 S. Turchikhin^{99.ag}, D. Turecek¹²⁸, R. Turra^{91a,91b}, A.J. Turvey⁴⁰, P.M. Tuts³⁵, A. Tykhonov⁴⁹,
 M. Tylmad^{146a,146b}, M. Tyndel¹³¹, I. Ueda¹⁵⁵, R. Ueno²⁹, M. Ughetto^{146a,146b}, M. Uglan¹⁴,
 M. Uhlenbrock²¹, F. Ukegawa¹⁶⁰, G. Unal³⁰, A. Undrus²⁵, G. Unel¹⁶³, F.C. Ungaro⁴⁸, Y. Unno⁶⁶,
 C. Unverdorben¹⁰⁰, J. Urban^{144b}, P. Urquijo⁸⁸, P. Urrejola⁸³, G. Usai⁸, A. Usanova⁶², L. Vacavant⁸⁵,
 V. Vacek¹²⁸, B. Vachon⁸⁷, C. Valderanis⁸³, N. Valencic¹⁰⁷, S. Valentini^{20a,20b}, A. Valero¹⁶⁷,
 L. Valery¹², S. Valkar¹²⁹, E. Valladolid Gallego¹⁶⁷, S. Vallecorsa⁴⁹, J.A. Valls Ferrer¹⁶⁷,
 W. Van Den Wollenberg¹⁰⁷, P.C. Van Der Deijl¹⁰⁷, R. van der Geer¹⁰⁷, H. van der Graaf¹⁰⁷,
 R. Van Der Leeuw¹⁰⁷, N. van Eldik¹⁵², P. van Gemmeren⁶, J. Van Nieuwkoop¹⁴², I. van Vulpen¹⁰⁷,

M.C. van Woerden³⁰, M. Vanadia^{132a,132b}, W. Vandelli³⁰, R. Vanguri¹²², A. Vaniachine⁶, F. Vannucci⁸⁰, G. Vardanyan¹⁷⁷, R. Vari^{132a}, E.W. Varnes⁷, T. Varol⁴⁰, D. Varouchas⁸⁰, A. Vartapetian⁸, K.E. Varvell¹⁵⁰, F. Vazeille³⁴, T. Vazquez Schroeder⁸⁷, J. Veatch⁷, L.M. Veloce¹⁵⁸, F. Veloso^{126a,126c}, T. Velz²¹, S. Veneziano^{132a}, A. Ventura^{73a,73b}, D. Ventura⁸⁶, M. Venturi¹⁶⁹, N. Venturi¹⁵⁸, A. Venturini²³, V. Vercesi^{121a}, M. Verducci^{132a,132b}, W. Verkerke¹⁰⁷, J.C. Vermeulen¹⁰⁷, A. Vest⁴⁴, M.C. Vetterli^{142,d}, O. Viazlo⁸¹, I. Vichou¹⁶⁵, T. Vickey¹³⁹, O.E. Vickey Boeriu¹³⁹, G.H.A. Viehhauser¹²⁰, S. Viel¹⁵, R. Vigne⁶², M. Villa^{20a,20b}, M. Villaplana Perez^{91a,91b}, E. Vilucchi⁴⁷, M.G. Vincter²⁹, V.B. Vinogradov⁶⁵, I. Vivarelli¹⁴⁹, F. Vives Vaque³, S. Vlachos¹⁰, D. Vladioiu¹⁰⁰, M. Vlasak¹²⁸, M. Vogel^{132a}, P. Vokac¹²⁸, G. Volpi^{124a,124b}, M. Volpi⁸⁸, H. von der Schmitt¹⁰¹, H. von Radziewski⁴⁸, E. von Toerne²¹, V. Vorobel¹²⁹, K. Vorobev⁹⁸, M. Vos¹⁶⁷, R. Voss³⁰, J.H. Vosseveld⁷⁴, N. Vranjes¹³, M. Vranjes Milosavljevic¹³, V. Vrba¹²⁷, M. Vreeswijk¹⁰⁷, R. Vuillermet³⁰, I. Vukotic³¹, Z. Vykydal¹²⁸, P. Wagner²¹, W. Wagner¹⁷⁵, H. Wahlberg⁷¹, S. Wahrmund⁴⁴, J. Wakabayashi¹⁰³, J. Walder⁷², R. Walker¹⁰⁰, W. Walkowiak¹⁴¹, C. Wang^{33c}, F. Wang¹⁷³, H. Wang¹⁵, H. Wang⁴⁰, J. Wang⁴², J. Wang^{33a}, K. Wang⁸⁷, R. Wang⁶, S.M. Wang¹⁵¹, T. Wang²¹, X. Wang¹⁷⁶, C. Wanotayaroj¹¹⁶, A. Warburton⁸⁷, C.P. Ward²⁸, D.R. Wardrope⁷⁸, M. Warsinsky⁴⁸, A. Washbrook⁴⁶, C. Wasicki⁴², P.M. Watkins¹⁸, A.T. Watson¹⁸, I.J. Watson¹⁵⁰, M.F. Watson¹⁸, G. Watts¹³⁸, S. Watts⁸⁴, B.M. Waugh⁷⁸, S. Webb⁸⁴, M.S. Weber¹⁷, S.W. Weber¹⁷⁴, J.S. Webster³¹, A.R. Weidberg¹²⁰, B. Weinert⁶¹, J. Weingarten⁵⁴, C. Weiser⁴⁸, H. Weits¹⁰⁷, P.S. Wells³⁰, T. Wenaus²⁵, T. Wengler³⁰, S. Wenig³⁰, N. Wermes²¹, M. Werner⁴⁸, P. Werner³⁰, M. Wessels^{58a}, J. Wetter¹⁶¹, K. Whalen¹¹⁶, A.M. Wharton⁷², A. White⁸, M.J. White¹, R. White^{32b}, S. White^{124a,124b}, D. Whiteson¹⁶³, F.J. Wickens¹³¹, W. Wiedenmann¹⁷³, M. Wielers¹³¹, P. Wienemann²¹, C. Wiglesworth³⁶, L.A.M. Wiik-Fuchs²¹, A. Wildauer¹⁰¹, H.G. Wilkens³⁰, H.H. Williams¹²², S. Williams¹⁰⁷, C. Willis⁹⁰, S. Willocq⁸⁶, A. Wilson⁸⁹, J.A. Wilson¹⁸, I. Wingerter-Seez⁵, F. Winklmeier¹¹⁶, B.T. Winter²¹, M. Wittgen¹⁴³, J. Wittkowski¹⁰⁰, S.J. Wollstadt⁸³, M.W. Wolter³⁹, H. Wolters^{126a,126c}, B.K. Wosiek³⁹, J. Wotschack³⁰, M.J. Woudstra⁸⁴, K.W. Wozniak³⁹, M. Wu⁵⁵, M. Wu³¹, S.L. Wu¹⁷³, X. Wu⁴⁹, Y. Wu⁸⁹, T.R. Wyatt⁸⁴, B.M. Wynne⁴⁶, S. Xella³⁶, D. Xu^{33a}, L. Xu^{33b,ak}, B. Yabsley¹⁵⁰, S. Yacoub^{145a}, R. Yakabe⁶⁷, M. Yamada⁶⁶, Y. Yamaguchi¹¹⁸, A. Yamamoto⁶⁶, S. Yamamoto¹⁵⁵, T. Yamanaka¹⁵⁵, K. Yamauchi¹⁰³, Y. Yamazaki⁶⁷, Z. Yan²², H. Yang^{33e}, H. Yang¹⁷³, Y. Yang¹⁵¹, W.-M. Yao¹⁵, Y. Yasu⁶⁶, E. Yatsenko⁵, K.H. Yau Wong²¹, J. Ye⁴⁰, S. Ye²⁵, I. Yeletsikh⁶⁵, A.L. Yen⁵⁷, E. Yildirim⁴², K. Yorita¹⁷¹, R. Yoshida⁶, K. Yoshihara¹²², C. Young¹⁴³, C.J.S. Young³⁰, S. Youssef²², D.R. Yu¹⁵, J. Yu⁸, J.M. Yu⁸⁹, J. Yu¹¹⁴, L. Yuan⁶⁷, A. Yurkewicz¹⁰⁸, I. Yusuff^{28,al}, B. Zabinski³⁹, R. Zaidan⁶³, A.M. Zaitsev^{130,ab}, J. Zalieckas¹⁴, A. Zaman¹⁴⁸, S. Zambito⁵⁷, L. Zanello^{132a,132b}, D. Zanzi⁸⁸, C. Zeitnitz¹⁷⁵, M. Zeman¹²⁸, A. Zemla^{38a}, K. Zengel²³, O. Zenin¹³⁰, T. Ženiš^{144a}, D. Zerwas¹¹⁷, D. Zhang⁸⁹, F. Zhang¹⁷³, H. Zhang^{33c}, J. Zhang⁶, L. Zhang⁴⁸, R. Zhang^{33b}, X. Zhang^{33d}, Z. Zhang¹¹⁷, X. Zhao⁴⁰, Y. Zhao^{33d,117}, Z. Zhao^{33b}, A. Zhemchugov⁶⁵, J. Zhong¹²⁰, B. Zhou⁸⁹, C. Zhou⁴⁵, L. Zhou³⁵, L. Zhou⁴⁰, N. Zhou¹⁶³, C.G. Zhu^{33d}, H. Zhu^{33a}, J. Zhu⁸⁹, Y. Zhu^{33b}, X. Zhuang^{33a}, K. Zhukov⁹⁶, A. Zibell¹⁷⁴, D. Zieminska⁶¹, N.I. Zimine⁶⁵, C. Zimmermann⁸³, S. Zimmermann⁴⁸, Z. Zinonos⁵⁴, M. Zinser⁸³, M. Ziolkowski¹⁴¹, L. Živković¹³, G. Zobernig¹⁷³, A. Zoccoli^{20a,20b}, M. zur Nedden¹⁶, G. Zurzolo^{104a,104b}, L. Zwalinski³⁰.

¹ Department of Physics, University of Adelaide, Adelaide, Australia

² Physics Department, SUNY Albany, Albany, New York, USA

³ Department of Physics, University of Alberta, Edmonton, Alberta, Canada

⁴ (a) Department of Physics, Ankara University, Ankara; (c) Istanbul Aydin University, Istanbul; (d)

Division of Physics, TOBB University of Economics and Technology, Ankara, Turkey

⁵ LAPP, CNRS/IN2P3 and Université Savoie Mont Blanc, Annecy-le-Vieux, France

⁶ High Energy Physics Division, Argonne National Laboratory, Argonne, Illinois, USA

⁷ Department of Physics, University of Arizona, Tucson, Arizona, USA

- ⁸ Department of Physics, The University of Texas at Arlington, Arlington, Texas, USA
- ⁹ Physics Department, University of Athens, Athens, Greece
- ¹⁰ Physics Department, National Technical University of Athens, Zografou, Greece
- ¹¹ Institute of Physics, Azerbaijan Academy of Sciences, Baku, Azerbaijan
- ¹² Institut de Física d'Altes Energies and Departament de Física de la Universitat Autònoma de Barcelona, Barcelona, Spain
- ¹³ Institute of Physics, University of Belgrade, Belgrade, Serbia
- ¹⁴ Department for Physics and Technology, University of Bergen, Bergen, Norway
- ¹⁵ Physics Division, Lawrence Berkeley National Laboratory and University of California, Berkeley, California, USA
- ¹⁶ Department of Physics, Humboldt University, Berlin, Germany
- ¹⁷ Albert Einstein Center for Fundamental Physics and Laboratory for High Energy Physics, University of Bern, Bern, Switzerland
- ¹⁸ School of Physics and Astronomy, University of Birmingham, Birmingham, United Kingdom
- ¹⁹ ^(a) Department of Physics, Bogazici University, Istanbul; ^(b) Department of Physics, Dogus University, Istanbul; ^(c) Department of Physics Engineering, Gaziantep University, Gaziantep, Turkey
- ²⁰ ^(a) INFN Sezione di Bologna; ^(b) Dipartimento di Fisica e Astronomia, Università di Bologna, Bologna, Italy
- ²¹ Physikalisches Institut, University of Bonn, Bonn, Germany
- ²² Department of Physics, Boston University, Boston MA, United States of America
- ²³ Department of Physics, Brandeis University, Waltham MA, United States of America
- ²⁴ ^(a) Universidade Federal do Rio De Janeiro COPPE/EE/IF, Rio de Janeiro; ^(b) Electrical Circuits Department, Federal University of Juiz de Fora (UFJF), Juiz de Fora; ^(c) Federal University of Sao Joao del Rei (UFSJ), Sao Joao del Rei; ^(d) Instituto de Fisica, Universidade de Sao Paulo, Sao Paulo, Brazil
- ²⁵ Physics Department, Brookhaven National Laboratory, Upton, New York, USA
- ²⁶ ^(a) National Institute of Physics and Nuclear Engineering, Bucharest; ^(b) National Institute for Research and Development of Isotopic and Molecular Technologies, Physics Department, Cluj Napoca; ^(c) University Politehnica Bucharest, Bucharest; ^(d) West University in Timisoara, Timisoara, Romania
- ²⁷ Departamento de Física, Universidad de Buenos Aires, Buenos Aires, Argentina
- ²⁸ Cavendish Laboratory, University of Cambridge, Cambridge, United Kingdom
- ²⁹ Department of Physics, Carleton University, Ottawa, Ontario, Canada
- ³⁰ CERN, Geneva, Switzerland
- ³¹ Enrico Fermi Institute, University of Chicago, Chicago, Illinois, USA
- ³² ^(a) Departamento de Física, Pontificia Universidad Católica de Chile, Santiago; ^(b) Departamento de Física, Universidad Técnica Federico Santa María, Valparaíso, Chile
- ³³ ^(a) Institute of High Energy Physics, Chinese Academy of Sciences, Beijing; ^(b) Department of Modern Physics, University of Science and Technology of China, Anhui; ^(c) Department of Physics, Nanjing University, Jiangsu; ^(d) School of Physics, Shandong University, Shandong; ^(e) Department of Physics and Astronomy, Shanghai Key Laboratory for Particle Physics and Cosmology, Shanghai Jiao Tong University, Shanghai; ^(f) Physics Department, Tsinghua University, Beijing 100084, China
- ³⁴ Laboratoire de Physique Corpusculaire, Clermont Université and Université Blaise Pascal and CNRS/IN2P3, Clermont-Ferrand, France
- ³⁵ Nevis Laboratory, Columbia University, Irvington, New York, USA
- ³⁶ Niels Bohr Institute, University of Copenhagen, Kobenhavn, Denmark
- ³⁷ ^(a) INFN Gruppo Collegato di Cosenza, Laboratori Nazionali di Frascati; ^(b) Dipartimento di Fisica, Università della Calabria, Rende, Italy
- ³⁸ ^(a) AGH University of Science and Technology, Faculty of Physics and Applied Computer Science,

Krakow; ^(b) Marian Smoluchowski Institute of Physics, Jagiellonian University, Krakow, Poland

³⁹ Institute of Nuclear Physics Polish Academy of Sciences, Krakow, Poland

⁴⁰ Physics Department, Southern Methodist University, Dallas, Texas, USA

⁴¹ Physics Department, University of Texas at Dallas, Richardson, Texas, USA

⁴² DESY, Hamburg and Zeuthen, Germany

⁴³ Institut für Experimentelle Physik IV, Technische Universität Dortmund, Dortmund, Germany

⁴⁴ Institut für Kern- und Teilchenphysik, Technische Universität Dresden, Dresden, Germany

⁴⁵ Department of Physics, Duke University, Durham, North Carolina, USA

⁴⁶ SUPA - School of Physics and Astronomy, University of Edinburgh, Edinburgh, United Kingdom

⁴⁷ INFN Laboratori Nazionali di Frascati, Frascati, Italy

⁴⁸ Fakultät für Mathematik und Physik, Albert-Ludwigs-Universität, Freiburg, Germany

⁴⁹ Section de Physique, Université de Genève, Geneva, Switzerland

⁵⁰ ^(a) INFN Sezione di Genova; ^(b) Dipartimento di Fisica, Università di Genova, Genova, Italy

⁵¹ ^(a) E. Andronikashvili Institute of Physics, Iv. Javakhishvili Tbilisi State University, Tbilisi; ^(b) High Energy Physics Institute, Tbilisi State University, Tbilisi, Georgia

⁵² II Physikalisches Institut, Justus-Liebig-Universität Giessen, Giessen, Germany

⁵³ SUPA - School of Physics and Astronomy, University of Glasgow, Glasgow, United Kingdom

⁵⁴ II Physikalisches Institut, Georg-August-Universität, Göttingen, Germany

⁵⁵ Laboratoire de Physique Subatomique et de Cosmologie, Université Grenoble-Alpes, CNRS/IN2P3, Grenoble, France

⁵⁶ Department of Physics, Hampton University, Hampton, Virginia, USA

⁵⁷ Laboratory for Particle Physics and Cosmology, Harvard University, Cambridge, Massachusetts, USA

⁵⁸ ^(a) Kirchhoff-Institut für Physik, Ruprecht-Karls-Universität Heidelberg, Heidelberg; ^(b) Physikalisches Institut, Ruprecht-Karls-Universität Heidelberg, Heidelberg; ^(c) ZITI Institut für technische Informatik, Ruprecht-Karls-Universität Heidelberg, Mannheim, Germany

⁵⁹ Faculty of Applied Information Science, Hiroshima Institute of Technology, Hiroshima, Japan

⁶⁰ ^(a) Department of Physics, The Chinese University of Hong Kong, Shatin, N.T., Hong Kong; ^(b) Department of Physics, The University of Hong Kong, Hong Kong; ^(c) Department of Physics, The Hong Kong University of Science and Technology, Clear Water Bay, Kowloon, Hong Kong, China

⁶¹ Department of Physics, Indiana University, Bloomington, Indiana, USA

⁶² Institut für Astro- und Teilchenphysik, Leopold-Franzens-Universität, Innsbruck, Austria

⁶³ University of Iowa, Iowa City, Iowa, USA

⁶⁴ Department of Physics and Astronomy, Iowa State University, Ames, Iowa, USA

⁶⁵ Joint Institute for Nuclear Research, JINR Dubna, Dubna, Russia

⁶⁶ KEK, High Energy Accelerator Research Organization, Tsukuba, Japan

⁶⁷ Graduate School of Science, Kobe University, Kobe, Japan

⁶⁸ Faculty of Science, Kyoto University, Kyoto, Japan

⁶⁹ Kyoto University of Education, Kyoto, Japan

⁷⁰ Department of Physics, Kyushu University, Fukuoka, Japan

⁷¹ Instituto de Física La Plata, Universidad Nacional de La Plata and CONICET, La Plata, Argentina

⁷² Physics Department, Lancaster University, Lancaster, United Kingdom

⁷³ ^(a) INFN Sezione di Lecce; ^(b) Dipartimento di Matematica e Fisica, Università del Salento, Lecce, Italy

⁷⁴ Oliver Lodge Laboratory, University of Liverpool, Liverpool, United Kingdom

⁷⁵ Department of Physics, Jožef Stefan Institute and University of Ljubljana, Ljubljana, Slovenia

⁷⁶ School of Physics and Astronomy, Queen Mary University of London, London, United Kingdom

⁷⁷ Department of Physics, Royal Holloway University of London, Surrey, United Kingdom

- ⁷⁸ Department of Physics and Astronomy, University College London, London, United Kingdom
- ⁷⁹ Louisiana Tech University, Ruston, Louisiana, USA
- ⁸⁰ Laboratoire de Physique Nucléaire et de Hautes Energies, UPMC and Université Paris-Diderot and CNRS/IN2P3, Paris, France
- ⁸¹ Fysiska institutionen, Lunds universitet, Lund, Sweden
- ⁸² Departamento de Física Teórica C-15, Universidad Autónoma de Madrid, Madrid, Spain
- ⁸³ Institut für Physik, Universität Mainz, Mainz, Germany
- ⁸⁴ School of Physics and Astronomy, University of Manchester, Manchester, United Kingdom
- ⁸⁵ CPPM, Aix-Marseille Université and CNRS/IN2P3, Marseille, France
- ⁸⁶ Department of Physics, University of Massachusetts, Amherst, Massachusetts, United States of America
- ⁸⁷ Department of Physics, McGill University, Montreal, Quebec, Canada
- ⁸⁸ School of Physics, University of Melbourne, Victoria, Australia
- ⁸⁹ Department of Physics, The University of Michigan, Ann Arbor MI, United States of America
- ⁹⁰ Department of Physics and Astronomy, Michigan State University, East Lansing, Michigan, USA
- ⁹¹ ^(a) INFN Sezione di Milano; ^(b) Dipartimento di Fisica, Università di Milano, Milano, Italy
- ⁹² B.I. Stepanov Institute of Physics, National Academy of Sciences of Belarus, Minsk, Republic of Belarus
- ⁹³ National Scientific and Educational Centre for Particle and High Energy Physics, Minsk, Republic of Belarus
- ⁹⁴ Department of Physics, Massachusetts Institute of Technology, Cambridge, Massachusetts, USA
- ⁹⁵ Group of Particle Physics, University of Montreal, Montreal, Quebec, Canada
- ⁹⁶ P.N. Lebedev Institute of Physics, Academy of Sciences, Moscow, Russia
- ⁹⁷ Institute for Theoretical and Experimental Physics (ITEP), Moscow, Russia
- ⁹⁸ National Research Nuclear University MEPhI, Moscow, Russia
- ⁹⁹ D.V. Skobeltsyn Institute of Nuclear Physics, M.V. Lomonosov Moscow State University, Moscow, Russia
- ¹⁰⁰ Fakultät für Physik, Ludwig-Maximilians-Universität München, München, Germany
- ¹⁰¹ Max-Planck-Institut für Physik (Werner-Heisenberg-Institut), München, Germany
- ¹⁰² Nagasaki Institute of Applied Science, Nagasaki, Japan
- ¹⁰³ Graduate School of Science and Kobayashi-Maskawa Institute, Nagoya University, Nagoya, Japan
- ¹⁰⁴ ^(a) INFN Sezione di Napoli; ^(b) Dipartimento di Fisica, Università di Napoli, Napoli, Italy
- ¹⁰⁵ Department of Physics and Astronomy, University of New Mexico, Albuquerque, New Mexico, USA
- ¹⁰⁶ Institute for Mathematics, Astrophysics and Particle Physics, Radboud University Nijmegen/Nikhef, Nijmegen, Netherlands
- ¹⁰⁷ Nikhef National Institute for Subatomic Physics and University of Amsterdam, Amsterdam, Netherlands
- ¹⁰⁸ Department of Physics, Northern Illinois University, DeKalb, Illinois, USA
- ¹⁰⁹ Budker Institute of Nuclear Physics, SB RAS, Novosibirsk, Russia
- ¹¹⁰ Department of Physics, New York University, New York, New York, USA
- ¹¹¹ Ohio State University, Columbus, Ohio, USA
- ¹¹² Faculty of Science, Okayama University, Okayama, Japan
- ¹¹³ Homer L. Dodge Department of Physics and Astronomy, University of Oklahoma, Norman, Oklahoma, USA
- ¹¹⁴ Department of Physics, Oklahoma State University, Stillwater, Oklahoma, USA
- ¹¹⁵ Palacký University, RCPTM, Olomouc, Czech Republic
- ¹¹⁶ Center for High Energy Physics, University of Oregon, Eugene, Oregon, USA

- 117 LAL, Université Paris-Sud and CNRS/IN2P3, Orsay, France
- 118 Graduate School of Science, Osaka University, Osaka, Japan
- 119 Department of Physics, University of Oslo, Oslo, Norway
- 120 Department of Physics, Oxford University, Oxford, United Kingdom
- 121 ^(a) INFN Sezione di Pavia; ^(b) Dipartimento di Fisica, Università di Pavia, Pavia, Italy
- 122 Department of Physics, University of Pennsylvania, Philadelphia, Pennsylvania, USA
- 123 National Research Centre "Kurchatov Institute" B.P.Konstantinov Petersburg Nuclear Physics Institute, St. Petersburg, Russia
- 124 ^(a) INFN Sezione di Pisa; ^(b) Dipartimento di Fisica E. Fermi, Università di Pisa, Pisa, Italy
- 125 Department of Physics and Astronomy, University of Pittsburgh, Pittsburgh, Pennsylvania, USA
- 126 ^(a) Laboratório de Instrumentação e Física Experimental de Partículas - LIP, Lisboa; ^(b) Faculdade de Ciências, Universidade de Lisboa, Lisboa; ^(c) Department of Physics, University of Coimbra, Coimbra; ^(d) Centro de Física Nuclear da Universidade de Lisboa, Lisboa; ^(e) Departamento de Física, Universidade do Minho, Braga; ^(f) Departamento de Física Teórica y del Cosmos and CAFPE, Universidad de Granada, Granada (Spain); ^(g) Dep Física and CEFITEC of Faculdade de Ciências e Tecnologia, Universidade Nova de Lisboa, Caparica, Portugal
- 127 Institute of Physics, Academy of Sciences of the Czech Republic, Praha, Czech Republic
- 128 Czech Technical University in Prague, Praha, Czech Republic
- 129 Faculty of Mathematics and Physics, Charles University in Prague, Praha, Czech Republic
- 130 State Research Center Institute for High Energy Physics, Protvino, Russia
- 131 Particle Physics Department, Rutherford Appleton Laboratory, Didcot, United Kingdom
- 132 ^(a) INFN Sezione di Roma; ^(b) Dipartimento di Fisica, Sapienza Università di Roma, Roma, Italy
- 133 ^(a) INFN Sezione di Roma Tor Vergata; ^(b) Dipartimento di Fisica, Università di Roma Tor Vergata, Roma, Italy
- 134 ^(a) INFN Sezione di Roma Tre; ^(b) Dipartimento di Matematica e Fisica, Università Roma Tre, Roma, Italy
- 135 ^(a) Faculté des Sciences Ain Chock, Réseau Universitaire de Physique des Hautes Energies - Université Hassan II, Casablanca; ^(b) Centre National de l'Énergie des Sciences Techniques Nucleaires, Rabat; ^(c) Faculté des Sciences Semlalia, Université Cadi Ayyad, LPHEA-Marrakech; ^(d) Faculté des Sciences, Université Mohamed Premier and LPTPM, Oujda; ^(e) Faculté des sciences, Université Mohammed V-Agdal, Rabat, Morocco
- 136 DSM/IRFU (Institut de Recherches sur les Lois Fondamentales de l'Univers), CEA Saclay (Commissariat à l'Énergie Atomique et aux Énergies Alternatives), Gif-sur-Yvette, France
- 137 Santa Cruz Institute for Particle Physics, University of California Santa Cruz, Santa Cruz, California, USA
- 138 Department of Physics, University of Washington, Seattle, Washington, USA
- 139 Department of Physics and Astronomy, University of Sheffield, Sheffield, United Kingdom
- 140 Department of Physics, Shinshu University, Nagano, Japan
- 141 Fachbereich Physik, Universität Siegen, Siegen, Germany
- 142 Department of Physics, Simon Fraser University, Burnaby, British Columbia, Canada
- 143 SLAC National Accelerator Laboratory, Stanford, California, USA
- 144 ^(a) Faculty of Mathematics, Physics & Informatics, Comenius University, Bratislava; ^(b) Department of Subnuclear Physics, Institute of Experimental Physics of the Slovak Academy of Sciences, Kosice, Slovak Republic
- 145 ^(a) Department of Physics, University of Cape Town, Cape Town; ^(b) Department of Physics, University of Johannesburg, Johannesburg; ^(c) School of Physics, University of the Witwatersrand, Johannesburg, South Africa

- ¹⁴⁶ (a) Department of Physics, Stockholm University; (b) The Oskar Klein Centre, Stockholm, Sweden
- ¹⁴⁷ Physics Department, Royal Institute of Technology, Stockholm, Sweden
- ¹⁴⁸ Departments of Physics & Astronomy and Chemistry, Stony Brook University, Stony Brook, New York, USA
- ¹⁴⁹ Department of Physics and Astronomy, University of Sussex, Brighton, United Kingdom
- ¹⁵⁰ School of Physics, University of Sydney, Sydney, Australia
- ¹⁵¹ Institute of Physics, Academia Sinica, Taipei, Taiwan
- ¹⁵² Department of Physics, Technion: Israel Institute of Technology, Haifa, Israel
- ¹⁵³ Raymond and Beverly Sackler School of Physics and Astronomy, Tel Aviv University, Tel Aviv, Israel
- ¹⁵⁴ Department of Physics, Aristotle University of Thessaloniki, Thessaloniki, Greece
- ¹⁵⁵ International Center for Elementary Particle Physics and Department of Physics, The University of Tokyo, Tokyo, Japan
- ¹⁵⁶ Graduate School of Science and Technology, Tokyo Metropolitan University, Tokyo, Japan
- ¹⁵⁷ Department of Physics, Tokyo Institute of Technology, Tokyo, Japan
- ¹⁵⁸ Department of Physics, University of Toronto, Toronto, Ontario, Canada
- ¹⁵⁹ (a) TRIUMF, Vancouver BC; (b) Department of Physics and Astronomy, York University, Toronto, Ontario, Canada
- ¹⁶⁰ Faculty of Pure and Applied Sciences, University of Tsukuba, Tsukuba, Japan
- ¹⁶¹ Department of Physics and Astronomy, Tufts University, Medford, Massachusetts, USA
- ¹⁶² Centro de Investigaciones, Universidad Antonio Narino, Bogota, Colombia
- ¹⁶³ Department of Physics and Astronomy, University of California Irvine, Irvine, California, USA
- ¹⁶⁴ (a) INFN Gruppo Collegato di Udine, Sezione di Trieste, Udine; (b) ICTP, Trieste; (c) Dipartimento di Chimica, Fisica e Ambiente, Università di Udine, Udine, Italy
- ¹⁶⁵ Department of Physics, University of Illinois, Urbana, Illinois, USA
- ¹⁶⁶ Department of Physics and Astronomy, University of Uppsala, Uppsala, Sweden
- ¹⁶⁷ Instituto de Física Corpuscular (IFIC) and Departamento de Física Atómica, Molecular y Nuclear and Departamento de Ingeniería Electrónica and Instituto de Microelectrónica de Barcelona (IMB-CNM), University of Valencia and CSIC, Valencia, Spain
- ¹⁶⁸ Department of Physics, University of British Columbia, Vancouver, British Columbia, Canada
- ¹⁶⁹ Department of Physics and Astronomy, University of Victoria, Victoria, British Columbia, Canada
- ¹⁷⁰ Department of Physics, University of Warwick, Coventry, United Kingdom
- ¹⁷¹ Waseda University, Tokyo, Japan
- ¹⁷² Department of Particle Physics, The Weizmann Institute of Science, Rehovot, Israel
- ¹⁷³ Department of Physics, University of Wisconsin, Madison, Wisconsin, USA
- ¹⁷⁴ Fakultät für Physik und Astronomie, Julius-Maximilians-Universität, Würzburg, Germany
- ¹⁷⁵ Fachbereich C Physik, Bergische Universität Wuppertal, Wuppertal, Germany
- ¹⁷⁶ Department of Physics, Yale University, New Haven, Connecticut, USA
- ¹⁷⁷ Yerevan Physics Institute, Yerevan, Armenia
- ¹⁷⁸ Centre de Calcul de l'Institut National de Physique Nucléaire et de Physique des Particules (IN2P3), Villeurbanne, France
- ^a Also at Department of Physics, King's College London, London, United Kingdom
- ^b Also at Institute of Physics, Azerbaijan Academy of Sciences, Baku, Azerbaijan
- ^c Also at Novosibirsk State University, Novosibirsk, Russia
- ^d Also at TRIUMF, Vancouver, British Columbia, Canada
- ^e Also at Department of Physics, California State University, Fresno, California, USA
- ^f Also at Department of Physics, University of Fribourg, Fribourg, Switzerland

- ^g Also at Departamento de Fisica e Astronomia, Faculdade de Ciencias, Universidade do Porto, Portugal
- ^h Also at Tomsk State University, Tomsk, Russia
- ⁱ Also at CPPM, Aix-Marseille Université and CNRS/IN2P3, Marseille, France
- ^j Also at Università di Napoli Parthenope, Napoli, Italy
- ^k Also at Institute of Particle Physics (IPP), Canada
- ^l Also at Particle Physics Department, Rutherford Appleton Laboratory, Didcot, United Kingdom
- ^m Also at Department of Physics, St. Petersburg State Polytechnical University, St. Petersburg, Russia
- ⁿ Also at Louisiana Tech University, Ruston, Louisiana, USA
- ^o Also at Institutio Catalana de Recerca i Estudis Avancats, ICREA, Barcelona, Spain
- ^p Also at Department of Physics, National Tsing Hua University, Taiwan
- ^q Also at Department of Physics, The University of Texas at Austin, Austin, Texas, USA
- ^r Also at Institute of Theoretical Physics, Ilia State University, Tbilisi, Georgia
- ^s Also at CERN, Geneva, Switzerland
- ^t Also at Georgian Technical University (GTU), Tbilisi, Georgia
- ^u Also at Ochadai Academic Production, Ochanomizu University, Tokyo, Japan
- ^v Also at Manhattan College, New York, New York, USA
- ^w Also at Hellenic Open University, Patras, Greece
- ^x Also at Institute of Physics, Academia Sinica, Taipei, Taiwan
- ^y Also at LAL, Université Paris-Sud and CNRS/IN2P3, Orsay, France
- ^z Also at Academia Sinica Grid Computing, Institute of Physics, Academia Sinica, Taipei, Taiwan
- ^{aa} Also at School of Physics, Shandong University, Shandong, China
- ^{ab} Also at Moscow Institute of Physics and Technology State University, Dolgoprudny, Russia
- ^{ac} Also at Section de Physique, Université de Genève, Geneva, Switzerland
- ^{ad} Also at International School for Advanced Studies (SISSA), Trieste, Italy
- ^{ae} Also at Department of Physics and Astronomy, University of South Carolina, Columbia, South Carolina, USA
- ^{af} Also at School of Physics and Engineering, Sun Yat-sen University, Guangzhou, China
- ^{ag} Also at Faculty of Physics, M.V.Lomonosov Moscow State University, Moscow, Russia
- ^{ah} Also at National Research Nuclear University MEPhI, Moscow, Russia
- ^{ai} Also at Department of Physics, Stanford University, Stanford, California, United States of America
- ^{aj} Also at Institute for Particle and Nuclear Physics, Wigner Research Centre for Physics, Budapest, Hungary
- ^{ak} Also at Department of Physics, The University of Michigan, Ann Arbor MI, USA
- ^{al} Also at University of Malaya, Department of Physics, Kuala Lumpur, Malaysia
- * Deceased